Autism Spectrum Disorder and Mitochondrial Dysfunction: The Role of Mitochondrial Dynamics

Erin Buchanan

Dissertation presented for the degree of Master of Science

Department of Molecular and Cell Biology

Science Faculty

University of Cape Town

August 2022

Supervisor: Dr Colleen O'Ryan

Declaration

I am presenting this dissertation in full fulfilment of the requirements for my degree.

I know the meaning of plagiarism and declare that all of the work in the dissertation, save for that which is properly acknowledged, is my own.

Signature: Signed by candidate

Acknowledgements

Thank you to everyone who contributed to my research and supported me during my MSc.

Thank you to my supervisor, Dr Colleen O'Ryan, for her support and guidance over the past few years. Thank you for always being willing to chat and give advice, even when there were a million other things on your to-do list. Your enthusiasm for my project and our lab's research is constantly inspiring and I could not have asked for a more supportive supervisor.

Thank you to the Lab 405 members, Sophia Bam, Emma Frickel, Caitlyn Mahony and Mignon Van Der Watt for all your support with difficult qPCRs and multiple writing drafts. Your help both in the lab and while writing was invaluable. I wouldn't have finished without you.

Thank you to Mohamed Jaffer for his support, training and advice at the EM Unit. You made the imaging part of my project possible, and I am so grateful that you were willing to teach me the EM techniques. Thank you for your continued interest in my project and your expert advice. Thank you also to Dr Trevor Sewell and Dr Jeremy Woodward for their advice on EM techniques and analysis.

A huge thank you to Dr Caron Jacobs for all her help and advice on my EM image analysis. You took time out of your extremely busy schedule to help me even though the project wasn't based in your department. Without your assistance, I wouldn't have been able to finish my analyses.

Thank you to Shakiera Sattar for her training and support in the MCB tissue culture unit. Thank you to Elle Van Der Colff for helping me with tissue culture at the start of this project.

Thank you to the parents and children who participated in our cohort study.

Thank you to the National Research Foundation for funding this project and to the University of Cape Town for conference travel assistance.

Lastly, thank you to my family and friends for their continuous support and guidance. To my mom, Nora Buchanan, for all her endless support, encouragement and patience throughout my university career, and to my fellow postgrads and best friends, Abby Gwynn and Arron Correia, for all their support as we tackled postgrad together.

Abstract

Numerous genes and biological pathways are implicated in the aetiology of the neurodevelopmental disorder, autism spectrum disorder (ASD). Our research group reported that mitochondrial dysfunction was associated with ASD in South African children diagnosed with ASD using differential methylation and metabolomics studies. Propionyl-CoA Carboxylase Subunit Beta (*PCCB*) was differentially methylated in our cohort ASD study, and its dysregulation can lead to the accumulation of propionic acid. This links *PCCB*'s function to a well-established animal model that uses sodium propionate (NaP) to study ASD in rats.

This thesis aimed to **i)** examine ASD-associated mitochondrial dysfunction in a neuronal-like cell model using NaP and to investigate its effects on mitochondrial dynamics and morphology; **ii)** investigate the application of this in a South African ASD cohort by measuring differential methylation of essential genes involved in mitochondrial dynamics.

Undifferentiated, neuronal-like SH-SY5Y cells were treated with NaP at 1.5mM, 3mM and 5mM to induce mitochondrial stress. The effects of NaP mitochondrial-induced stress were quantified using MTT and ATP assays. Transmission electron microscopy (TEM), using cryogenic techniques, was used to examine mitochondrial morphology by measuring nine parameters: area, area^2, form factor, area-weighted form factor, aspect ratio, perimeter, circularity, Feret's diameter and roundness. TEM images were analysed using Fiji/Image J. Mitochondrial DNA (MT-DNA) copy number and *STOML2* expression were measured using RT-qPCR, and these data were compared to TEM data. *STOML2* was the most differentially methylated gene in our ASD cohort in our previous study. Differential methylation of six essential genes (*DRP1, FIS1, MFN1, MFN2*, *OPA1, STOML2*) involved in mitochondrial fusion and fission were examined using targeted next-generation bisulfite sequencing (tNGBS) between ASD and control participants in a South African cohort. Significance for all experiments was determined using unpaired t-tests, one-way ANOVA and correlation analysis ($p<0.05$).

SH-SY5Y cells treated with NaP showed mitochondrial dysfunction as reflected in changes in ATP levels and no changes in cell viability were observed except at 9mM NaP. In addition, NaP treatments led to significant changes in mitochondrial morphology with significant decreases

in mitochondrial area, perimeter, form factor and Feret's diameter between NaP treatments and control and a significant increase in circularity. These changes in morphological data were supported by a significant increase in MT-DNA copy number at 5mM and significant decreases in *STOML2* expression at all concentrations. Together, the TEM and expression data highlight the balancing act between mitochondrial fusion and fission, with increasing levels of fission occurring with increasing NaP concentrations. In the South African cohort, there were significant differences in methylation between the ASD group compared to controls at two CpG sites in *MFN2,* two CpG sites in *STOML2* and one CpG site in *FIS1* (significant increases) and two CpG sites in *OPA1* (significant decreases). The increase in *FIS1* and decrease in *OPA1* methylation are consistent with this balancing act between mitochondrial fusion and fission in mitochondrial dysfunction in this cohort.

These results suggest a potential link between mitochondrial dysfunction and the fluctuation in mitochondrial dynamics and morphology. The inclusion of TEM demonstrates its unique ability to visualise mitochondrial ultrastructure and the effect changes in mitochondrial dynamics have on morphology as opposed to only examining these changes through gene expression and metabolic assays. Although the exact relationship between the TEM and gene expression data could not be fully explained in this study, it highlights the need to explore further the relationship between mitochondrial dynamics, biogenesis and mitophagy in the context of ASD aetiology and neuronal development.

Table of Contents

List of Abbreviations

In the text, gene names are capitalised and italicised; protein names are capitalised.

ANOVA: Analysis of variance

ASD: Autism spectrum disorder

ATP: Adenosine triphosphate

B2M: Beta-2-microglobulin

cDNA: Complementary DNA

Ct: Cycling threshold

DMSO: Dimethyl sulfoxide

DMEM: Dulbecco's modified eagle medium

DNA: Deoxyribonucleic acid

Dnmt: DNA methyltransferase

DRP1: Dynamin-related protein 1

DSM: Diagnostic and statistical manual of mental disorders

EDTA: Ethylenediamine tetraacetic acid

ER: Endoplasmic reticulum

ETC: Electron transport chain

FBS: Fetal bovine serum

FIS1: Mitochondrial fission protein 1

HIV: Human immunodeficiency virus

L-OPA: Long isoforms of OPA1

MeCP2: Methyl CpG binding protein 2

MFF: Mitochondrial fission factor

MFN1: Mitofusin 1

MFN2: Mitofusin 2

MiD49: mitochondrial dynamics protein 49

MiD51: mitochondrial dynamics protein 51

mRNA: Messenger RNA

MT-DNA: Mitochondrial DNA

MT-ND1: Mitochondrial NADH dehydrogenase 1

MTT: 3-(4,5-dimethylthiazol-2-yl)-2,5-diphenyl-2H-tetrazolium bromide

NaP: Sodium propionate

NaCl: Sodium chloride

nDNA: Nuclear DNA

OPA1: Dominant optic atrophy 1

PBS: Phosphate-buffered saline

PCC: Propionyl-CoA carboxylase

PCCB: Propionyl-CoA carboxylase subunit beta

PCR: Polymerase chain reaction

PGC-1α: Peroxisome proliferator-activated receptor-gamma coactivator-1 alpha

PINK1: PTEN Induced Kinase 1

PPA: Propionic acid

RNA: Ribonucleic acid

ROI: Region of interest

ROS: Reactive oxygen species

RT-qPCR: Real-time quantitative PCR

S-OPA1: short isoforms of OPA1

STOML2: Stomatin-like protein 2

TE: Tris-EDTA

TEM: Transmission electron microscopy

tNGBS: Targeted next-generation bisulfite sequencing

TSS: Transcription start site

Measurements

g: gram

ml: milli-litre

mM: millimolar

ng: nanogram

µl: micro-litre

µm: micromolar

°C: degrees Celsius

List of Figures and Tables

Chapter 1

Literature Review

1.1. Introduction

The roles assigned to mitochondria in cellular functioning are constantly evolving. Mitochondria are known primarily for producing adenosine triphosphate (ATP). However, their other functions include calcium signalling and apoptosis, confirming mitochondria's dynamic capabilities. Proper mitochondrial morphology, driven by mitochondrial dynamics, is often overlooked but is imperative to mitochondrial and cellular function. The shape, connectivity and cristae structure of mitochondria are essential in generating energy and ensuring mitochondrial survival (Belenguer *et al.*, 2019; Wang *et al.*, 2021).

Mitochondrial dysfunction has been implicated in many neurological disorders, from psychiatric disorders, such as bipolar disorder and depression, to neurodegenerative (Parkinson's disease and dementia) and neurodevelopmental disorders (Mattson, Gleichmann and Cheng, 2008). In addition, efficient mitochondrial function is crucial in neurons for neurogenesis, plasticity and function (Rugarli and Langer, 2012; Rangaraju *et al.*, 2019).

The neurodevelopmental disorder autism spectrum disorder (ASD) has been associated with mitochondrial dysfunction (Siddiqui, Elwell and Johnson, 2016; Griffiths and Levy, 2017; Frye *et al.*, 2021). Recently, the *Diagnostic and Statistical Manual of Mental Disorders* (DSM-5th edition) merged autism, Asperger's syndrome, pervasive developmental disorder and childhood disintegrative disorder into ASD to reflect the overlapping characteristics of individuals diagnosed with these disorders. Usually diagnosed during early childhood, ASD behaviours impair social and occupational functioning (American Psychiatric Association, 2013). ASD individuals often display co-morbidities with other neurodevelopmental or health conditions such as gastrointestinal disorders or metabolic disorders (Al-Beltagi, 2021). Mitochondrial dysfunction could explain a wide range of the symptoms associated with ASD (Frye and Rossignol, 2011).

1.2. Mitochondrial function

The primary role of mitochondria is to generate energy in the form of ATP, primarily through oxidative phosphorylation, driven by the four electron transport chain (ETC) complexes housed in the inner mitochondrial membrane (Rossignol and Frye, 2012; Siddiqui, Elwell and Johnson, 2016). The movement of these electrons through the transport chain creates a proton gradient across the inner membrane, which drives complex V (ATP synthase) to produce ATP (Mattson, Gleichmann and Cheng, 2008). Primary mitochondrial dysfunction occurs when mutations or damages directly disrupt the ATP production pathway (Rossignol and Frye, 2012).

However, mitochondria have functions in other pathways aside from energy production. These include calcium homeostasis, production of reactive oxygen species (ROS) and regulation of programmed cell death (apoptosis) (Siddiqui, Elwell and Johnson, 2016). Mitochondrial homeostasis regulates these processes and the mitochondrial network, which is composed of connected mitochondria in a branched system (Hoitzing, Johnston and Jones, 2015; Siddiqui, Elwell and Johnson, 2016). If any dysfunction occurs in these processes, it is known as secondary mitochondrial dysfunction (Rossignol and Frye, 2012).

Multiple copies of mitochondria are present in each cell, and each mitochondrion contains multiple copies of its genome. Mitochondrial DNA (MT-DNA) copy number varies between cell types depending on their energy demands. Changes in MT-DNA copy number can be used as a marker for mitochondrial dysfunction as numerous studies have associated it with mitochondrial diseases and as a response to oxidative stress (Grady *et al.*, 2014; Thompson *et al.*, 2016; Zeng *et al.*, 2019). Because it can suggest changes in mitochondrial function, fluctuations in MT-DNA copy number can also indicate changes in mitochondrial dynamics. The mitochondrial genome consists of 37 genes that encode ETC complex subunits and proteins needed for transcription and translation. All other genes needed for mitochondrial machinery or function are part of the cell's nuclear DNA (nDNA). As both MT-DNA and nDNA encode mitochondrial proteins, mutations in either genome affect mitochondrial function (Rossignol and Frye, 2012; Siddiqui, Elwell and Johnson, 2016).

1.3. The importance of mitochondria in neurons

Neuronal cells are an interesting case for mitochondrial function as they are high-energy demanding, non-replicating and have varying morphologies (Chang and Reynolds, 2006; Rossignol and Frye, 2012). Neurons extend over relatively long distances compared to other cell types and consist of axons, dendrites and cell bodies (Misgeld and Schwarz, 2017). Maintenance of a healthy mitochondrial network is known as mitostasis, which "can be thought of as a specialized form of homeostasis, a mechanism by which mitochondrial number and quality are maintained over time in each compartment of the neuron" (Misgeld and Schwarz, 2017). Mitostasis involves processes such as mitochondrial dynamics (fusion and fission), mitophagy and mitochondrial transport (Frederick and Shaw, 2007). Fission and fusion are essential processes in modulating mitostasis to ensure mitochondria are well dispersed to meet the energy demands of the neuron (Chang and Reynolds, 2006; Misgeld and Schwarz, 2017). Mitophagy, the autophagy of mitochondria, is another essential process in mitostasis. The mitochondrial population goes through a regular turn-over to ensure that any damaged mitochondria are removed via mitophagy to prevent excess ROS from being produced (Fan *et al.*, 2022). Mitochondria are also highly mobile in neurons, and their transport throughout the neuronal network is essential in maintaining mitostasis. The organelles can be transported both toward axons (anterograde movement) and towards cell bodies (retrograde movement) (Mandal *et al.*, 2021). Any changes in mitochondrial dynamics, mitophagy or mitochondrial transport could affect mitostasis and thus the overall health of the neuronal network.

Recent reviews have outlined the importance of mitochondria and mitostasis in neurogenesis, differentiation, maturation and plasticity (Belenguer *et al.*, 2019; Rangaraju *et al.*, 2019; Wang *et al.*, 2021). Any dysfunction which occurs in the mitochondrial pathways would impact these processes and lead to the development of neurological disorders. This is particularly important during neurodevelopment as reliable energy production and distribution are essential for neurogenesis and synaptic connectivity of axons and dendrites (Mattson, Gleichmann and Cheng, 2008; Haas, 2010; Rangaraju *et al.*, 2019).

Disruptions in mitostasis have been associated with many neurological disorders aside from ASD. Neurodegenerative diseases, such as Alzheimer's and Parkinson's, are associated with

oxidative stress and changes in energy metabolism. Parkinson's disease has specifically implicated Parkin and PINK1, involved in mitophagy, in its pathology and patients have decreased ETC complex activity (Mattson, Gleichmann and Cheng, 2008). Psychiatric disorders such as depression, bipolar disorder and schizophrenia are also associated with mitochondrial dysfunction (Mattson, Gleichmann and Cheng, 2008; Gandal *et al.*, 2018). These neurological disorders and diseases highlight mitochondria's essential role in ensuring the health of the neuronal network.

1.4. Mitochondrial dynamics and morphology

Mitochondrial morphology constantly changes due to fluctuations in mitochondrial dynamics. Once considered a fixed shape, we now know that it is a plastic structure – it can adapt to the needs of the organelle and the cell (Cogliati, Enriquez and Scorrano, 2016). Three main processes govern mitochondrial morphology: fusion, fission and cristae structure (Baker, Patel and Khacho, 2019). The balance between these processes sustains mitochondrial metabolism and influences mitochondrial function. Shifting mitochondria "from highly branched to fragmented morphologies" (Karbowski and Youle, 2003) allows the organelles to adapt to their environment when confronted with toxins, changing energy demands and nutrient availability (Youle and Bliek, 2012; Cogliati *et al.*, 2013; Baker, Patel and Khacho, 2019). Proteins that directly participate in mammalian fission, fusion and cristae structure, as well as accessory proteins, have been identified, although pieces of the puzzle are still missing (Karbowski and Youle, 2003).

1.4.1. Fusion

Fusion refers to joining or fusing two or more mitochondria. Mitochondria have an outer and inner membrane, with both membranes needing to fuse with neighbouring mitochondria. Three main proteins, mitofusins 1 and 2 (MFN1 and MFN2) and dominant optic atrophy (OPA1), control fusion together with other accessory proteins such as STOML2 (Figure 1). Although these three primary proteins are known to control fusion, the roles of other accessory proteins are still being investigated.

Mitofusins 1 and 2 (MFN1 and MFN2) fuse the outer membrane (Figure 1) (Santel and Fuller, 2001; Chen *et al.*, 2003). Losing either or both mitofusins increases fragmented mitochondria

and changes respiration activity and mitochondrial mobility (Chen *et al.*, 2003; Tondera *et al.*, 2009). MFN1 and MFN2 co-localise with mitochondrial markers confirming they interact directly with the mitochondrial membrane (Santel and Fuller, 2001). Although they appear to have the same function, both mitofusins are essential for fusion. Loss of MFN2 after losing MFN1 confirms this as it produces an additive effect of mitochondrial fragmentation. Together, the mitofusins form homotypic and heterotypic complexes corroborating that they interact during fusion (Chen *et al.*, 2003).

A different protein is responsible for fusing the inner mitochondrial membrane. The cell transcribes and translates dominant optic atrophy (OPA1) into one protein and processes it into different splice variants (Duvezin-Caubet *et al.*, 2006; Ishihara *et al.*, 2006). Like the mitofusins, loss of OPA1 leads to increased mitochondrial fragmentation. However, it is specifically the long isoforms of OPA1 (L-OPA1), not the short isoforms (S-OPA1), which are essential for fusion. Expressing L-OPA1 alone, after causing mitochondrial fragmentation, can restore the mitochondrial network (Ishihara *et al.*, 2006). On the other hand, stimulating proteolytic processing of L-OPA1 into S-OPA1 coincides with increased fragmentation, while blocking this proteolytic processing does not affect the tubular shape of mitochondria (Duvezin-Caubet *et al.*, 2006; Ishihara *et al.*, 2006; Anand *et al.*, 2014). Instead, S-OPA1 is associated with mitochondrial fission. Two proteases, YME1L and OMA1, process L-OPA1 into its short isoforms (Anand *et al.*, 2014). A decrease in mitochondrial membrane potential triggers proteolytic processing of L-OPA1 to S-OPA1 – an event associated with apoptosis (Duvezin-Caubet *et al.*, 2006; Anand *et al.*, 2014).

Stomatin-like protein 2 (STOML2, also known as SLP2) is a protein involved in mitochondrial function, although its exact roles in various mitochondrial pathways are still unknown. Currently, we know that it is indirectly involved in fusion as it maintains the long isoforms of OPA1. It is especially important during hyperfusion when the rate of fusion increases under stress conditions (Tondera *et al.*, 2009). Its role in fusion is further supported by the discovery that it is associated with MFN2 though the exact mechanism behind this is unclear (Hájek, Chomyn and Attardi, 2007). It is also involved in maintaining coupled mitochondrial respiration and the formation of respiratory chain complexes (Christie *et al.*, 2012; Mitsopoulos *et al.*, 2015). However, upregulation of STOML2 has also been associated with

certain cancers, increased cell proliferation, tumour progression and mitophagy (Qu *et al.*, 2019; Zheng *et al.*, 2021).

1.4.2. Fission

Mitochondrial fission (or fragmentation) involves dividing a mitochondrion into smaller mitochondria. Dynamin-related protein 1 (DRP1) divides the outer membrane (Figure 1). Fission of the inner membrane remains a mystery as no proteins dividing this membrane have been identified (Wai and Langer, 2016). DRP1 localises to the mitochondrial outer membrane before division and forms spirals to constrict the membrane (Smirnova *et al.*, 2001). Mutations or knockouts of DRP1 lead to increased mitochondrial network connectivity and no fission occurs (Smirnova *et al.*, 2001; Otera *et al.*, 2016). This DRP1-null phenotype is the most severe compared with the loss of any other fission protein (Losón *et al.*, 2013; Otera *et al.*, 2016). However, although it is responsible for dividing the outer membrane, DRP1 is mainly found in the cytosol (Smirnova *et al.*, 2001; Losón *et al.*, 2013). Thus, other proteins must recruit DRP1 to the mitochondrial membrane before fission.

Mitochondrial fission factor (MFF) is the primary protein that recruits DRP1 to the membrane (Figure 1). Losing MFF results in a decrease in DRP1 localisation and elongated mitochondria (a more severe phenotype than losing other DRP1 recruitment proteins) (Otera *et al.*, 2010; Losón *et al.*, 2013). MFF functions independently of other recruitment proteins and localises to the mitochondrial membrane in the absence of DRP1, suggesting that it acts independently of DRP1 (Otera *et al.*, 2010; Friedman *et al.*, 2011; Losón *et al.*, 2013).

Researchers have debated the importance of the next fission protein, mitochondrial fission protein 1 (FIS1). Some studies conclude that FIS1 interacts with DRP1, and losing it decreases fission (Stojanovski *et al.*, 2004; Losón *et al.*, 2013). Others find that FIS1 is dispensable to fission (Otera *et al.*, 2010; Elgass *et al.*, 2015). Stojanovski *et al*. (2004) and Losón *et al*. (2013) locate FIS1 on the mitochondrial outer membrane. When knocked out, mitochondria significantly elongate and DRP1 recruitment decreases. Although Losón *et al*. (2013) observed that the morphological changes in FIS1-null cells were more moderate compared to MFF-null cells, they were still apparent, and FIS1 acted independently of MFF. However, Elgass *et al*. (2015) found no interactions between DRP1 and FIS1 proteins. In a knockout model of FIS1 after the knockout of MFF, there was no increase in mitochondrial elongation or reduced DRP1

protein levels in cell fractionations. The study conceded, though, that FIS1 did associate with DRP1 under mild stress conditions and that overexpressing FIS1 affected the mitochondrial network (Otera *et al.*, 2010). One possibility is that the role of FIS1 in fission depends on the cell type. Another possibility is that MFF and FIS1 are involved in different DRP1 pathways (Otera *et al.*, 2010; Losón *et al.*, 2013). Either way, FIS1's potential role in mitochondrial fission cannot be excluded (Figure 1).

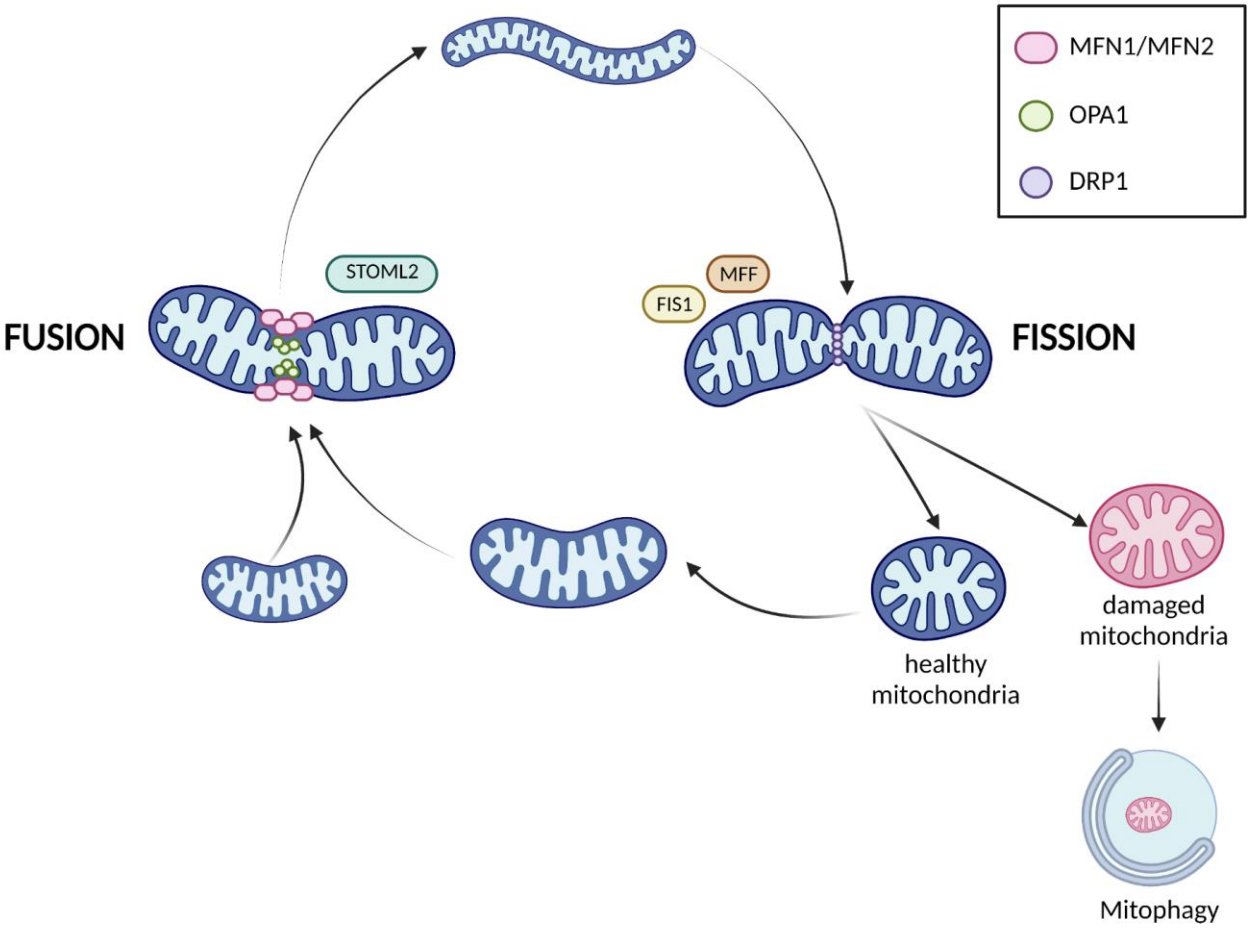

FIGURE 1: The mitochondrial fusion and fission cycle. Mitochondria undergo fusion and fission to maintain homeostasis. During fusion, separate mitochondria fuse and the resulting mitochondrion is elongated. During fission, damaged mitochondria are separated from healthy mitochondria. The damaged mitochodnria undergo mitophagy, while healthy mitochondria continue in the cycle. The key genes involved in fusion (*MFN1, MFN2, OPA1* and *STOML2*) and key genes involved in fission (*FIS1, MFF* and *DRP1*) are shown. Figure made in BioRender.com

Two mitochondrial dynamics proteins 49 and 51 kDa (MiD49 and MiD51) also mediate DRP1's recruitment to the mitochondria. Both interact with DRP1, MFF, and each other (Elgass *et al.*, 2015). A double knockout of MFF and FIS1 resulted in increased elongation but some fission was still present, indicating that other fission proteins can recruit DRP1 (Losón *et al.*, 2013). Overexpressing Mid49 and MiD51 proteins in MFF-null and/or FIS1-null cells can restore fission to a small extent. Knocking out Mid49 and MiD51 increases elongation and decreases DRP1 recruitment, though more moderately than in MFF-null cells (Losón *et al.*, 2013; Otera *et al.*, 2016). Some studies show that overexpression of Mid49 or MiD51 has been associated with increased elongation, but this is thought to be because they associate with an inactive form of DRP1 (Losón *et al.*, 2013). Although MFF, FIS1, MiD49 and MiD51 act independently, they could co-localise with DRP1 to form one fission machine (Elgass *et al.*, 2015).

1.4.3. Cristae structure

Cristae are the folds of the mitochondrial inner membrane and regularly change their morphology, known as cristae remodelling, such as elongation and shortening (Hu *et al.*, 2020). Although they are known to be essential for mitochondrial functioning, the exact mechanism around their functions and changing morphologies are still being investigated (Zick, Rabl and Reichert, 2009). OPA1, MiD49 and MiD51 act independently of their roles in fusion and fission when regulating cristae remodelling (Frezza *et al.*, 2006; Otera *et al.*, 2016). As OPA1 is an integral intermembrane protein, it is no surprise that it participates in cristae remodelling. OPA1 regulates cristae junctions and length and prevents the widening of cristae (Frezza *et al.*, 2006). Narrow cristae junctions delay cytochrome c release, which occurs when cristae widen. Cytochrome c needs to be released before apoptosis, indicating that OPA1 is anti-apoptotic (Frezza *et al.*, 2006; Cogliati, Enriquez and Scorrano, 2016). The importance of OPA1 in cytochrome c release varies between studies. Frezza *et al.* (2006) concluded that OPA1 controls cytochrome c mobilisation through cristae remodelling. However, Otera *et al*. (2016) found that increasing proteolytic processing of L-OPA1 to its short isoforms did not affect cytochrome c release.

MiD49 and MiD51 prepare cristae for apoptosis and cytochrome c release. Cells lacking MiD49 and MiD51 display tight cristae during apoptosis and resist cytochrome c release (Otera *et al.*, 2016). Although the roles of these proteins in cristae remodelling are still being explored, they are essential for maintaining and regulating cristae structure.

1.4.4. Fusion/fission and the endoplasmic reticulum

The endoplasmic reticulum (ER) transports different substrates to various organelles in the cell. It specifically transfers calcium ions to mitochondria which play a significant role in calcium signalling (Elgass *et al.*, 2015). However, the ER also plays a role in fusion and fission. MFN2 appears at the ER-mitochondrial interface and losing MFN2 alters ER morphology and disrupts this connection (de Brito and Scorrano, 2008). The contact sites of the ER-mitochondria interface are also sites of mitochondrial division, pointing to an ER role in fission. DRP1 and MFF localise at these points of contact. Even in cells lacking DRP1 and MFF, mitochondria still constrict at the ER-mitochondria interface. This suggests the ER acts independently of these fission proteins in mitochondrial division (Friedman *et al.*, 2011).

1.4.5. The importance of mitochondrial dynamics and morphology

Various reviews and studies have outlined how mitochondrial morphology is linked to mitochondrial function, cell function, bioenergetics and apoptosis (Karbowski and Youle, 2003; Liesa and Shirihai, 2013; Cogliati, Enriquez and Scorrano, 2016; Wai and Langer, 2016). It is widely accepted that "The morphology of mitochondria is inextricably linked to its function" (Wai and Langer, 2016). Different cellular stresses have differing impacts on mitochondrial dynamics and morphology. Increases in oxidative stresses favour fission and mitophagy, while energy stresses favour fusion (Fu, Liu and Yin, 2019).

Both mitofusins (MFN1 and MFN2) are essential in embryonic development as homozygous embryos lacking either or both mitofusins fail to survive (Chen *et al.*, 2003). Fusion also allows mitochondria to complement each other's defects. When fusing, mitochondria share MT-DNA, ensuring that any deleterious mutations are compensated for and do not affect the overall health of the mitochondrial network (Karbowski and Youle, 2003; Youle and Bliek, 2012). Fusion can be a protective mechanism to prevent mitochondria and the cell from undergoing apoptosis (Tondera *et al.*, 2009; Anand *et al.*, 2014).

Fission also plays a role in different cellular pathways. Fission can be divided into two categories. Firstly, it can play a role in cellular division when mitochondria must be separated between daughter cells (Youle and Bliek, 2012). It is also needed during differentiation to divide mitochondria and when the energy demands of the cell increase (Smirnova *et al.*, 2001). Fission's other role is to assist in preparing damaged mitochondria for mitophagy or the cell

for apoptosis (Figure 1). Fission separates severely damaged mitochondria from the mitochondrial network to prevent further damage to the overall network (Youle and Bliek, 2012). The membrane potential of these damaged mitochondria decreases to promote ubiquitinylation, which marks them for the mitophagy pathway. After the decrease in membrane potential, factors process L-OPA1 to S-OPA1 to block fusion and promote fission and mitophagy (Duvezin-Caubet *et al.*, 2006). The protein Parkin (encoded by the *PARK2* gene) ubiquitylates MFN1 and MFN2 to assist in preventing fusion (Escobar-Henriques and Langer, 2014). Mitophagy usually occurs after mitochondrial fission, meaning that fission machinery may interact with mitophagy factors such as Parkin and PINK1 (Youle and Bliek, 2012). Ubiquitylating other outer mitochondrial proteins signals to lysosomes that the marked mitochondrion can be engulfed and degraded (Youle and Bliek, 2012). As previously discussed, cristae remodelling controls the release of cytochrome c, which is needed for apoptosis. Without changes in cristae structure, the cell would be unable to complete apoptosis (Cogliati *et al.*, 2013).

Balancing the opposing processes of fusion and fission is a delicate act. Disrupted, it can lead to mitochondrial dysfunction and disease (Baker, Patel and Khacho, 2019). For example, Chen *et al.* (2015) found that mice lacking MFF develop cardiomyopathy and do not survive. These mutant mice had decreased mitochondrial respiration and electron transport chain activity. However, when they introduced a mutation for MFN1, the mice were rescued (to a certain degree) and survived for longer (Chen *et al.*, 2015). Mutations or loss of any of the proteins mentioned can lead to various mitochondrial disorders such as dominant optic atrophy 1 (defects in OPA1), fatal infantile encephalomyopathy (defects in DRP1 or MFF), Parkinson's disease type 2 (defects in *PARK2*) and many others (Area-Gomez and Schon, 2014).

Changes in morphology affect and are affected by changes in energy production. Nutrient availability in the cell affects the balance of fusion and fission. When starved, mitochondria fuse to increase ATP production, while mitochondria fragment when the cell has excess nutrients (Tondera *et al.*, 2009; Liesa and Shirihai, 2013). Cristae remodelling affects mitochondrial oxidative phosphorylation by changing the structures of ETC complexes and super complexes (Cogliati, Enriquez and Scorrano, 2016; Baker, Patel and Khacho, 2019). Fusion and cristae remodelling can also increase ATP production when nutrients are low to sustain the cell's energy demands (Cogliati, Enriquez and Scorrano, 2016).

1.5. Mitochondrial dysfunction is implicated in ASD

There is increasing evidence that mitochondrial dysfunction is associated with ASD. A higher percentage of mitochondrial disease in the ASD population compared to the total population, demonstrates this. Rossignol and Frye's (2012) meta-analysis estimated that the prevalence of mitochondrial disease in the ASD population is 5% compared to 0.01% in the general population. Other studies have given even higher estimates, such as 7.2% and 8% (Oliveira *et al.*, 2005; Haas, 2010). Patients with ASD regularly have mitochondrial biochemical, genetic and physiological abnormalities compared to controls (Siddiqui, Elwell and Johnson, 2016; Griffiths and Levy, 2017).

Differences in gene or protein expression and activities of ETC complexes point towards dysregulation of energy metabolism in ASD groups. Reduced levels of complex I, III and V in both brain and skin tissue occur most frequently in ASD patients compared to controls (Filiano *et al.*, 2002; Weissman *et al.*, 2008; Gu *et al.*, 2013). Weismann *et al*. (2008) found 64% and 20% deficiencies in complexes I and III, respectively, while Gu *et al.* (2013) found complex I, III and V were reduced by 43%, 29% and 43%, respectively, with 14% of their ASD patients having reductions in all complexes. ASD brain tissue also displays reduced gene expression of complex I, III, IV and V subunits (Anitha *et al.*, 2013).

Changes in metabolite levels are also seen in ASD groups compared to controls. Increases in lactate and pyruvate levels indicate changes in mitochondrial function in ASD patients (Haas, 2010; Rossignol and Frye, 2012). Metabolomics data from urine samples showed mitochondrial metabolites were elevated in the ASD individuals. This was supported by differential methylation of genes linked to mitochondrial metabolism (Stathopoulos *et al.*, 2020). ASD individuals have also shown reduced expression for genes involved in mitochondrial localisation and protein transport (Anitha *et al.*, 2012). Oliveira *et al*. (2005) diagnosed specific ASD patients with mitochondrial respiratory chain disorder. Differences in MT-DNA levels show evidence of dysfunction. Differences in MT-DNA levels imply different levels of ETC complex proteins and other mitochondrial proteins (Gu *et al.*, 2013; Carrasco *et al.*, 2019), although these differences are not found in all studies (Oliveira *et al.*, 2005; Tang *et al.*, 2013).

There are two opposing viewpoints on mitochondrial dysfunction in the ASD population. One viewpoint is that mitochondrial dysfunction affects a sub-population of those diagnosed with ASD, while the other is that most ASD individuals have mitochondrial dysfunction at different severity levels (Haas, 2010; Rossignol and Frye, 2012). Most individuals with ASD present with co-morbidities such as epilepsy and gastrointestinal dysfunction, proving that ASD can affect multiple systems in the body (Weissman *et al.*, 2008; Frye and Rossignol, 2011). However, Weismann *et al.* (2008) note that their ASD patients with mitochondrial dysfunction have other distinct characteristics not found in the general ASD population. These range from developmental issues such as an increased occurrence of regression to muscular symptoms of excessive fatigability (Weissman *et al.*, 2008). This would point to ASD and mitochondrial dysfunction individuals being part of a separate group. However, clinicians note that mitochondrial dysfunction is difficult to diagnose as changes in lactate levels and other markers might not be seen in test results (Haas, 2010; Rossignol and Frye, 2012). Additionally, clinicians do not regularly test for mitochondrial dysfunction in ASD individuals (Oliveira *et al.*, 2005). Because of this, mitochondrial dysfunction may occur more frequently in the ASD population than estimated and could instead exist on a spectrum of severity.

1.6. Mitochondrial dynamics are associated with ASD

Although researchers now study mitochondrial dysfunction associations with ASD more widely, few studies examine the role mitochondrial dynamics and morphology play in the disorder. Even fewer studies examine the gene or protein expression of mitochondrial dynamics factors and visualise mitochondrial morphology in ASD individuals. As a result, this specific area of research has been understudied, and the role that mitochondrial dynamics play in ASD lacks clarity. Furthermore, when studies do include mitochondrial dynamics factors and/or morphology these are usually secondary results to support differences found in ETC complexes or other mitochondrial pathways.

Anitha *et al.* (2012) and Tang *et al.* (2013) used post-mortem brains from individuals with ASD to examine mitochondrial dysfunction and abnormal mitochondrial dynamics. Anitha *et al*. (2012) examined gene expression levels and found a significant decrease in *MFN2* expression in the anterior cingulate gyrus region. Tang *et al.* (2013) found differences in protein expression in the brain samples from patients aged between two and nine years. Fusion

proteins MFN1, MFN2 and OPA1 had decreased expression, while fission proteins DRP1 and FIS1 had increased expression levels.

Carrasco *et al.* (2019), Pecorelli *et al*. (2020) and Stathopoulos *et al*. (2020) used non-neurological cells from oral mucosa samples, skin biopsies and buccal swabs in their studies. Carrasco *et al*. (2019) found significantly increased gene expression of *MFN2* and increasing trends of *MFN1*, *OPA1*, *DRP1* and *FIS1*. Pecorelli *et al*. (2020) examined mRNA and protein levels of fusion and fission factors with slightly differing results. There was a significant increase in the gene expression of *MFN1*, *MFN2*, *DRP1*, *FIS1* and PINK1 and a significant decrease in Parkin. However, significant differences in protein expression only occurred for MFN1, FIS1 and PINK1 (increased) and DRP1 (decreased). When examining differential methylation in ASD individuals, Stathopoulos *et al*. (2020) had *STOML2* as their topmost differentially methylated gene. This suggested that *STOML2* expression differed between ASD individuals and controls, implying that fusion was altered in ASD individuals.

Weismann *et al*. (2008) and Filiano *et al.* (2002) found mitochondrial shape abnormalities in four out of 25 ASD individuals and three out of four ASD individuals, respectively, but did not go into more detail. Pecorelli *et al*. (2020) used electron microscopy to visualise mitochondria and observed an increase in interconnected mitochondria and swelled cristae compared to control cells.

In the research mentioned above, changes in mitochondrial function and dynamics differed between the studies. This could be explained by the different cell types used, which ranged from brain tissue to buccal samples. Post-mortem brain tissue samples are difficult to obtain, and only non-neurological samples such as buccal cells, blood samples and skin fibroblasts can be collected from living participants. Because of this, the different cell types used in these studies could explain the differences in directionality. Fission seems to be favoured over fusion in brain tissue samples, although these studies only concluded that mitochondrial dynamics differ between ASD and controls (Anitha *et al.*, 2013; Tang *et al.*, 2013). Non-neurological sample studies have found fusion to be favoured over fission (Carrasco *et al.*, 2019; Pecorelli *et al.*, 2020), with others only mentioning that there were differences (Filiano *et al.*, 2002; Weissman *et al.*, 2008). Although the direction of fusion and fission differs between these studies, they all demonstrate that differences in mitochondrial fusion and fission between ASD individuals and controls are consistent across different cell types.

1.7. Limitations of ASD studies

Studies researching the association of ASD with mitochondrial function have a variety of limitations. The sample sizes of case and control groups in studies are the most obvious limitation (Rossignol and Frye, 2012). Four studies that link changes in mitochondrial dynamics to ASD had 20 or fewer samples in the ASD group (Anitha *et al.*, 2012; Tang *et al.*, 2013; Carrasco *et al.*, 2019; Pecorelli *et al.*, 2020). Examining all the studies mentioned in this review which studied mitochondrial function and ASD, the sample size ranged from 8-69 ASD participants, and the median number of participants was 13. As these studies have small sample sizes, conclusions about ASD's relationship to mitochondrial dysfunction might not apply to the whole ASD population.

The method of ASD diagnosis also varies between studies (Frye and Rossignol, 2011). Many research papers rely on a previous diagnosis of the individual by other clinicians who use numerous diagnostic methods (Weissman *et al.*, 2008; Carrasco *et al.*, 2019; Pecorelli *et al.*, 2020). Some researchers confirm the clinical ASD diagnosis using a "research-standard" ASD assessment before including them in their ASD study group (Oliveira *et al.*, 2005; Stathopoulos *et al.*, 2020). Additionally, many studies do not specify if the control individuals were assessed for ASD characteristics before being included in the control group. This could lead to individuals with an incorrect ASD diagnosis being included in the case group or individuals showcasing ASD traits in the control group. Variability within the groups would influence the outcomes of the experiments and could cause inconclusive results.

The diagnosis of mitochondrial dysfunction is also a limitation of these studies (Haas, 2010; Frye and Rossignol, 2011). Definitive proof of mitochondrial dysfunction usually requires a biopsy from the individual but this is an invasive procedure, and most participants do not consent to this. For example, in this study carried out by Oliveira *et al*. (2005) only 11 participants consented to skin biopsies. Although only 14 participants showed increased lactate levels, other participants (of the total group of 69 ASD individuals) may have had mitochondrial dysfunction, which would only be apparent after a skin biopsy.

ASD individuals can display co-morbidities such as epilepsy and seizures (Frye and Rossignol, 2011). These co-morbidities negatively impact these studies. Sometimes ASD patients are excluded if they present with any neurological co-morbidities, thus decreasing the sample size

(Oliveira *et al.*, 2005). At other times these individuals are still included but this creates a confounding factor as the co-morbidities might be responsible for any found mitochondrial dysfunction rather than ASD (Weissman *et al.*, 2008).

ASD is a neurodevelopmental disorder, meaning that brain tissue or neuronal cells are the best candidates. However, retrieving brain tissue samples from living individuals is impossible, leading to most studies using other tissues such as skeletal muscle, fibroblasts or blood/oral mucosa cells. These studies assume that factors affecting mitochondria in these cell types will affect neuronal cells in the same way. This may not be true as mitochondrial function and morphology can differ between cell types (Chang and Reynolds, 2006).

Although these limitations exist in ASD studies, findings of mitochondrial dysfunction in ASD are consistent across multiple studies examining different populations. The overall conclusions reached in ASD studies still support the association between mitochondrial dysfunction and ASD. Hopefully, as ASD research continues to grow, the impact of these limitations will reduce.

1.8. Conclusion

The association between mitochondrial dysfunction and ASD has been well established in current literature (Citrigno *et al.*, 2020; Balachandar *et al.*, 2021; Frye *et al.*, 2021). As neurons are particularly vulnerable to mitochondrial damage and dysfunction, the role of mitochondria in ASD as a neurodevelopmental disorder is no surprise. The presence of mitochondrial dysfunction in other neurological disorders aside from ASD further promotes the idea that mitochondria play an important role in the brain.

The primary functions of mitochondria are widely known and garner the most attention when examining mitochondrial dysfunction in ASD. Defects in ETC complexes have been studied multiple times, and changes in primary mitochondrial pathways have also been found. However, research examining the role of mitochondrial dynamics and subsequently morphology in ASD remains underrepresented.

Mitochondrial dynamics involves many key factors regulating fusion, fission and cristae structure. These include MFN1, MFN2, OPA1 and STOML2 in fusion; DRP1, Mff, FIS1, MiD49 and MiD51 in fission; OPA1, MiD49 and MiD51 in cristae structure and the ER. The importance

of these factors is highlighted in their effects on mitochondrial morphology and function when their protein expression levels are changed and by the diseases caused by mutations in these genes. The few studies which do examine mitochondrial dynamics in ASD provide promising results that changes in mitochondrial dynamics are associated with ASD. Therefore, by continuing to look for changes in morphological factors and visualising mitochondrial morphology in ASD individuals, the role of mitochondrial dynamics and morphology in ASD can be established.

1.9. Aims and objectives

This thesis tests the hypothesis that sodium propionate results in mitochondrial morphological changes, and that these changes in mitochondrial dynamics play a role in ASD aetiology. The overarching aim of the thesis is to investigate the relationship between mitochondrial dysfunction and ASD, specifically the role of mitochondrial dynamics. This will be carried out using a neuronal-like SH-SY5Y cell culture model and will be supported by findings from a South African cohort study. The project is broken down into the following aims and objectives as outlined in Figure 2:

Aim 1:

To recapitulate an ASD/mitochondrial dysfunction model using a neuronal cell line.

i. Treat SHSY-5Y neuronal-like cells with sodium propionate (NaP) at a range of concentrations to induce mitochondrial dysfunction.
ii. Cell viability at the different NaP concentrations will be tested using an MTT assay.
iii. Mitochondrial stress will be characterised using an ATP assay, with rotenone as a positive control.

Aim 2:

To investigate if mitochondrial dynamics and morphology are altered during mitochondrial stress.

i. Mitochondrial morphology will be examined using transmission electron microscopy (TEM) qualitatively and quantitatively.

Aim 3:

To investigate if changes in mitochondrial morphology are supported by changes in gene expression associated with mitochondrial dysfunction and dynamics.

i. Mitochondrial copy number will be quantified using gene expression of *MT-ND1* and *B2M*.
ii. The expression of *STOML2*, the mitochondrial gene involved in fusion, will be quantified.

Aim 4:

To support findings from the cell culture model, differential methylation of key mitochondrial genes will be examined in a wider South African ASD cohort.

i. Key mitochondrial genes will be selected for further targeted next-generation bisulfite sequencing (tNGBS) analysis. Key fusion and fission genes will be analysed for differential methylation between the ASD and control groups.

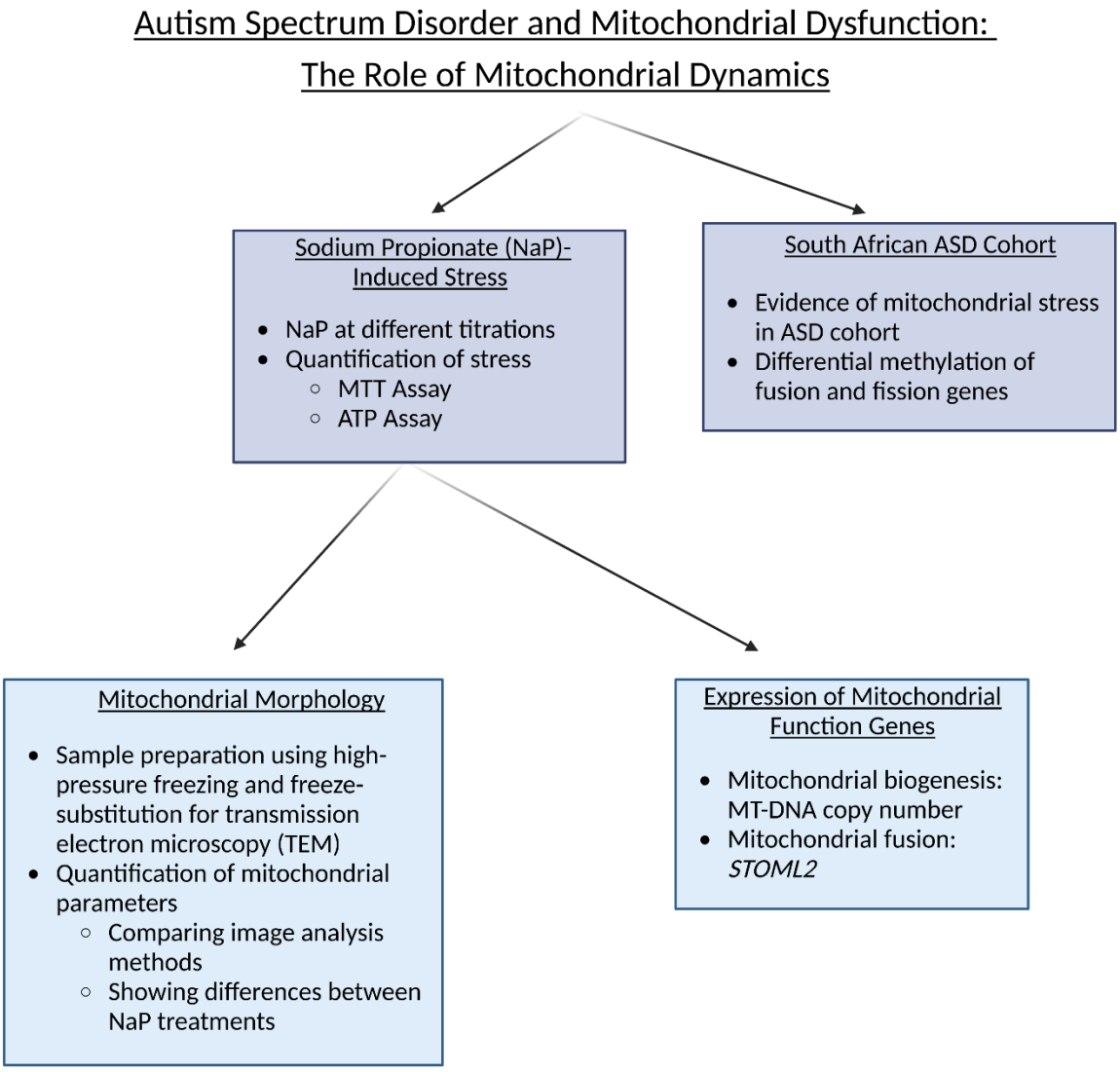

FIGURE 2: Overview of the project's workflow. Figure made in BioRender.com

Chapter 2

Sodium Propionate-Induced Mitochondrial Stress in a SH-SY5Y Cell Model

2.1. Introduction

Cell models provide a useful system to investigate the numerous biological pathways associated with ASD. NaP or other propionic acid (PPA) derivatives have been used in previous studies to recapitulate an ASD-like phenotype in rat and cell models (El-Ansary, Bacha and Kotb, 2012; Frye *et al.*, 2016; Khera *et al.*, 2022). Moreover, NaP directly recapitulates molecular disruptions previously reported by our group in a South African ASD cohort where ASD was associated with significant differential methylation of Propionyl-CoA Carboxylase Subunit Beta (*PCCB*) (Stathopoulos *et al.*, 2020). Differential methylation of *PCCB* can alter its gene expression resulting in changes to the function or activity of propionyl-CoA carboxylase (PCC) (Jin and Liu, 2018; Ehrlich, 2019). Disruptions to PCC function prevent the breakdown of PPA, causing it to accumulate to toxic levels. For example, mitochondrial dysfunction caused by toxic levels of PPA is observed in metabolic disorders caused by mutations in PCC, like propionic acidemia (Desviat *et al.*, 2004). Treating SH-SY5Y cells with NaP recapitulates this metabolic phenotype by adding propionate to the cells, mimicking the same result of increased levels of PPA leading to metabolic/mitochondrial dysfunction. Disruptions to mitochondrial metabolism were confirmed by measuring cell viability and ATP production after NaP treatment.

Several genes could have been chosen to measure RNA expression to investigate whether this NaP-induced mitochondrial dysfunction in SH-SY5Y cells affects mitochondrial fusion and fission. The key genes involved in fusion are *MFN1*, *MFN2*, *OPA1* and *STOML2,* while the key genes in fission are *DRP1*, *FIS1* and *MFF*. For this study, *STOML2*, implicated in fusion and hyperfusion, was selected to measure gene expression. This is because *STOML2* was the most differentially methylated gene between ASD and control groups in a previous study conducted by our research group (Stathopoulos *et al.*, 2020). *STOML2* plays an essential role in fusion and hyperfusion by maintaining the long isoforms of OPA1 responsible for fusion of the inner

mitochondrial membrane (Tondera *et al.*, 2009). Due to its essential role in fusion and its connection to previous research, it was considered the gene best suited to indicate if fusion or fission was favoured in this model.

RNA or protein expression helps give insight into the role of specific target genes in response to mitochondrial stress. However, this approach is limited in isolation, as differential expression of mitochondrial dynamics genes is an indirect proxy for changes in mitochondrial morphology. The morphology of mitochondria can be directly visualised by transmission electron microscopy (TEM), which shows cell ultrastructure and gives a more detailed examination of morphological parameters. TEM is an ideal tool as it provides an overview of the whole mitochondria and directly visualises its shape and morphology as opposed to only relying on gene and/or protein expression (Winey *et al.*, 2014).

Conventional EM sample preparation uses glutaraldehyde and osmium tetroxide to fix cells before dehydrating the samples using ethanol and/or acetone. These methods can lead to artefacts and distorted cellular membranes and organelles (Winey *et al.*, 2014). Previous research conducted in our research group using these conventional methods led to inadequate images due to the disruption of cellular membranes and distorted mitochondrial morphology in controls (data not shown). On the other hand, the high-pressure freezing and freeze substitution methods used in cryogenic sample preparation result in minimal changes to cellular structure, making it the ideal preparation method for TEM (Giddings, 2003; Hawes *et al.*, 2007). Therefore, cryogenic sample preservation or cryo-fixation was used to better preserve cellular ultrastructure.

However, examining morphology qualitatively is often insufficient to make firm conclusions as individual images can be misleading. To utilise the full potential of TEM images, cell and organelle parameters such as area and perimeter should be measured to quantify any differences between cases and controls. Numerous software programmes can be used to analyse mitochondrial parameters, such as Fiji/ImageJ, CellProfiler and MATLAB and various pre-processing methods can be used to improve the images before processing and quantification (Chu *et al.*, 2022). The ideal method must be reproducible and time efficient as TEM analysis can involve processing hundreds of images. Additionally, it needs to be as accurate as possible in selecting or outlining the objects of interest, in this case mitochondria,

compared to the raw images. In this study, three different analysis methods were tested in a pilot study to determine which one would best address the research question.

Determining the pre-processing and analysis methods is only the first step in TEM analysis. The second is determining which mitochondrial parameters to measure during the analysis workflow. There is no single specific parameter that distinguishes differences in mitochondrial morphology. Instead, it is more important to find differences across multiple parameters to show changes in morphology between cases and controls confidently. After reviewing the literature, nine parameters were chosen to quantify mitochondrial morphology in this study (Merrill, Flippo and Strack, 2017; Collins *et al.*, 2021; Lam *et al.*, 2021). Mitochondria undergoing fusion would be characterised by elongated shapes with greater area and perimeter as multiple mitochondria would have joined together. On the other hand, mitochondrial fission is characterised by smaller mitochondria (decreased area and perimeter) which are more spherical (Yu *et al.*, 2020). This is because fission is the splitting of one mitochondrion into many, essentially dividing up the mitochondrial volume into multiple new mitochondria. Examining mitochondrial morphology using visual parameters and gene expression levels demonstrates how two different methods can be used to complement one another.

In this chapter, a cell model system recapitulating ASD-associated mitochondrial dysfunction was set up using SH-SY5Y neuronal-like cells treated with NaP. The role of mitochondrial dynamics in this mitochondrial dysfunction was examined by measuring MT-DNA copy number, ATP levels, gene expression of *STOML2* and quantifying morphological parameters visualised using TEM. Any changes in the expression of these genes, activities or morphological parameters could point to changes in the balance between fusion and fission in this model system. This would indicate that dysfunction of these mitochondrial dynamics pathways could be associated with ASD and contribute to ASD's association with mitochondrial dysfunction.

2.2. Materials and methods

2.2.1. Mammalian tissue culture

The human neuroblastoma cell line SH-SY5Y (ECACC 94030304-1VL) was purchased from Sigma-Aldrich. Cells were grown in 25cm^2 flasks in Dulbecco's Modified Eagle Medium /

Nutrient Mixture F-12 (DMEM/F-12) with L-Glutamine (SC09411, ScienCell) supplemented with 20% Foetal Bovine Serum (FBS) (10493106,ThermoFisher Scientific) and 1% Penicillin-Streptomycin (P4333-20ML,Sigma-Aldrich) at 37°C and 5% CO_2. Cells were sub-cultured at 80% confluency using 0.05% Trypsin-EDTA (15400054, ThermoFisher Scientific), centrifuged at 300 rpm (Hermle Z383 centrifuge, rotor number 221.08, max speed 4500 rpm, serial number 30110022) and seeded at approximately 7 x 10^5 cells/ml. All experiments were done on SH-SY5Y cells between passages 19–22.

2.2.2. Sodium propionate (NaP) treatment

Sodium propionate (CAS number 137-40-6, chemical formula $C_3H_5NaO_2$, hereafter referred to as NaP) (P5436-100G, Sigma-Aldrich) powder was dissolved in warm MilliQ water to a concentration of 1M and stored at 4°C. This NaP solution was diluted in serum-free media (DMEM/F-12 with L-Glutamine without FBS) to treatment concentrations of 1.5mM, 3mM and 5mM on the day of treatment.

2.2.3. MTT assay

The Thiazolyl Blue Tetrazolium Bromide or MTT assay (M5655-500MG, Sigma-Aldrich) was used according to the manufacturer's instructions. The SH-SY5Y cells were seeded in a clear 96-well plate at 8 x 10^5 cells/ml in 100µl of serum-free media per well and allowed to adhere for 24 hours. The media was removed, and cells were washed with 1x phosphate-buffered saline (PBS) before NaP treatment. NaP concentrations ranged from 1mM to 9mM for 24 hours. The MTT powder was dissolved in MilliQ water for a stock solution of 5mg/ml and diluted in serum-free media to a working solution of 0.5mg/ml. The NaP treatment solutions were removed from the cell, and the cells were washed with 1x PBS before adding 100µl of MTT reagent (5mg/ml) to each well. Plates were wrapped in aluminium foil and incubated for three hours at 37°C. The MTT reagent was removed and 100µl of tissue culture grade dimethyl sulfoxide (DMSO) was added to each well. The solutions were mixed by shaking the plate for 10 minutes to dissolve the purple formazan crystals before measuring absorbance at 570nm. Each treatment was performed in triplicate per plate and across seven biological repeats. For the assay to be accurate, absorbance readings were required to be above 0.5 AU, leading to two assays being excluded. Cell viability for each NaP treatment was calculated as a percentage of the control (no NaP treatment).

2.2.4. ATP assay

ATP concentrations were calculated using the Luminescent ATP Detection Assay Kit (AB113849, Abcam). The SH-SY5Y cells were plated at 2.4 x 10^4 cells/100µl in a white 96-well plate. After 24 hours, the cells were treated with NaP treatment solutions (1.5mM, 3mM, 5mM) or Rotenone (5µM) for 24 hours. Following treatment, the cells were washed with 1x PBS before performing the assay according to the manufacturer's instructions. ATP concentration was calculated using the standard curve for each plate, and the percentage of ATP for each treatment was calculated relative to the average ATP for the control. Standard curves were performed in duplicate and each treatment was performed in triplicate per plate and across two biological repeats.

2.2.5. DNA extraction

DNA was extracted from the SH-SY5Y cells using a standard protocol (Aljanabi and Martinez, 1997) with the following modifications: The cells were grown in a six-well plate at a density of 0.3 x 10^6 cells/ml for 24 hours before treatment. After treatment, the cells were washed with 1x PBS before adding 500µl lysis buffer (Saline/EDTA; 10mM EDTA, 40mM NaCl; pH8) and incubating for five minutes. The cells were scraped from the wells, and samples were transferred to Eppendorf tubes before adding 50µl of 10% SDS and 20µl proteinase K (20mg/ml). Samples were mixed and incubated for two hours at 56°C before adding 225µl of saturated NaCl (6M), mixing and incubating at room temperature for one hour. Following this, samples were centrifuged at 10 000 rpm (Eppendorf – Netheler – Hinz 5426 centrifuge , max speed 13200 rpm, serial number 542601273) for 10 minutes at room temperature. The supernatant was transferred to new Eppendorf tubes, and the pellets were discarded. Centrifugation was repeated before adding 1ml isopropanol to each tube and storing the samples overnight at -20°C. Next, samples were centrifuged at 10 000 rpm for 20 minutes, and the supernatants were discarded. The pellets were washed by adding 1ml of 70% ethanol and mixing, followed by centrifuging at 10 000 rpm for 20 minutes. The supernatants were discarded, and the pellets were air-dried before being resuspended in 30µl TE buffer (10mM Tris pH8; 1mM EDTA pH8) and stored at -20°C. The quantity and quality of the samples were checked using the NanoDrop ND-1000 UV-Vis Spectrophotometer.

2.2.6. RNA extraction

RNA was extracted from SH-SY5Y cells using the Quick-RNA™ Miniprep (ZR R1055, Zymo Research) quick protocol with minor modifications. SH-SY5Y cells were grown at a density of 0.3 x 10^6 cells/ml in six-well plates for 24 hours before treatment. After treatment, 300µl of RNA lysis buffer was added to each well, and the cells were scraped from the well. Samples were transferred to Eppendorf tubes, and the protocol was followed according to the manufacturer's instructions. For each sample, RNA was eluted in 30µl DNase/RNase-free water and centrifuged at 16 000 x g for two minutes. RNA samples were stored at -80°C. The quantity and quality of the samples were checked using the NanoDrop ND-1000 UV-Vis Spectrophotometer.

2.2.7. cDNA synthesis

For real-time quantitative PCR (RT-qPCR), cDNA was synthesised using the Tetro™ cDNA Synthesis Kit (BIO-65043, Meridian Bioscience) according to the kit instructions. Random Hexamer primers and a total RNA amount of 850ng were used in each reaction. The cDNA samples were stored at -80°C for up to a week.

2.2.8. Quantitative real-time PCR

Mitochondrial DNA (MT-DNA) copy number and expression of *STOML2* were measured using RT-qPCR. The primer sets used *MT-ND1* for MT-DNA copy number (Grady *et al.*, 2014) and *STOML2* for *STOML2* expression (Hu *et al.*, 2018), and both primer sets were normalised to *B2M* (Grady *et al.*, 2014) (Table S1). Primers were purchased from inqaba biotec™. Luna® Universal qPCR Master Mix (NEB M3003L, New England BioLabs) was used according to the manufacturer's instructions, and the master mix included 5µl LUNA Taq polymerase, 0.5µl forward and reverse primers, 1µl (2ng/µl) DNA (MT-DNA copy number) or 0.8µl cDNA synthesised from 850ng RNA per cDNA reaction (*STOML2*). PCR-grade water was added to a final volume of 10µl per reaction. Rotor-Gene Q 6-plex (QIAGEN RG – Serial Number: R0618110) was used to perform the RT-qPCR with the following cycling conditions: MT-DNA copy number: 95°C 10 minutes (1x cycle) followed by 95°C for 5 seconds and 60°C for 30 seconds (40x cycles); *STOML2*: 95°C 10 minutes (1x cycle) followed by 95°C for 15 seconds and 62°C for 30 seconds (40x cycles). Data was analysed using Rotor-Gene Q Software 2.3.5. All samples were amplified in triplicate, and standard curves were generated for each primer set

using DNA or cDNA pools. Standard curve efficiencies and R^2 values were between 0.83-1.14 and 0.85-0.99, respectively. The standard deviation for the cycling threshold (Ct) values for the technical repeats was below 0.42. MT-DNA copy number and *STOML2* expression were calculated using the delta delta Ct method ($2^{-\text{delta delta Ct}}$) (Livak and Schmittgen, 2001). Samples were analysed from three biological repeats.

2.2.9. Transmission electron microscopy

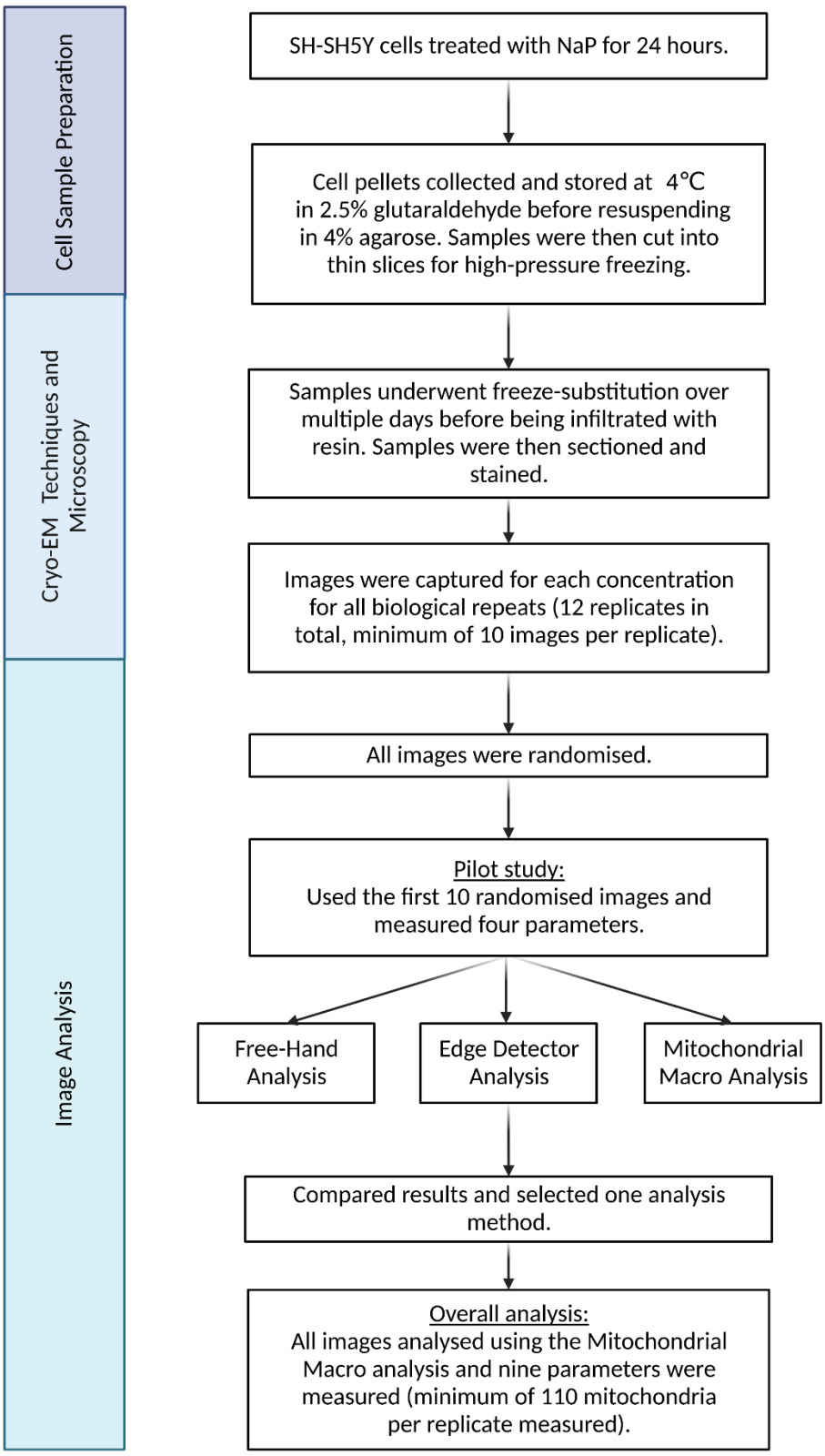

FIGURE 3: Overview of the transmission electron microscopy workflow. Figure made in BioRender.com

An overview of the TEM methods workflow is described in Figure 3 and the methods are described in more detail in the following sub-sections.

2.2.9.1. Cell sample preparation

The SH-SY5Y cells were seeded at 5.5 x 10^5 cells/ml in 25cm^2 flasks and grown for 24 hours. NaP treatments (1.5mM, 3mM and 5mM) were added to the flasks before incubating for 24 hours. Routine mammalian tissue sub-culturing protocol (as described in section 2.2.1) was followed to collect cell pellets. Pellets were resuspended in 100µl 2.5% glutaraldehyde, 1x PBS transferred to Eppendorf tubes and stored at 4°C. Samples were centrifuged for 10 000 x g for 30 seconds to pellet the cells and remove the 2.5% glutaraldehyde, 1x PBS solution. The pellet was then resuspended in 4% agarose gel made with distilled water (1:1 ratio agarose to pellet volume) and allowed to set. Samples were then sectioned into thin slices using a scalpel.

2.2.9.2. High-pressure freezing, freeze-substitution, resin infiltration and staining

Agarose slices were placed onto grids on a flat planchette and covered with 1-hexadecene before high-pressure freezing. Samples were removed and transferred for freeze substitution. Samples were freeze substituted at -90°C for 24 hours in 100% dry acetone. This was followed by raising the temperature to -80°C and adding a solution of 1% osmium tetroxide and 0.1% glutaraldehyde. Samples were kept at -80 °C for 24 hours. Following this, the temperature was gradually increased to room temperature over multiple days: from -80°C to -50°C for 24 hours, to -30°C for 24 hours, to -10°C for 24 hours and finally to room temperature. Samples were infiltrated with resin, and ultrathin sections (~100nm) were cut with a Leica Reichert UltracutS Ultramicrotome (Leica Microsystems). Sections were stained with 2% uranyl acetate and lead citrate (also known as Reynold's stain) (Reynolds, 1963).

2.2.9.3. Microscopy

Samples were viewed using a FEI Tecnai 20 transmission electron microscope (ThermoFisher (formerly FEI), Eindhoven, Netherlands) operating at 200kV (Lab6 emitter) and fitted with a Tridiem energy filter using a Gatan CCD camera (Gatan, UK). Images were captured at x3600 magnification, and scale bars were added to all images.

2.2.10. TEM image analysis

SH-SY5Y cells were treated with three concentrations of NaP (1.5mM, 3mM and 5mM) and controls (no NaP) and were prepared over three biological repeats (12 replicates in total). A minimum of 10 images was captured per replicate, and only whole cells (where the complete cell membrane is captured) were analysed, with a total of 144 images being included in the analysis. Representative images of NaP treatment and control samples are included in the supplementary material (Figure S1).

2.2.10.1. Pilot study

A pilot study was performed to determine the most suitable analysis method to measure mitochondrial parameters using Fiji/ImageJ (Schindelin *et al.*, 2012). All images across the 12 replicates were randomised, and the first 10 randomised images were used in the pilot study. There is no standard analysis method to measure mitochondrial morphology. After reviewing the literature, three image analysis methods were created based on a combination of analysis methods (Merrill, Flippo and Strack, 2017; Collins *et al.*, 2021; Lam *et al.*, 2021). The three methods of analysis were Free-Hand analysis, Edge Detector Macro analysis and Mitochondrial Macro analysis.

Free-Hand analysis used the drawing tool to manually outline mitochondria in the images. The Edge Detector Macro first applied a band filter to the image to remove noise. It then used the Canny Edge Detector plug-in for Fiji/ImageJ to detect and outline objects in the image. These outlined particles were then measured. The Mitochondrial Macro first subtracted the background from the original image to remove noise before applying a threshold to create a binary image. Masks of the detected objects were then created and measured. Before running the Edge Detector Macro and the Mitochondrial Macro, another macro, called the ROIBatchGen Macro, was used to select regions of interest (ROIs) in the image. ROIs were selected by outlining the areas containing mitochondria using the drawing tool and saving them to the ROI manager. This meant that when running the two analysis macros (Edge Detector Macro and Mitochondrial Macro), the program would not measure the entire image but only the ROIs that contained the mitochondria. This made the macros more time-efficient, and more specific as only the mitochondria in the cell were measured instead of all organelles being measured. The Edge Detector Macro, Mitochondrial Macro and ROIBatchGen Macro

were written by Dr Caron Jacobs, based at the University of Cape Town and the author. All macros are included in the supplementary materials.

In the pilot study, four parameters were measured: area, perimeter, circularity and aspect ratio. The average measurements (in pixels) for each parameter were compared across the three analysis methods to find out if the three methods gave the same results and were equally adequate analysis methods.

2.2.10.2. Image analysis

The pilot study revealed that not all the methods yielded the same results, so one analysis method needed to be chosen for the overall image analysis. The Mitochondrial Macro was chosen as the final analysis method for all images as it was the least labour intensive and provided the most accurate representation of the mitochondria, in relation to the objects measured. ROIs for all images were selected before running the Mitochondrial Macro. On average, 2 000 mitochondria were analysed for each NaP treatment, and approximately 8 200 mitochondria were analysed overall (data not shown). No mandatory parameters are needed to be measured to quantify differences in mitochondrial morphology. Given this, the nine parameters chosen were selected based on prior research that also aimed to investigate mitochondrial morphology, dynamics and function specifically (Merrill, Flippo and Strack, 2017; Collins *et al.*, 2021; Lam *et al.*, 2021). The parameters measured were area, area^2, form factor, area-weighted form factor, aspect ratio, perimeter, circularity, Feret's diameter and roundness. Equations for all parameters can be found in the supplementary materials (Figure S2).

2.2.11. Statistical analysis

Each data set was tested for normality using the Shapiro-Wilks test before assuming Gaussian distribution and equal standard deviations and proceeding with the analysis (unless otherwise stated). For data sets containing two samples, unpaired t-tests were performed with $p<0.05$ considered significant. For data sets containing more than two samples, one-way ANOVA (mean of treatments compared to controls) and Dunnett's test for multiple comparisons were used to determine significance ($p<0.05$). Correlation analysis was performed using Pearson's correlation, with $p<0.05$ considered significant. All statistical analyses and graphs were performed and generated using GraphPad Prism 9.4.0.

2.3. Results

2.3.1. Sodium propionate (NaP) alters mitochondrial function

The SH-SY5Y cells were first treated with 1mM – 9mM NaP for 24 hours to assess cell viability. Any significant changes in cell viability induced by NaP would negatively affect subsequent experiments as cell numbers would not be the same. The only significant decrease in cell viability was at 9mM NaP (Figure 4) using the MTT assay. This agrees with previous studies where high concentrations of PPA lead to increased oxidative stress and eventually apoptosis (El-Ansary, Bacha and Kotb, 2012). Due to these results, further experiments could use NaP at concentrations below 9mM to induce mild but not toxic mitochondrial stress without inducing cell death.

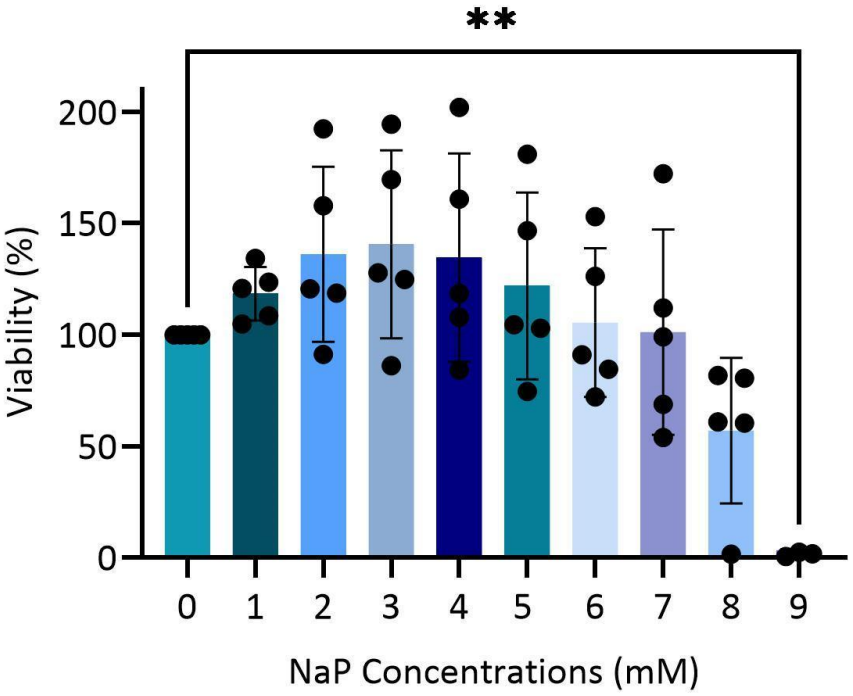

FIGURE 4: Cell viability is not affected by mild sodium propionate (NaP)-induced stress. SH-SY5Y cells were treated with NaP (1mM–9mM in 1mM increments) for 24 hours. Cell viability was measured using the MTT assay and viability was calculated as a percentage of the control. Significant differences were identified using one-way ANOVA (control compared to treatments) and Dunnett's test for multiple comparisons ($p<0.05$). Bars represent the mean percentage viability; error bars represent standard deviations. Data shown represents n=5 biological repeats, ** indicates $p<0.01$.

Changes in ATP levels occur during mitochondrial stress and can indicate mitochondrial dysfunction. To confirm that NaP induced mitochondrial stress, resulting in changes in mitochondrial function, ATP concentration in the SH-SY5Y cells was measured following NaP treatment. Rotenone treatment was used as a positive control as it is a known inhibitor of Complex I in the electron transport chain (Heinz *et al.*, 2017; Peng *et al.*, 2017). The cells were treated with 1.5mM, 3mM and 5mM NaP and 5µM rotenone for 24 hours. As expected, there was a significant decrease in ATP levels after rotenone treatment (Figure 5B). Conversely, NaP treatment increased ATP levels significantly at 3mM and 5mM (Figure 5A).

ATP is primarily derived from oxidative phosphorylation, and so any changes in mitochondrial function could increase or decrease ATP levels. These changes in ATP levels thus show that there may be alterations in mitochondrial function. Specifically, the increases in ATP may be an indication of increased mitochondrial biogenesis (Fu *et al.*, 2016; Vaarmann *et al.*, 2016).

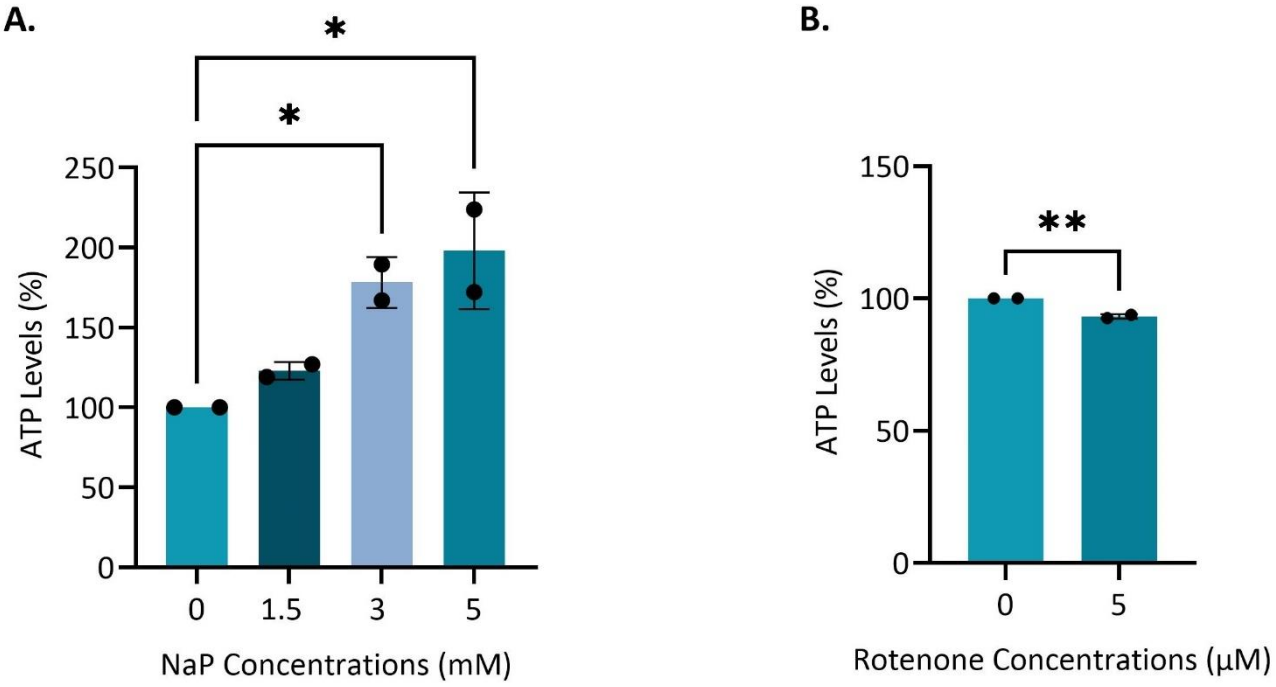

FIGURE 5: Sodium propionate (NaP) increases ATP levels. A. ATP concentration significantly increased in comparison to controls after 3mM and 5mM NaP treatment. **B.** ATP concentration significantly decreased after treatment with 5µM rotenone. SH-SY5Y cells were treated with NaP (1.5mM, 3mM and 5mM) and rotenone (5µM) as a positive control for 24 hours. ATP concentration (µM) was measured and the percentage of ATP compared to controls was calculated. Significant differences were identified using unpaired t-tests with equal variance (rotenone) or one-way ANOVA (control compared to treatments) and Dunnett's test for multiple comparisons (NaP) ($p<0.05$); significant differences for rotenone was identified using unpaired t-test with equal variance. Bars represent the mean percentage ATP; error bars represent standard deviations. Data shown represents n=2 biological repeats, * indicates $p<0.05$, ** indicates $p<0.01$.

2.3.2. Determining an analysis method for transmission electron microscopy: a pilot study

Three analysis methods (Free-Hand, Edge Detector Macro and Mitochondrial Macro) were used to quantify mitochondrial morphological parameters for a pilot group of images to determine the most suitable method for subsequent analysis. As all three analysis methods were analysing the same group of images, the hypothesis was that there should be no

differences in the parameters measured based on the analysis method. If this were the case, any analysis method could be chosen.

The pilot group consisted of images across all biological repeats and treatments and measured the following parameters: area, perimeter, circularity and aspect ratio. Four parameters were chosen from Fiji/ImageJ's standard shape descriptors to ensure that if there were any differences between the analysis methods they would be found, improving the reliability of the pilot study as opposed to only measuring one parameter. The two automated methods, Edge Detector Macro and Mitochondrial Macro, apply different pre-processing and processing methods to identify mitochondria before analysing the particles, whereas the Free-Hand method relies on the researcher to identify the outlines/edges of mitochondria.

A disadvantage of the Free-Hand analysis method is that it can differ between individuals as the researcher has to manually trace the outlines of the organelles. To account for this variance, a different researcher from our laboratory performed an additional Free-Hand analysis using the pilot images to compare the four parameters between the images. Pairwise comparison of the same image measured by the two researchers showed significant differences in perimeter, circularity and aspect ratio (data not shown). However, unpaired comparisons of all 10 images as a group measured by the two researchers showed no significant differences in any parameters (Figure S3). These results allowed it to be included as a potential candidate for an analysis method.

When comparing the parameters after using the three analysis methods, it was found that there were significant differences in area, perimeter, circularity and aspect ratio between Free-Hand, Edge Detector Macro and Mitochondrial Macro analyses (Figure 6). The Free-Hand analysis method and the Mitochondrial Macro method differed in area and perimeter (Figure 6A, B), while the Free-Hand analysis and the Edge Detector Macro analysis differed between perimeter, circularity and aspect ratio (Figure 6B, C, D). Mitochondrial Macro and Edge Detector Macro showed substantial differences between all four parameters. Despite the fact that they all used the same images, the differences in the processing of the images were significantly different enough to yield different results. The next step to determine which of

the three analysis methods was the most reproducible and preserved the most data from the raw image to the final processed image.

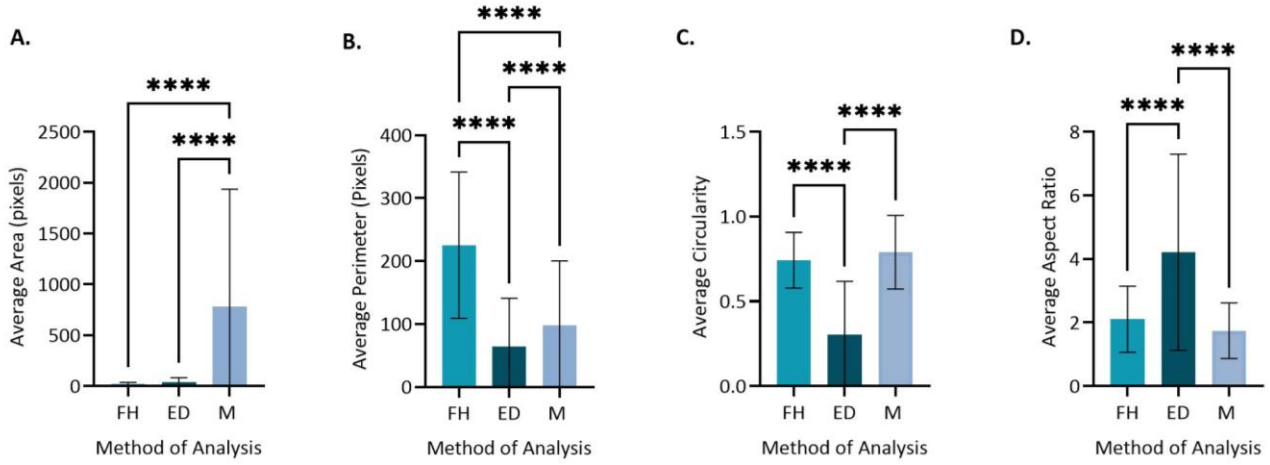

FIGURE 6: **Pilot study compares three methods of image analysis.** Three methods of analysis used were Free-Hand analysis (FH), Edge Detector Macro analysis (ED) and Mitochondrial Macro analysis (M), measuring four parameters: **A.** Average Area (pixels), **B.** Average Perimeter (pixels), **C.** Average Circularity and **D.** Average Aspect Ratio. The pilot study consisted of 10 randomised images across three biological repeats and controls, 1.5mM, 3mM and 5mM NaP treatments. Significant differences were identified using one-way ANOVA and Dunnett's test for multiple comparisons ($p<0.05$). Bars represent the mean parameter; error bars represent standard deviations. Data shown represents n=3 biological repeats, **** indicates $p<0.0001$.

To determine this, the raw image was compared to the final processed image across the 10 pilot images to see which analysis method most accurately outlined the mitochondria. The Edge Detector Macro analysis method showed a lot of background noise in the final processed image, as can be seen by the small lines surrounding the mitochondrion (Figure 7; B4). The macro outlined this background noise and included it in the measurements. This eliminated the Edge Detector Macro as a suitable analysis method.

The Free-Hand and Mitochondrial Macro analysis methods accurately outlined the mitochondrion compared to the original raw image and showed no background noise (Figure 7; A1 and A4; C1 and C4). The Free-Hand method manually outlined the mitochondrion (Figure

7; A4), while the Mitochondrial Macro processed the image to display the mitochondrion as a solid object in the ROI (Figure 7; C4).

However, the Free-Hand method was highly labour intensive as each mitochondrion had to be outlined manually. Across all 144 images, this could lead to inaccuracy. Additionally, as it was labour intensive it was also not time efficient. From this it was concluded that the Mitochondrial Macro method was the most suitable analysis method as it accurately outlined the mitochondrion and, as it was mostly automated, was the most time-efficient option.

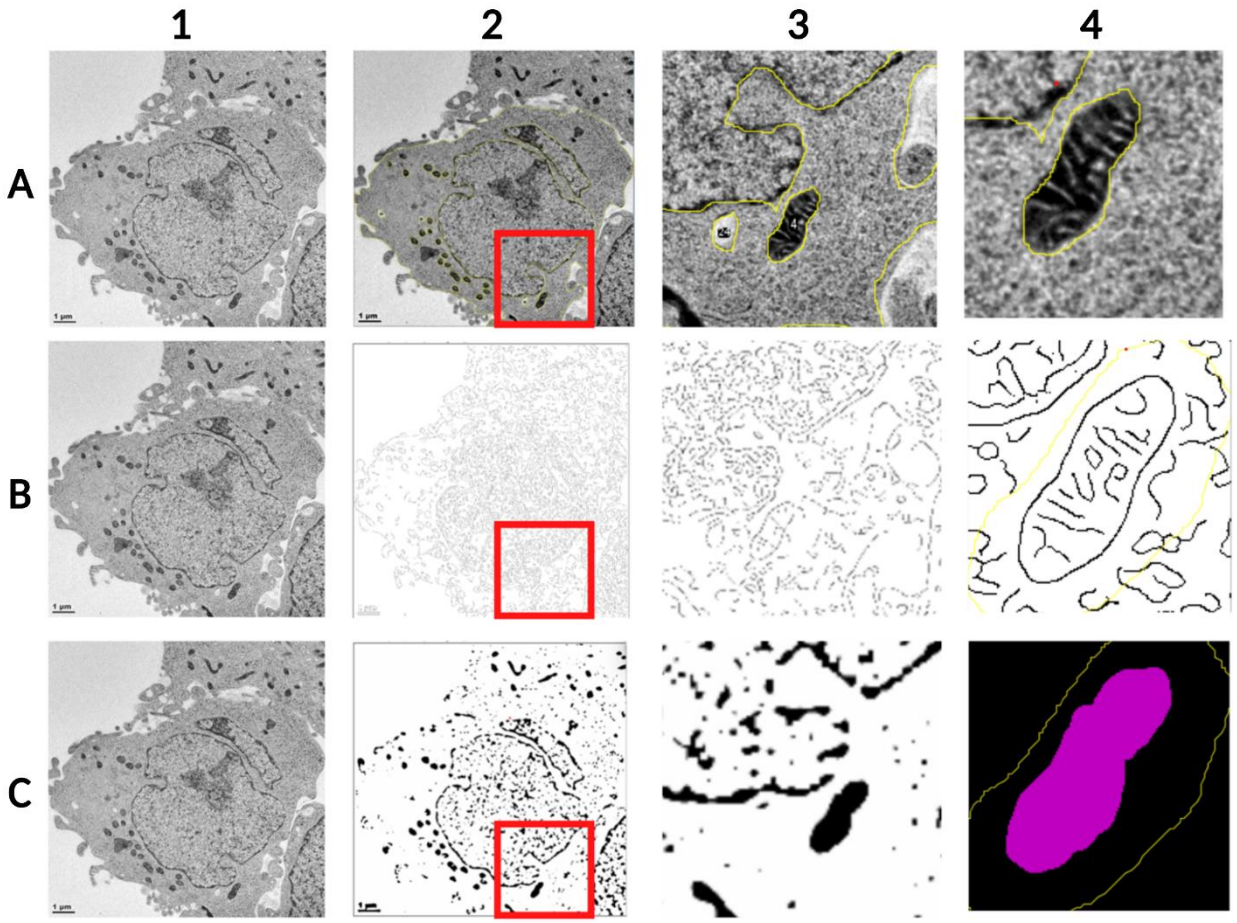

FIGURE 7: Comparison of raw image versus processed image of three analysis methods used in the pilot study for transmission electron microscopy (TEM) analysis. Rows A-C show the three different analysis methods. **A.** Free-Hand analysis, **B.** Edge Detector Macro analysis, **C.** Mitochondrial Macro analysis. Columns 1-4 are different steps in the analysis workflow. Columns **1** and **2** are images of the whole cell. Column **1** is the raw image before processing and Column **2** shows the image after processing for the macros in **B** and **C**. Columns **3** and **4** are zoomed in images to show one mitochondrion. The zoomed in area of the cell is outlined in red in column **2**. Column **4** shows how one mitochondrion looks at the last step in each analysis workflow in the final processed image. The yellow outline in column **4** is the region of interest (ROI) that is measured. These images represent 10 randomised images across three biological repeats and controls, 1.5mM, 3mM and 5mM NaP treatments that were used in the pilot study. Figure made in BioRender.com

2.3.3. Mitochondrial morphology under NaP-induced mitochondrial stress

The relationship between mitochondrial function and morphology has been well established and explored in several reviews (Mattson, Gleichmann and Cheng, 2008; Palmer *et al.*, 2011; Galloway, Lee and Yoon, 2012). Despite this, many studies that examine morphology only report qualitative findings and often use fluorescent microscopy. TEM provides an opportunity to observe the ultrastructure of mitochondria and have a more detailed examination of morphological parameters. The SH-SY5Y cells treated with three concentrations of NaP (1.5mM, 3mM, 5mM) underwent TEM preparation, high-pressure freezing and freeze substitution for TEM image analysis. Nine parameters were used to analyse mitochondrial structure, which were compared among the treatments. These parameters were: area, area^2, area-weighted form factor, form factor, aspect ratio, perimeter, circularity, Feret's diameter and roundness. Of the nine parameters, there were significant differences between treatments and control in five of them: area, perimeter, circularity form factor and Feret's diameter (Figure 8).

The area was significantly decreased in all treatment groups compared to controls (Figure 8A), perimeter and Feret's diameter were significantly decreased at 1.5mM and 5mM (Figure 8B, E) and form factor was significantly decreased at 5mM (Figure 8D). Circularity was the only parameter significantly increased at 5mM (Figure 8C). The decrease in area and perimeter and an increase in circularity indicate that cells treated with 5mM NaP have mitochondria that are not as elongated as those in control cells and are smaller and more circular. A decrease in Feret's diameter supports this as it independently shows that the longest distance between the edges of the particles (or a version of length) is decreasing. Whether these are existing mitochondria which are undergoing fission and becoming smaller and more circular or it is an increase in mitochondrial biogenesis with newly produced smaller mitochondria cannot be determined by TEM.

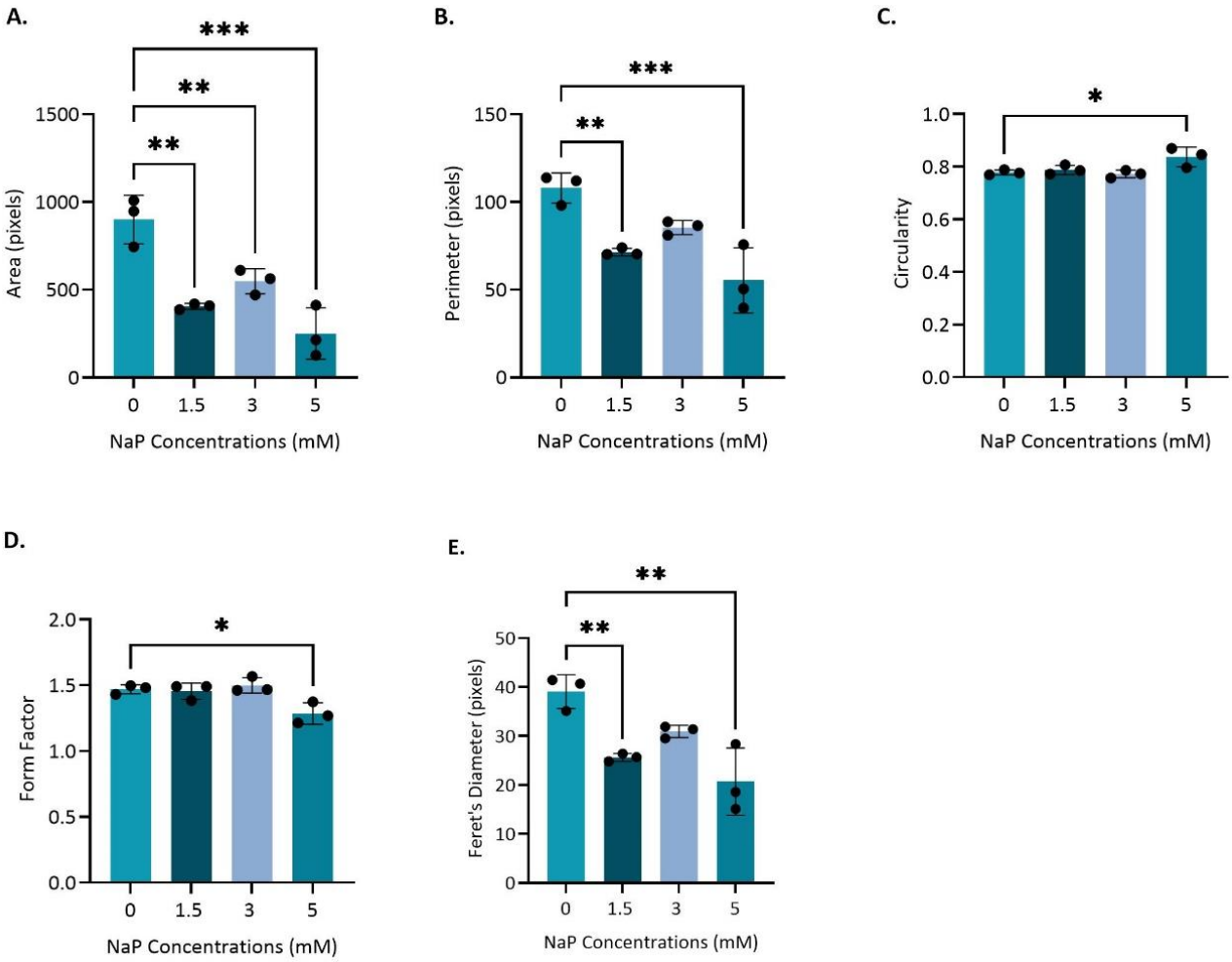

FIGURE 8: **Mitochondrial morphology is altered during mitochondrial stress.** SH-SY5Y cells treated with sodium propionate (NaP) for 24 hours underwent preparation for transmission electron microscopy (TEM) and results were analysed using Fiji/ImageJ. Five of the nine parameters showed significant differences between control (0mM NaP) and treated (1.5mM, 3mM, 5mM NaP) cells. **A.** Area, **B.** Perimeter, **C.** Circularity, **D.** Form Factor, **E.** Feret's Diameter. Significant differences were identified using one-way ANOVA (control compared to treatments) and Dunnett's test for multiple comparisons ($p<0.05$). Bars represent the mean parameters; error bars represent standard deviations. Data shown represents n=3 biological repeats; a total of 144 images; 2 000 mitochondria per treatment; 8 200 mitochondria in total; * indicates $p<0.05$, ** indicates $p<0.01$ and *** indicates $p<0.001$.

2.3.4. Mitochondrial copy number and *STOML2* expression are affected by NaP-induced mitochondrial stress

MT-DNA copy number is used as an indicator of mitochondrial function or homeostasis and is known to increase under oxidative stress (Gaziev, Abdullaev and Podlutsky, 2014). After 24 hours of NaP treatment, RT-qPCR of *MT-ND1* relative to *B2M* showed elevated levels of MT-DNA copy number across all NaP concentrations (Figure 9A). There was a significant increase in MT-DNA copy number at 5mM compared to the control using unpaired t-test analysis (Figure 9A), although there was no significant increase in MT-DNA copy number across the three concentrations when analysing with ANOVA.

STOML2 has a role in both mitochondrial hyperfusion and mitophagy (Tondera *et al.*, 2009). Therefore, any changes in its expression may reflect potential mitochondrial compensatory mechanisms that balance the effects of mitochondrial stress. *STOML2* expression was significantly decreased across all NaP treatments (Figure 9B). Therefore, both the MT-DNA copy number and *STOML2* expression data support the premise of mitochondrial morphology changes in response to NaP-induced mitochondrial stress.

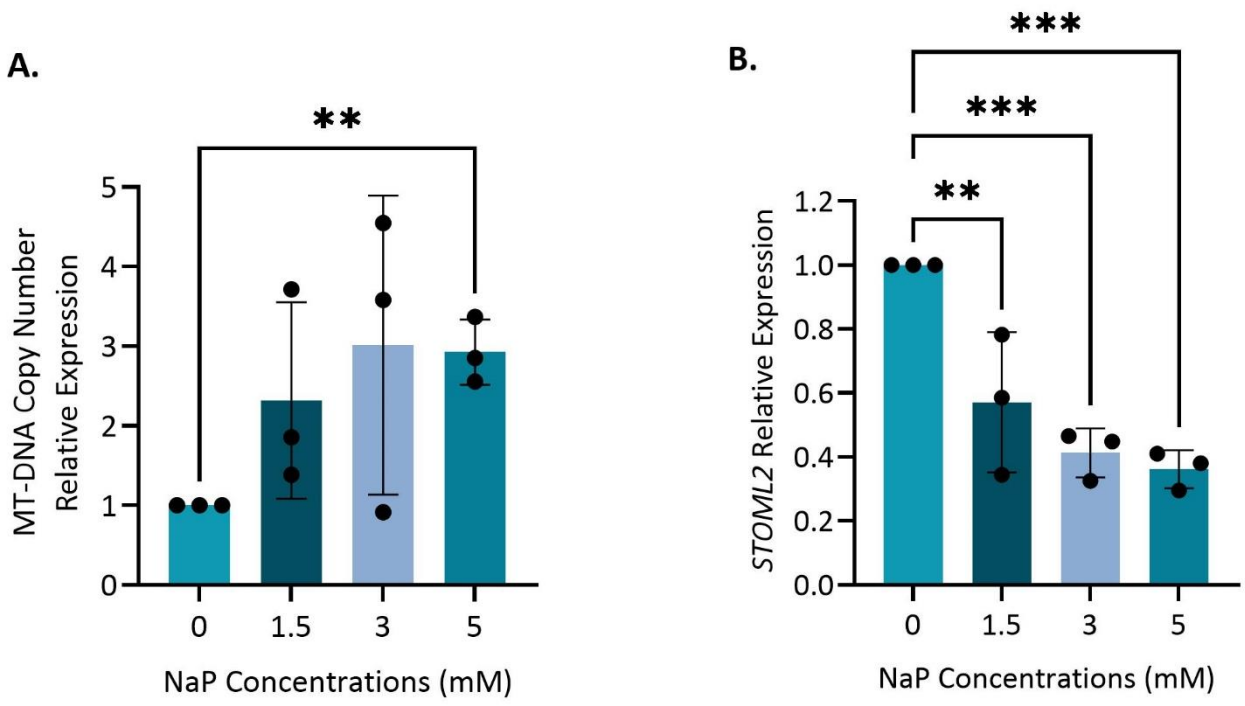

FIGURE 9: MT-DNA copy number and *STOML2* expression are altered during mitochondrial stress. A. MT-DNA copy number is significantly elevated after 5mM sodium propionate (NaP) treatment. Relative quantification of MT-DNA copy number was performed by RT-qPCR of *MT-ND1* and *B2M*. **B.** *STOML2* expression is significantly down regulated after 1.5mM, 3mM and 5mM NaP treatment. Relative quantification of *STOML2* expression was performed by RT-qPCR of *STOML2* and *B2M*. Significant differences were identified using one-way ANOVA (control compared to treatments) and Dunnett's test for multiple comparisons ($p<0.05$) for *STOML2* expression and unpaired t-test with equal variance for MT-DNA copy number (control compared to 5mM). Bars represent the mean expression; error bars represent standard deviations. All data shown represents n=3 biological repeats, * indicates $p<0.05$, ** indicates $p<0.01$ and *** indicates $p<0.001$.

2.3.5. Mitochondrial morphological parameters correlate significantly with mitochondrial gene expression

An increase in MT-DNA copy number and decrease in *STOML2* expression suggest that the mitochondrial morphology changes may be mediated by an increase in biogenesis and a decrease in mitochondrial fusion. To further explore this hypothesis, associations between the

five significant morphology parameters (area, perimeter, circularity, form factor and Feret's diameter) and/or MT-DNA copy number and *STOML2* expression were investigated.

Significant correlations existed between area, perimeter, Feret's diameter and *STOML2* expression. These three morphology parameters all showed a positive correlation with *STOML2* (Pearson's area r=0.79, perimeter r=0.74, Feret's diameter r=0.72, p<0.01) (Figure 10). This positive correlation further supports the hypothesis of a decrease in fusion activity during NaP-induced stress as mitochondrial shape gets smaller as *STOML2* expression decreases. There was no significant correlation between morphology parameters and MT-DNA copy number or between MT-DNA copy number and *STOML2* (Figure S5).

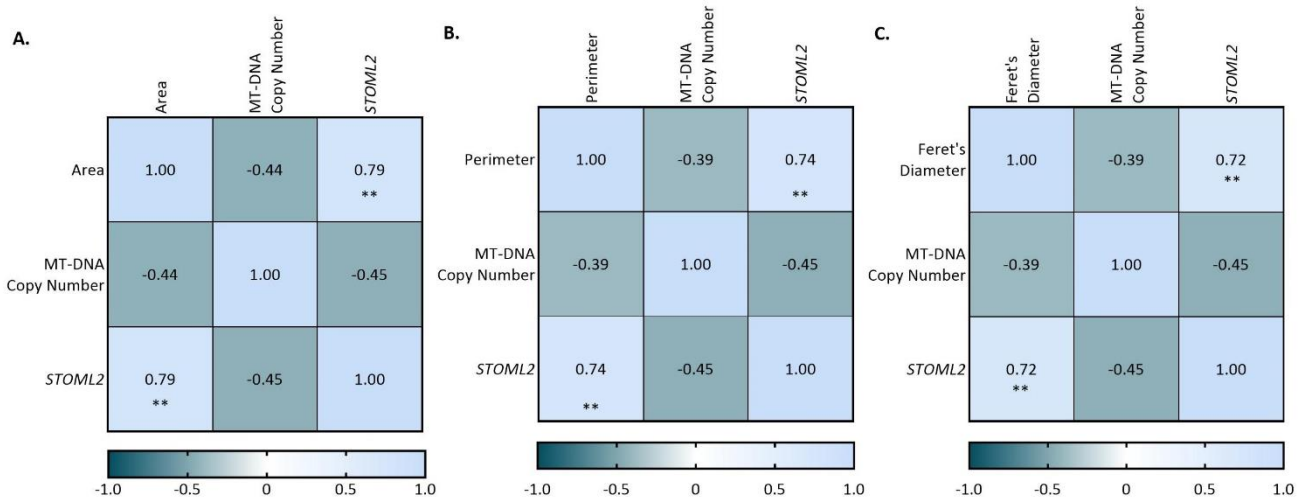

FIGURE 10: The relationship between MT-DNA copy number, *STOML2* and morphological parameters. Heatmaps show the Pearson's rank correlations between MT-DNA copy number, *STOML2* and the morphological parameters **A.** Area, **B.** Perimeter and **C.** Feret's diameter. Rho is represented according to the color key provided, **=p<0.01, n=3 biological repeats for all groups.

2.4. Discussion

Mitochondrial dynamics are essential for maintaining mitochondrial homeostasis and preserving the function of the mitochondrial network (Khacho and Slack, 2018). Any changes in these processes due to cellular stresses, such as oxidative stress, would impact the functioning of the mitochondrial network, which could have significant implications for the

function of neuronal cells. This is evident by mitochondrial dynamics being implicated in many neurological disorders (Yang *et al.*, 2021). The SH-SY5Y neuronal cell model used in this thesis successfully recapitulated "ASD-associated" mitochondrial dysfunction using NaP. Interestingly, the data presented indicate that the role played by mitochondrial dynamics in NaP-induced mitochondrial dysfunction may involve a broader systemic dysregulation of both mitochondrial biogenesis and mitophagy. However, it must be noted that this is a cell model system using the SH-SY5Y cell line, which are cancerous cells that have been transformed. Because of this SH-SY5Y cells may already have some level of mitochondrial dysfunction.

During NaP-induced stress, ATP concentration and MT-DNA copy number increased significantly (at 3mM and 5mM, and 5mM, respectively). The increase in MT-DNA copy number confirms mitochondrial dysfunction as it is regularly used as a marker for mitochondrial stress (Castellani *et al.*, 2020). The above-mentioned increases are consistent with changes in mitochondrial biogenesis.

Biogenesis is the process whereby mitochondrial mass in a cell is increased by MT-DNA copy number by DNA replication and the synthesis of new mitochondrial lipids and proteins to create new organelles. This increase in mitochondrial mass allows more ATP to be synthesised in the cell (Zhu, Wang and Chu, 2013; Uittenbogaard and Chiaramello, 2014). The complex mitochondrial biogenesis pathway involves many players, such as peroxisome proliferator-activated receptors (*PPARs*), transcription factor A, mitochondrial (*TFAM*), nuclear respiratory factors (*NRF1* and *NRF2)* and others (Zhu, Wang and Chu, 2013; Palikaras and Tavernarakis, 2014). A well-known key regulator in this pathway is PPAR gamma coactivator 1 alpha (*PGC-1α*), with increases in *PGC-1α* expression resulting in increases in MT-DNA copy number, mitochondrial mass and ATP (Viscomi *et al.*, 2011; Vaarmann *et al.*, 2016; Chaudhary *et al.*, 2021).

An increase in mitochondrial biogenesis in the context of this NaP-induced mitochondrial stress could indicate that biogenesis compensates for oxidative stress, as shown in previous studies (Chen *et al.*, 2011). Furthermore, this upregulation of biogenesis would lead to an increase in MT-DNA copy number. Investigating the expression or protein levels of biogenesis genes such as *PGC-1α* in this cell model system would support this hypothesis; this was not part of the scope of this project and this is currently an ongoing project in our research group. There are also other methods that can be used to determine increases in mitochondrial mass

such as citrate synthase activity and fluorescent dyes which can be used in future research (Stremming *et al.*, 2012; Doherty and Perl, 2017).

Mitochondrial dynamics intrinsically affect mitochondrial morphology. For example, fusion, fusing two or more mitochondria, would be characterized by an elongated mitochondrial shape and increased mitochondrial area and perimeter. On the other hand, fission, the splitting of one mitochondrion into individual mitochondria, would result in the opposite change in morphology, such as a smaller, more circular shape and decreases in area and perimeter. Maintenance of mitochondrial morphology by these dynamics is essential for proper functioning, and abnormal visible changes in morphology can signify mitochondrial dysfunction and cellular stress (Galloway, Lee and Yoon, 2012).

This cell model showed significant differences in mitochondrial morphology between controls and NaP-treated cells. From TEM analysis, five morphological parameters were significantly different (area, perimeter, circularity, form factor and Feret's diameter). Area, perimeter and form factor were significantly decreased (across all concentrations, at 1.5mM and 5mM, and 5mM, respectively), indicating that the average size of mitochondria was becoming smaller. Additionally, Feret's diameter was significantly decreased (at 1.5mM and 5mM) and circularity was significantly increased (at 5mM), showing that mitochondrial shape became more spherical. Together, all these changes in ultrastructure indicate that NaP treatment results in smaller, rounder mitochondria in the cell. This is consistent with fission, which is increased during NaP-induced mitochondrial stress.

In this cell model system, TEM was a useful tool to visualise changes in mitochondrial morphology instead of only relying on changes in fusion or fission genes to indicate morphological changes. However, there are limitations to the TEM methods. Capturing these cell images is a labour-intensive process, and it is nearly impossible to capture images of every cell in the sample which could lead to bias when choosing the images (Lam *et al.*, 2021). Additionally, sample preparation can result in artefacts leading to incorrect conclusions from the data, although this limitation can be solved to a certain extent if cryogenic techniques are used. Additionally, electron microscopy costs are relatively high compared to other imaging methods such as fluorescent microscopy. However, TEM remains a powerful tool to visualise mitochondrial morphology using a single method. In addition, collecting quantitative data

from TEM images, as opposed to only qualitative data, helps to further support the data gathered from gene expression.

The implications of these morphological changes are supported by the significant decrease in *STOML2* expression across all NaP treatments. The STOML2 protein is thought to be involved in fusion, specifically in maintaining the long isoforms of OPA1 (L-OPA1), the protein responsible for fusing the inner mitochondrial membrane (Hájek, Chomyn and Attardi, 2007; Tondera *et al.*, 2009). A significant decrease in *STOML2* expression would lead to a decrease in L-OPA1 downstream, inhibiting fusion of the inner mitochondrial membrane. Correlation analysis between the morphological parameters and *STOML2* expression revealed that area, perimeter and Feret's diameter were significantly positively correlated with *STOML2* expression. A decrease in fusion would have the same morphological consequences as an increase in fission. This imbalance in mitochondrial dynamics would be confirmed by measuring the expression and/or protein levels of key fusion and fission factors such as DRP1, FIS1, MFN1, MFN2 and OPA1 isoforms. Unfortunately, these experiments could not be explored in this thesis due to time constraints but is currently an ongoing project in our research group.

The favouring of fission over fusion is supported by previous studies examining mitochondrial dynamics and ASD. It has been reported that fusion gene expression and protein levels were decreased in brain tissue of ASD patients (Anitha *et al.*, 2012; Tang *et al.*, 2013). Additionally, this decrease in fusion proteins (MFN1, MFN2 and OPA1) was accompanied by an increase in fission proteins (DRP1 and FIS1) (Tang *et al.*, 2013). The favouring of fission over fusion in the context of NaP-induced oxidative stress is consistent with the changes that might be expected due to oxidative stress and ROS leading to mitochondrial damage. One of the primary roles of fission is to mitigate mitochondrial dysfunction as a precursor to mitophagy. Fission separates damaged mitochondrial components from the healthy mitochondrial network to preserve its function and prevent further damage (Youle and Bliek, 2012).

However, other studies on the relationship between fission and fusion in ASD have found conflicting evidence. For example, Carrasco *et al*. (2019) found increased expression of both fusion and fission genes (*MFN1, MFN2, OPA1, DRP1* and *FIS1*) in buccal mucosa samples in the ASD cohort, while Pecorelli *et al.* (2020), using fibroblasts from ASD patients and controls, found increased fusion and fission gene expression (*MFN1, MFN2, DRP1* and *FIS1*) with

correspondingly increased protein expression of MFN1 and FIS1, although DRP1 protein expression decreased. These differences in the reported expression of fusion/fission genes in ASD could be due to the different tissue types used. Alternatively, the differences could reflect the small sample sizes used in these studies (the number of participants in ASD and control groups ranged from 8-25) or the variance within ASD and the "mitochondrial-endophenotype" in the study. Even though there is no consensus on the direction of the relationship between fission and fusion in ASD, there is consistent evidence that alterations in mitochondrial dynamics play an essential role in ASD aetiology.

In this context, cell models can help to shed more light on the relationship between mitochondrial function, morphology and dynamics. The data presented here shows that increased MT-DNA copy number and ATP concentration are associated with increased fission activity and decreased fusion activity and is supported by decreased STOML2 expression *in vitro*. Several previous studies support these data. Tang *et al.* (2013) found evidence of increased mitochondrial mass with increased protein levels of DRP1 and FIS1 and decreased levels of MFN1, MFN2 and OPA1 in the primary neurons of ASD brain tissue. Kim et al. (2019) showed increased MT-DNA copy number and decreased mitochondrial size after PPA treatment in SH-SY5Y cells. Carrasco *et al*. (2019) also found increased MT-DNA copy number in ASD participants in upward trends for fission gene expression (although fusion gene expression was also elevated).

On the other hand, there is also evidence for an inverse relationship between mitochondrial biogenesis and fission. Studies have shown that *PGC-1α* upregulates fusion and downregulates fission suggesting that an increased MT-DNA copy number would correlate with a decrease rather than an increase in fission (Dabrowska *et al.*, 2015; Peng *et al.*, 2017). However, it is important to consider the complexity of the numerous pathways that converge on the regulation of biogenesis and mitochondrial dynamics. While *PGC-1α* is an essential transcriptional regulator of numerous key genes of mitochondrial biogenesis and dynamics, both processes are also regulated by independent pathways that respond to oxidative and metabolic stress. For example, NFE2L2 is an important redox-sensitive regulator of mitochondrial biogenesis (Ryoo and Kwak, 2018), while PINK1, Parkin and P62 are critical modulators of fusion and fission that respond to signals of mitochondrial dysfunction (Lim *et al.*, 2012). The increase in mitochondrial copy number reported in this study is not necessarily

PGC-1α dependent; moreover, an increase in *PGC-1α* signalling does not necessarily directly relate to an increase in fusion as many other factors could be mediating this relationship.

The relationship between increased mitochondrial biogenesis and increased fission activity could also be explained by an imbalance between biogenesis and mitochondrial degradation (Figure 11). This opens the possibility of biogenesis and mitophagy being involved in mitochondrial dynamics in ASD. Biogenesis and mitophagy are opposing processes that must strike a balance in the cell to maintain mitochondrial mass and homeostasis (Figure 11) (Palikaras and Tavernarakis, 2014; Popov, 2020). Biogenesis is needed to increase mitochondrial mass, but overexpression can cause abnormally high levels of ROS. On the other hand, mitophagy is needed to remove damaged mitochondrial components to maintain a healthy network as an accumulation of damaged mitochondria can increase oxidative stress and inflammation, but overactivity can lead to a dangerous decrease in mitochondrial mass (Palikaras and Tavernarakis, 2014).

An increase in biogenesis and fission activity indicates that the mitochondrial network is attempting to maintain this balance and sustain a consistent mitochondrial mass. However, the increase in MT-DNA copy number reported in this study may be due to a decrease in mitophagy rather than, or as well as, an upregulation of biogenesis (Figure 11). The smaller mitochondria visualized using TEM may represent healthy and damaged mitochondria that have been separated via fission but the latter not having undergone mitophagy (Figure 1 and Figure 11). This could be evidence of damaged/dysfunctional mitochondria being retained by the cell due to defects in the mitophagy pathway. This would also result in an increase in ROS in the cell as increased biogenesis with impaired mitophagy would allow damaged mitochondria to continue producing ROS and too many mitochondria in the cell (Wang *et al.*, 2021). There has been evidence of Parkin and PINK1 (key regulators of mitophagy) being altered in ASD and other mitophagy factors (Wang *et al.*, 2021). This hypothesis suggests another pathway that could be investigated in the future by using TEM to examine the expression of key mitophagy genes and quantifying mitophagy parameters. The exact interplay between these two processes in mitochondria is still unknown, and the possibility of mitochondrial dynamics being involved in this balance is an exciting one that should be further explored.

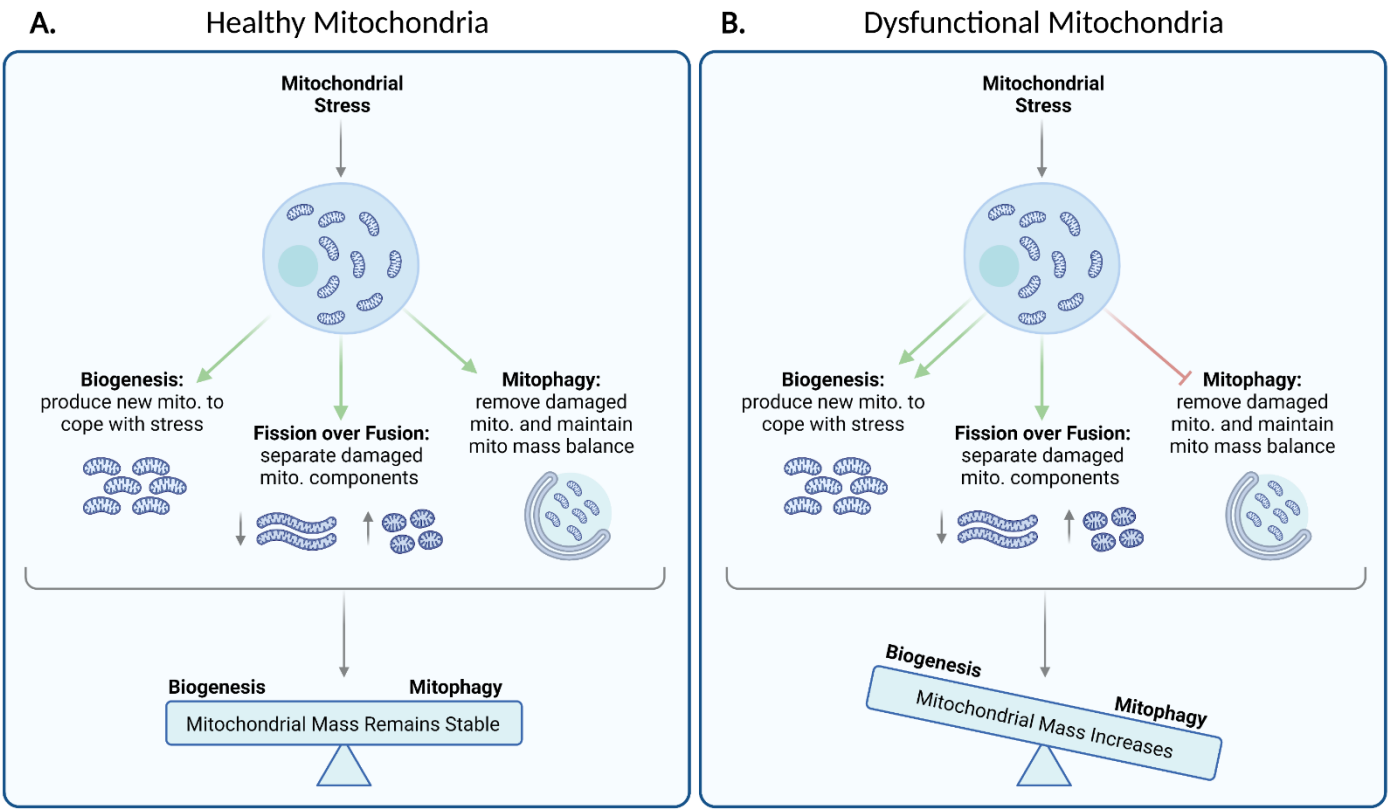

FIGURE 11: The imbalance between mitochondrial biogenesis and mitophagy in dysfunctional mitochondria. A. In healthy mitochondria, biogenesis, fission over fusion and mitophagy are activated during mitochondrial stress (shown by single green arrows), leading to mitochondrial mass remaining stable. **B.** In dysfunctional mitochondria, fission over fusion is activated (single green arrow) but biogenesis is overly upregulated (double green arrows) and/or mitophagy is impaired (red arrow). This leads to an overall increase in mitochondrial mass. Figure made in BioRender.com

Chapter 3

Differential DNA Methylation Analysis in a South African ASD Cohort

3.1. Introduction

Gene expression can be altered without changing the genetic sequence as a result of DNA methylation. The study of DNA methylation patterns falls under the umbrella term of epigenetics, referring to any changes in gene expression that occur without changing the DNA code. Epigenetic modifications include histone modifications, DNA methylation, chromatin re-structuring or non-coding RNAs (Jin and Liu, 2018; Tremblay and Jiang, 2019). During cell differentiation, DNA methylation specifies the development of different tissue types (Jaenisch and Bird, 2003). DNA methylation is also essential in regulating neurogenesis, highlighting its importance in the brain (Moore, Le and Fan, 2013). Although prevalent in development, DNA methylation changes continue to occur throughout childhood and adulthood to regulate cell function (Ciernia and LaSalle, 2016).

Differential DNA methylation can occur anywhere in the gene but was initially found in CpG islands. These DNA regions are usually non-methylated but when methylation occurs, it usually results in gene silencing. It is common for these CpG islands to occur in gene promoter regions, and most methylation studies have focused on this region (Weng *et al.*, 2013). However, emerging evidence shows that changes in methylation patterns can occur in the gene body, frequently in the region after the first exon, or in non-CpG islands (Maunakea *et al.*, 2010; Ladd-Acosta *et al.*, 2014; Nardone *et al.*, 2017; Ehrlich, 2019).

Changes in methylation patterns can lead to both increased and decreased gene expression. Hypermethylation in the promoter region has been associated with gene silencing, whereas in the gene body it has been associated with increased expression (Ehrlich, 2019). Similarly, hypomethylation is associated with increased and decreased gene expression (Hon *et al.*, 2012; Nardone *et al.*, 2014). This suggests that there is no fixed rule of hypermethylation leading to gene silencing and hypomethylation leading to increased expression. Instead, the

effect that hyper- or hypomethylation has on gene expression depends on the specific gene and where in the gene it occurs (Tremblay and Jiang, 2019). Additionally, the difference in methylation does not have to be large to have a significant effect. In a brain tissue study between ASD cases and controls, Ladd-Acosta *et al.* (2014) found methylation differences ranging from 6.6% - 15.8%, which were all statistically significant. Significant biological differences can exist between controls and the affected group, regardless of how large or small the percentage methylation differences are.

DNA methylation, in relation to diseases and disorders, occurs due to changes in any of the players involved in the methylation pathway. DNA methyltransferases (Dnmt) are known as the writers of DNA methylation because they add methyl groups to cytosine residues. Dnmt1 is involved in copying methylation patterns during cell replication in embryonic development, while Dnmt3a and Dnmt3b are involved in *de novo* DNA methylation (Weng *et al.*, 2013; Tremblay and Jiang, 2019). Mutations in the Dnmt genes themselves would lead to dysfunctional Dnmt proteins. This would affect their ability to successfully copy DNA methylation patterns (Klein *et al.*, 2011; Moore, Le and Fan, 2013). Other factors which influence Dnmt regulation could also impact their function leading to irregular methylation patterns (Moore, Le and Fan, 2013; Weng *et al.*, 2013; Semick *et al.*, 2019).

Other essential proteins in the methylation pathway are readers of DNA methylation, which 'interpret' methylation patterns (Weng *et al.*, 2013; Good, Vincent and Ausió, 2021). Mutations in DNA methylation readers are another way to introduce epigenetic changes. Although methylation patterns would not change, gene expression would change due to incorrect reading. An example of this is Rett's syndrome, caused by a mutation in the MeCP2 gene involved in reading DNA methylation (Good, Vincent and Ausió, 2021).

Rett's syndrome is an example of single gene methylation changes or mutations leading to changes in gene expression. However, most neurological disorders are more complex, with multiple genes and pathways involved (Moore, Le and Fan, 2013). For example, studies examining bipolar disorder have found differences in DNA methylation between patients and controls at multiple gene sites, and other psychiatric disorders, such as major depression and schizophrenia, have shown similar results (Kuratomi *et al.*, 2008; Mill *et al.*, 2008). In addition, differential methylation at multiple sites has also been studied in neurodegenerative disorders. For example, Alzheimer's and Parkinson's diseases have been associated with

multiple CpG sites and regions of differential methylation (Chuang *et al.*, 2017; Semick *et al.*, 2019).

The importance of epigenetics in ASD has been discussed in multiple reviews (Rylaarsdam and Guemez-Gamboa, 2019; Tremblay and Jiang, 2019; Wiśniowiecka-Kowalnik and Nowakowska, 2019; Yoon *et al.*, 2020). Wong *et al*. (2014) examined methylation patterns of 50 pairs of monozygotic twins regarding ASD. As monozygotic twins have identical gene sequences, any discordance between the twins can be attributed to epigenetic factors. There were both CpG site-specific and region-specific differences in methylation patterns between the discordant twin pairs. This study was seminal in demonstrating that ASD has an epigenetic component (Wong *et al.*, 2014). Other studies have found differential methylation at specific CpG sites and gene regions in ASD (Ladd-Acosta *et al.*, 2014; Nardone *et al.*, 2014).

DNA methylation is a useful biomarker for various diseases and disorders. As cancers have been found to have epigenetic signatures, tests are being developed to use methylation to detect different types (Levenson, 2010; Feinberg, Koldobskiy and Göndör, 2016). Certain neurological disorders, such as fragile X syndrome, Angelman syndrome and Prader-Willi syndrome, can also be diagnosed through DNA methylation assays (Ai *et al.*, 2012). For example, fragile X syndrome is caused by repeats of the CGG nucleotide in the FMR1 gene, which are subsequently methylated, leading to gene suppression. The disorder is diagnosed by measuring the size of the FMR1 gene but can also be diagnosed by measuring the DNA methylation levels of the FMR1 gene (Schenkel *et al.*, 2016). In comparison, ASD is a more complex disorder as DNA methylation at several genes has been associated with its aetiology (Ciernia and LaSalle, 2016). Thus, for DNA methylation to potentially be used as a biomarker for ASD, a methylation test would require examining a group of genes rather than just one gene. Although these tests are still under development, this would be an interesting concept for future studies to explore (Ehrlich, 2019).

Examining DNA methylation in neurological disorders is difficult because access to brain samples from living patients is unattainable. Although post-mortem brain tissue is used in many studies to show epigenetic differences (Corley *et al.*, 2019), access to these types of samples is limited. Therefore, a proxy for brain DNA methylation is needed (Jin and Liu, 2018). Blood has traditionally been used, but recently buccal and saliva samples have proven to be as useful, if not more useful, as blood samples. Furthermore, both buccal and saliva samples

have been shown to overlap in DNA methylation patterns in brain tissue, making them an adequate proxy (Lowe *et al.*, 2013; Smith *et al.*, 2015).

This chapter reports the use of buccal samples from a previously established South African ASD cohort, an understudied population, to measure DNA methylation (Stathopoulos *et al.*, 2020). The genes analysed are based on their roles in mitochondrial dynamics (specifically fusion and fission) and the RNA expression work done in a cell model system described in chapter two of this thesis. The analysis of this chapter explores the hypothesis that changes in gene expression and mitochondrial morphology in the cell model system may be associated with changes in DNA methylation at these genes in our ASD cohort. If this were the case, it would support the utility of the cell culture model system used to recapitulate "ASD-like" mitochondrial stress and support the overall hypothesis of mitochondrial dynamics contributing to the ASD aetiology. The data presented and analyses I performed, as described in this chapter, have also been included in a recent publication by Bam *et al.* (2021).

3.2. Materials and methods

3.2.1. Study participants and DNA sample collection

DNA samples previously collected from an established South African cohort of children were used (Stathopoulos *et al.*, 2020). Male and female participants were recruited in the original cohort study, but only male participants (6-12 years) were used due to insufficient female participants. This also served to "narrow" our ASD phenotype, given the sex differences in ASD (Ferri, Abel and Brodkin, 2018). All participants were assessed using the Autism Diagnostic Observation Schedule, Second Edition (ADOS-2) to ensure that ASD and control participants displayed the correct phenotype for their group. The cohort included children diagnosed with ASD and age- and gender-matched controls (included in this analysis were ASD: n=55; controls: n=43). DNA was previously extracted from buccal cell samples from participants. This study involving participants was reviewed and approved by the University of Cape Town, FSREC076-2014. The legal guardians or parents supplied their written informed consent to the participation of the children in the study. The participants also agreed to participate as any participants not willing to complete the ADOS-2 assessment or provide a buccal sample were excluded from the study.

3.2.2. Targeted next-generation bisulfite sequencing (tNGBS)

DNA samples were sent to EpigenDx, Inc. (MA, USA) for tNGBS. Six genes were selected for tNGBS based on their roles in mitochondrial fusion and fission and 25 assays across 98 CpG sites were designed (Table S2). Two assays covered 11 CpG sites for *DRP1*, four assays covered 30 CpG sites for *FIS1*, one assay covered 18 CpG sites for *MFN1*, five assays covered 26 CpG sites for *MFN2*, five assays covered 25 CpG sites for *OPA1* and eight assays covered 45 CpG sites for *STOML2*. Methylation levels at each CpG site were measured and calculated as a percentage of total reads. DNA methylation for *MFN1* and *STOML2* was quantified in a larger validation cohort of ASD (n=55) and controls (n=43). DNA methylation of the other four genes, *DRP1*, *FIS1*, *MFN2* and *OPA1*, was quantified in a subset of samples from the cohort of ASD (n=22) and controls (n=22).

3.2.3. Statistical analysis

Multiple unpaired t-tests, assuming Gaussian distribution and unequal variance, were performed to find significantly differentially methylated CpG sites between ASD and controls ($p<0.05$). The False Discovery Rate (FDR) test was used to correct for multiple comparisons using the Benjamini, Krieger, and Yekutieli method where Q=0.01. Simple logistic regression was performed on the seven significant CpG sites ($p<0.05$) across four genes. Percentage methylation was the independent variable and ASD vs Control was the dependent variable (ASD=1, Control=0). All analyses were performed in GraphPad Prism 9.4.0.

3.3. Results

3.3.1. Methylation patterns differ across CpG sites

Six genes were used in tNGBS to investigate whether changes in DNA methylation patterns affect genes implicated in mitochondrial fusion and fission. The fusion genes, *MFN1*, *MFN2*, *OPA1* and *STOML2*, and the fission genes, *DRP1* and *FIS1*, were chosen based on their roles in mitochondrial dynamics. The differential methylation between ASD and control groups across these six genes demonstrated how much DNA methylation can vary between different CpG sites (Figure 12). The methylation percentage ranged from 0% to 100% among different individuals. There were also large differences in methylation levels across CpG sites in the

same gene. However, there was no definitive direction of methylation across all genes when comparing the ASD and control groups. At some CpG sites, the ASD group was hypermethylated compared to the control group, while at other sites, the ASD group was hypomethylated compared to the control group (Figure 12).

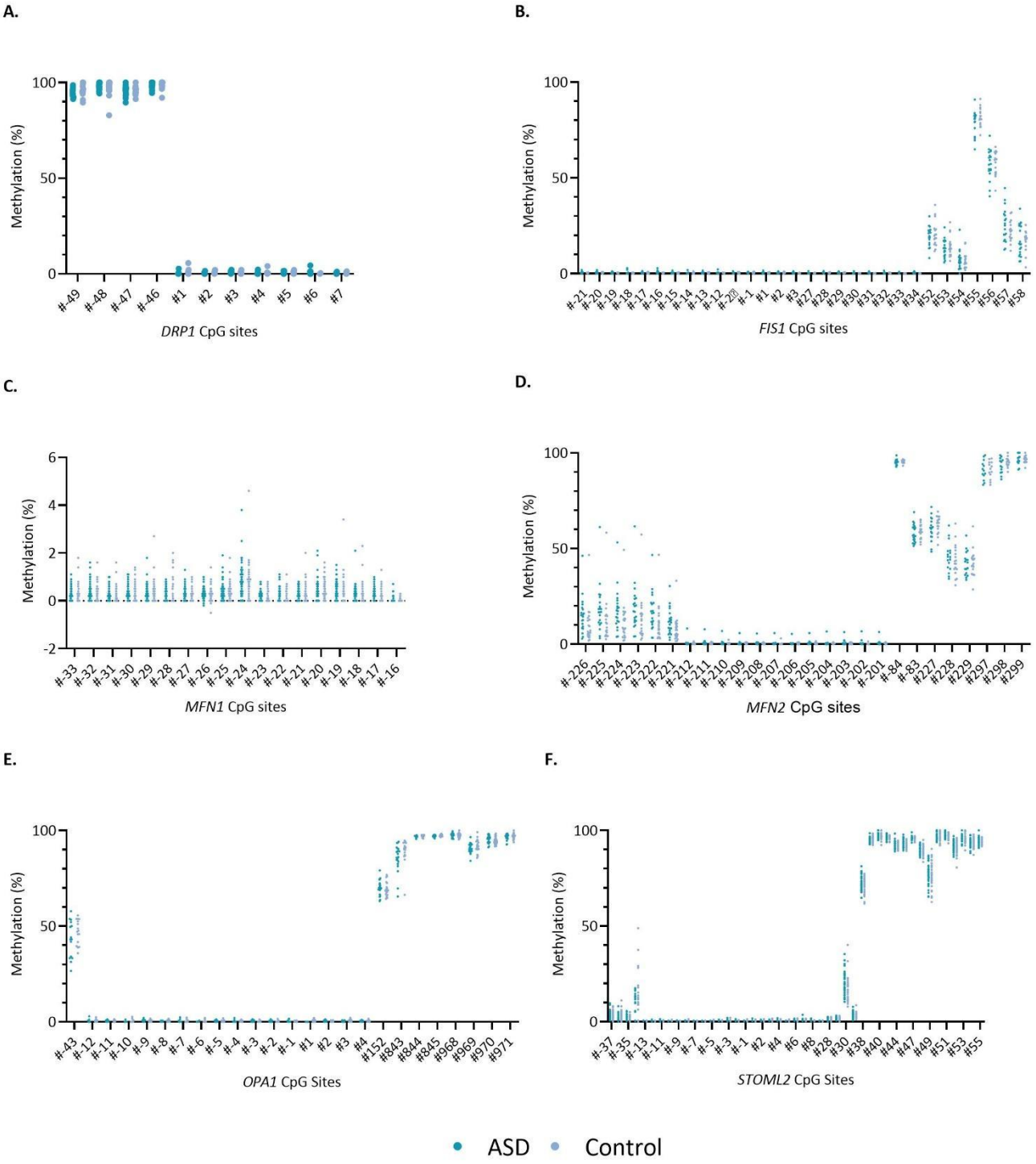

FIGURE 12: CpG sites located in mitochondrial fusion and fission genes were measured for differential methylation. Targeted next generation bisulfite sequencing (tNGBS) was used to measure percentage methylation. Individual percentage methylation readings for each CpG site for the ASD (dark blue) and control (light blue) groups are shown in the scatter plots with the bars representing the mean of each group. **A.** *DRP1* CpG sites, **B.** *FIS1* CpG sites, **C.** *MFN1* CpG sites, **D.** *MFN2* CpG sites, **E.** *OPA1* CpG sites, **F.** *STOML2* CpG sites. The individual values at each CpG site For *MFN1* and *STOML2* CpG sites, ASD=55, controls=43. For *DRP1, FIS1, MFN2* and *OPA1*, ASD=22, controls=22.

3.3.2. Fusion and fission genes are differentially methylated in ASD

Of the 98 CpG sites examined, seven sites were significantly differentially methylated between the ASD and control groups ($p<0.05$), with these sites located in *FIS1* (*FIS1* #31), *MFN2* (*MFN2* #-222, *MFN2* #-224), *OPA1* (*OPA* #1, *OPA* #845) and *STOML2* (*STOML2* #30, *STOML2* #43) (Table 1; Figure 13). A range of differential methylation was detected among these significant sites, ranging from 0.06% to 97.36%. CpG sites in *FIS1*, *MFN2* and *STOML2* were hypermethylated, while CpG sites in *OPA1* were hypomethylated in the ASD group (Table 1).

These results also demonstrated that even a small difference in methylation could be statistically significant. At CpG sites, *MFN2* #-222, *MFN2* #-224 and *STOML2* #30 there are relatively small differences in the mean methylation between the ASD and control group (Figure 13A, B, E). However, at *OPA1* #1, *OPA1* #845, *STOML2* #43 and *FIS1* #31 the difference in the mean methylation was large (Figure 13C, D, F, G).

TABLE 1: Significantly differentially methylated CpG sites. CpG sites of FIS1, MFN2, OPA1 (ASD=22, controls=22) and STOML2 (ASD=55, controls=43). CpG sites are numbered relative to the ATG translational start codon. The CpG site location is relative to the transcription start site (TSS). Mean percentage methylation of the ASD and control groups and p-values for each CpG site are displayed.

CpG Site	CpG Location from TSS	Mean Methylation (%)		P-value
		ASD	Control	
MFN2 #-224	5-Upstream	17,87	11,33	0,047
MFN2#-222	5-Upstream	17,11	10,60	0,032
OPA1 #1	Exon 1	0,06	0,41	0,016
OPA1 #845	Intron 28	97,05	97,36	0,038
STOML2 #30	Intron 2	19,28	16,29	0,011
STOML2 #43	Exon 5	96,52	96,11	0,044
FIS1 #31	Intron 1	0,24	0,11	0,041

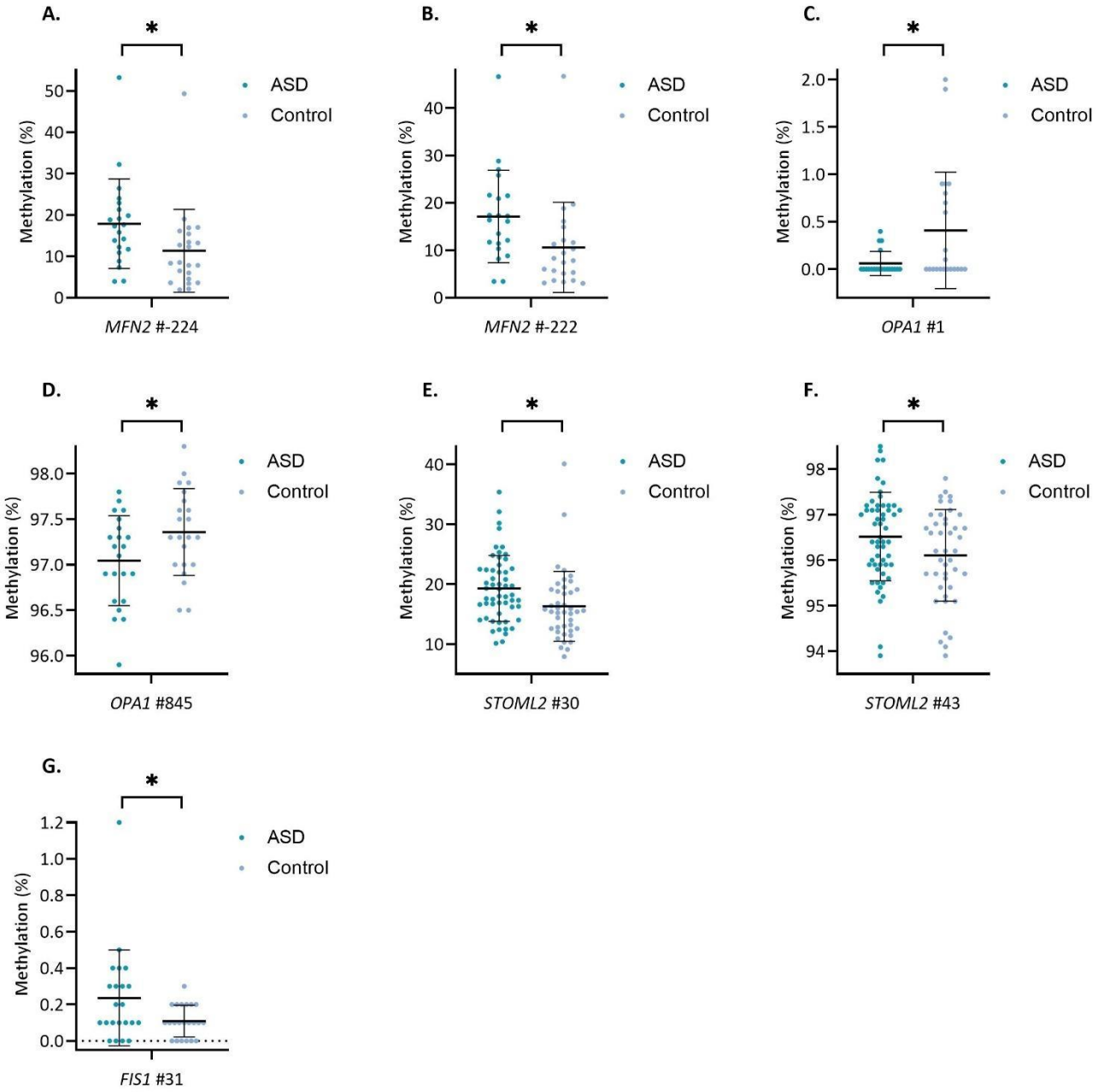

FIGURE 13: Mitochondrial fusion and fission factors are significantly differentially methylated in autism spectrum disorder (ASD). Percentage methylation was measured using targeted next generation bisulfite sequencing (tNGBS) of CpG sites and found significant differential methylation at **A.** *MFN2* #-224*,* **B.** *MFN* #-222, **C.** *OPA1* #1, **D.** *OPA1* #845, **E.** *STOML2* #30, **F.** *STOML2* #43 and ***F.*** *FIS1* #31. Data show the percentage methylation readings for all individuals in the ASD (dark blue) and control (light blue) groups for each CpG site. For *MFN2, OPA1* and *FIS1* CpG sites, ASD=22, controls=22. For *STOML2* CpG sites, ASD=55, controls=43. The mean percentage methylation for each group is shown, error bars represent standard deviation.

FIGURE 13 continued: Significantly differentially methylated CpG sites were identified using multiple unpaired two-tailed t-tests which assumed Gaussian distribution and unequal variance. All sites shown are significantly differentially methylated ($p<0.05$). This figure is similar to figure 2 in Bam *et al.* (2021).

The locations of the significantly differentially methylated sites were plotted on gene diagrams in relation to the transcription start site (TSS) (Figure 14). CpG sites for *FIS1* #31, OPA #845 and *STOML2* #30 are all located in introns, *OPA1* #1 and *STOML2* #43 are in exons and both *MFN2* #-224 and *MFN2* #-222 are located upstream of the TSS (Table 1; Figure 14). The differing locations of these CpG sites implies that DNA methylation across the gene could impact gene expression rather than being constricted to a particular area.

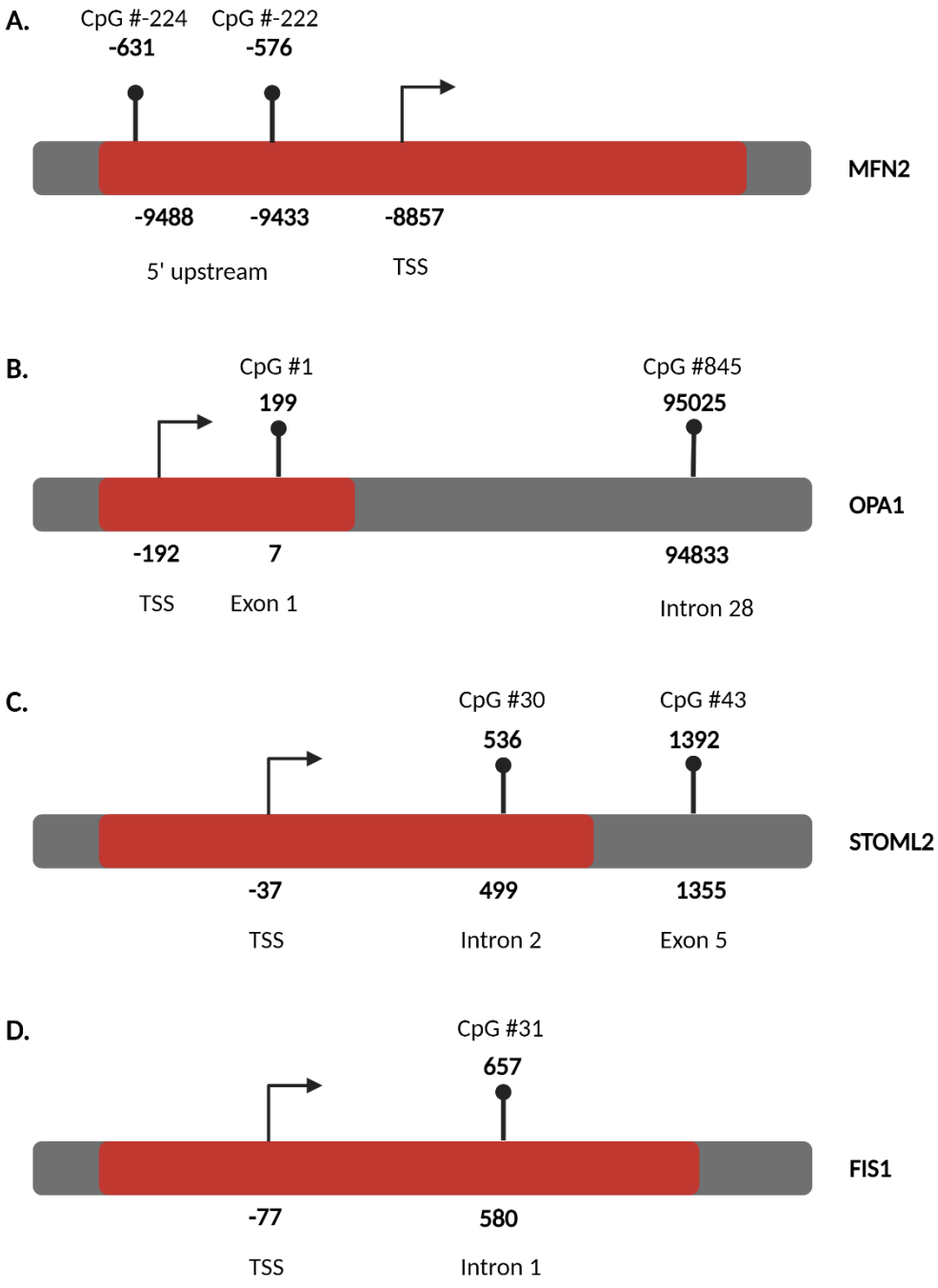

FIGURE 14: Gene diagrams of four fusion and fission genes showing the locations of the seven significantly differentially methylated CpG sites. Each diagram displays the significant CpG sites in relation to the transcription start site (TSS) (top number) and translational start codon (bottom number). The shaded red areas indicate the promoter region and the shaded grey areas indicate the rest of the gene body. The CpG sites are shown by the black pins. **A.** *MFN2* gene and the CpG sites #-224 and -222 **B.** *OPA1* gene and the CpG sites #1 and #845 **C.** *STOML2* gene and the CpG sites #30 and #43 **D.** *FIS1* gene and the CpG site #31. This figure is similar to figure 1A in Bam *et al.* (2021) and is based on diagrams provided by EpigenDx, Inc. Figure made in BioRender.com

3.3.3. Methylation patterns correlate significantly with ASD

DNA methylation can be used as a biomarker for certain neurological disorders (Ai *et al.*, 2012). Therefore, to explore whether the DNA methylation found in our cohort may potentially be used as biomarkers, models were created to test whether there was a relationship between percentage methylation at the seven significantly differentially methylated CpG sites and whether these sites were present in the ASD or control group. Simple logistic regression was used with percentage methylation as the independent variable and ASD or control as the dependent variable. Models were created for each of the seven CpG sites, and the likelihood ratio test was used to test the null hypothesis.

All seven CpG sites had significant relationships between the variables ($p<0.05$) (Table 2). The unadjusted odds ratios, X at 50% and the p-values of the likelihood ratio test for each site are also shown (Table 2). The odds ratios demonstrate how the odds of being grouped as ASD increases with a 1% increase in methylation. For example, at *STOML2* #30, for every 1% increase in methylation, the chances of being in the ASD group increase by 1.109. The percentage of methylation where the odds of being classified as ASD is 50% is shown as X at 50% (Table 2). These data show how combining different CpG sites in the future could lead to DNA methylation being used as a biomarker as an additional means to diagnose ASD.

TABLE 2: Simple logistic regression shows a relationship between DNA methylation at certain CpG sites and autism spectrum disorder (ASD) diagnosis. Simple logistic regression was performed where X=percentage methylation and Y=ASD or control (ASD=1, control=0). The CpG sites used were those that were determined to be significantly differentially methylated between the ASD control groups after multiple unpaired t-tests, assuming Gaussian distribution and unequal variance. The seven CpG sites are located across four genes: *STOML2* (ASD=55, controls=43); *FIS1*, *MFN2* and *OPA1* (ASD=55, controls=43). After modelling simple logistic regression, all seven CpG sites had slopes that had significant deviation from zero using the likelihood ratio test ($p<0.05$). The unadjusted odds ratios, X at 50% and p-values for the seven CpG sites are shown.

CpG Site	Unadjusted Odds Ratio	X at 50%	P-value
MFN2 #-224	1,076	14,62	0,0337
MFN2#-222	1,087	13,83	0,0232
OPA1 #1	0,05357	0,1339	0,0056
OPA1 #845	0,2499	97,21	0,0328
STOML2 #30	1,109	15,26	0,0082
STOML2 #43	1,534	95,74	0,0407
FIS1 #31	245,6	0,05886	0,0148

3.4. Discussion

Differential methylation of genes can affect numerous biological pathways and is implicated in many diseases and disorders such as autoimmune diseases, cancers, metabolic disorders and neurological disorders (Jin and Liu, 2018). Differential methylation, and the wider field of epigenetics, of which it is a part, provides an explanation for changes in gene expression, particularly in the context of disorders that are not linked to mutations.

It is well established that differential methylation is important in neurodevelopment and has been linked to ASD aetiology (Moore, Le and Fan, 2013; Corley *et al.*, 2019; Yoon *et al.*, 2020). In a previous study using this South African ASD cohort, multiple genes were screened for

differential methylation. Most of the identified genes converged on mitochondrial pathways, suggesting that mitochondrial dysfunction may be involved in ASD aetiology. The most differentially methylated gene was *STOML2,* whose protein is associated with mitochondrial fusion. Their genome-wide methylation data were supported by urinary metabolomic data (Stathopoulos *et al.*, 2020). Additionally, multiple studies have shown associations between mitochondrial dysfunction and ASD using gene and protein expression and biochemical data (Griffiths and Levy, 2017). The role of mitochondrial dynamics in maintaining mitochondrial function has been demonstrated in mitochondrial research, particularly the role it plays in neurological disorders (Yu *et al.*, 2020). Based on this research and the results described in the previous chapter in this thesis, the work described in this chapter focused on the potential involvement of mitochondrial dynamics genes in ASD through differential methylation.

The DNA methylation data in this chapter showed that seven CpG sites across four of the six genes were significantly differentially methylated. Three genes (*MFN2*, *OPA1, STOML2*) are involved in fusion and the fourth gene (*FIS1*) is involved in fission. MFN2 is one of the proteins responsible for fusing the outer mitochondrial membrane, while OPA1 fuses the inner mitochondrial membrane. STOML2, as previously mentioned, is indirectly involved in fusion as it maintains the long isoforms of the OPA1 protein, which are needed for fusion to occur. On the other hand, FIS1 is an accessory protein that maintains DRP1, the protein responsible for mitochondrial fission (Tondera *et al.*, 2009; Yu *et al.*, 2020). These four genes and their proteins are essential in maintaining the balance between fusion and fission. The locations of the differentially methylated CpG sites are also interesting, as five of the seven sites were located in the promoter regions of the genes. As the structure of the promoter region is tightly linked with gene expression, altering methylation patterns in this region could lead to downstream changes in gene expression (Juven-Gershon and Kadonaga, 2010). Previous studies examining differential methylation in other cases such as schizophrenia have found evidence of correlation in the promoter region between methylation patterns and changes in transcription (Dyrvig *et al.*, 2017). Additionally, simple logistic regression showed a significant relationship between ASD vs controls and the seven CpG sites. Examination of the mechanisms and specific transcription factors lay outside the scope of this thesis, but it suggests an interesting avenue for future research.

These findings of this study show that differential methylation of CpG sites in these genes suggests that mitochondrial dynamics could be involved in the aetiology of ASD. Unfortunately, the quality of RNA extracted from the buccal cells had low integrity, with RT-qPCR experiments requiring extensive optimisation, and therefore the expression of the chosen genes in this cohort could not be measured. However, data from the wider study found that MT-DNA copy number, urinary metabolomics and DNA methylation of PGC-1α were altered between ASD and control groups. This indicated that mitochondrial dysfunction was present in this cohort and that an increase in MT-DNA copy number could be a compensatory mechanism (Bam *et al.*, 2021). Additionally, these data align with previous studies which implicate mitochondrial dynamics in ASD through gene and protein expression data (Anitha *et al.*, 2012; Tang *et al.*, 2013; Carrasco *et al.*, 2019; Pecorelli *et al.*, 2020).

The directional changes in the differential methylation of these genes highlight that hyper- and hypomethylation alone cannot indicate the effect on gene expression and that they are gene dependent (Tremblay and Jiang, 2019). *FIS1, MFN2* and *STOML2* were hypermethylated, while *OPA1* was hypomethylated. If specific increases or decreases in methylation directly indicated increased or decreased gene expression, it would be expected that the fusion genes (*MFN2, STOML2* and *OPA1*) would have the same directional change in methylation and the opposite directional change in methylation to *FIS1*. Whether the hypo- and hypermethylation of these genes in this cohort lead to increased or decreased gene expression must still be investigated.

This unanswered research question points to a limitation of differential methylation studies. These studies are valuable in identifying whether certain pathways are associated with a specific disorder or disease and can account for changes that cannot be explained by genetic mutations. However, RNA or protein expression studies need to be performed to confirm if these differences in methylation result in expression changes. Additionally, a limitation of this study is that changes seen in differential methylation between ASD and controls could be due to other variation within the groups because of different environmental exposures or genetic variation.

Despite this, the interplay between fusion and fission in mitochondrial dynamics is so complex that gene and/or protein expression data, in addition to differential methylation data, may

not fully explain the changes between these processes. Previous studies that examined the gene expression levels of these genes in a similar context found increased expression of both fusion and fission genes/proteins (Carrasco *et al.*, 2019; Pecorelli *et al.*, 2020). Additionally, gene expression data did not always correspond with subsequent protein expression levels. In this context, morphological studies using fluorescence or electron microscopy can be useful.

The differential methylation reported in this thesis may result in changes in gene expression and has been shown to result in other physiological changes such as MT-DNA copy number and urinary metabolomics (Bam *et al.*, 2021). This points to an imbalance in mitochondrial homeostasis in the South African ASD cohort. This exploratory investigation of mitochondrial dysfunction associations in ASD provides more reason to further explore this association in future studies. Additionally, it continues to support the hypothesis that mitochondrial dynamics are involved in regulating mitochondrial function and are involved in ASD aetiology.

The findings of this study from a South African cohort are valuable as they add to the body of literature concerning ASD and mitochondrial dysfunction and, more importantly, they provide evidence of the association between ASD and mitochondrial dysfunction in an understudied population. There is a substantial knowledge gap in ASD research in sub-Saharan Africa. Two recent reviews that looked at the number of ASD papers emanating from sub-Saharan Africa up until mid-2016 found only 47 and 53 ASD papers, respectively, from the region (Abubakar, Ssewanyana and Newton, 2016; Franz *et al.*, 2017). Of those papers, only six and two, respectively, focused on genetics and ASD. This is compared to the approximately 7 500 papers on ASD published in Europe and the approximately 11 500 ASD papers published in North America in the same time frame (Franz *et al.*, 2017). These statistics demonstrate a need for more research focusing on ASD in the sub-Saharan African region, especially because the genetic diversity in these populations could provide novel perspectives into the genes and pathways associated with ASD (Abubakar *et al.*, 2016). Given the need for more research focusing on ASD in sub-Saharan African populations, the findings of this study also demonstrate the success of using buccal samples, a relatively cheap and easily accessible method, to obtain DNA. This method could be used in various studies as a proxy for examining neurological disorders (Lowe *et al.*, 2013; Smith *et al.*, 2015).

Chapter 4

Summary and Concluding Remarks

In general, the investigation of the genetics underlying many disorders remains understudied in African populations. Most genetic studies focus on the populations of high-income countries. The lack of inclusion of African populations is due to multiple reasons, such as lack of access to technology, laboratory equipment, and the high cost of scientific research (Martin *et al.*, 2018). ASD is one disorder that remains understudied in African populations and has a significant genetic contribution to its aetiology.

ASD is a heterogenous disorder involving multiple genes and pathways in its aetiology such as neurotransmission, metabolism, synaptic integrity and neurodevelopment (Baranova et al., 2021; Rodriguez-Gomez et al., 2021). It is estimated that 1 in 100 children are diagnosed with ASD globally (Zeidan *et al.*, 2022). Of the studies based in sub-Saharan Africa, relatively few investigate ASD compared to the number of studies on diseases such as human immunodeficiency virus (HIV) and tuberculosis (TB). (Franz *et al.*, 2017). Two of the most recent systematic reviews looking at ASD research in sub-Saharan Africa up until mid-2016 found only six papers investigating genetics and ASD up until 2016 (Abubakar, Ssewanyana and Newton, 2016; Franz *et al.*, 2017). Another recent scoping review has found that only three more papers from South Africa have been published between 2017-2021 (unpublished data from the research group). This situates genetics and ASD in the African context as a research area that requires further investigation.

One of the pathways implicated in ASD is mitochondrial dysfunction; this is supported by changes in gene and protein expression, the activity of the OXPHOS complexes and metabolic and biochemical changes (Citrigno *et al.*, 2020; Frye, 2020). These aspects of mitochondrial dysfunction and their association to ASD have been studied relatively well both in cell models and cohort studies. In comparison, mitochondrial dynamics and their role in mitochondrial dysfunction and autism remain unexplored. Mitochondrial dynamics are an essential part of mitochondrial function, especially in neurons. The balance between fusion and fission allows the mitochondrial network to adapt to cellular conditions either by becoming more

interconnected or by fragmenting. These processes are intrinsically linked to mitochondrial transport and mitophagy in maintaining mitostasis (Misgeld and Schwarz, 2017). Given the lack of research on ASD in African populations and that mitochondrial dysfunction is an established component of ASD aetiology, the aim of this thesis was to explore the role of mitochondrial dynamics, specifically fusion and fission, in ASD in a South African context.

The focus of our research group has been to identify the biological pathways associated with ASD in a South African cohort. Our group's first paper examined genome-wide differences between ASD and controls and found differential methylation of numerous genes that converged on nine canonical pathways linked to mitochondrial metabolism (Stathopoulos *et al.*, 2020). This genome-wide methylation data was supported by a second study in the same cohort that examined the differential methylation of specific genes linked to the identified mitochondrial pathways, such as mitochondrial biogenesis and mitochondrial dynamics (Bam *et al.*, 2021).

In chapter three of this thesis, the differential methylation of genes involved in mitochondrial dynamics is specifically compared between control and ASD groups. The genes chosen were key mitochondrial fusion and fission genes. Four of the six genes had significantly differentially methylated CpG sites (*MFN2, OPA1, STOML2* and *FIS1*), thus demonstrating an association between ASD and potential changes in mitochondrial dynamics. The data in chapter three built on the mitochondrial dysfunction hypothesis in ASD; it highlights the power of using epigenetics, specifically differential methylation, to find associations between specific biological pathways and disorders. Most importantly, an understudied population in the context of both genetics and ASD was explored.

In parallel to this epigenetics work, the data from the ASD epigenetics research was examined in a cell model system which was better suited to investigate the mechanisms behind the associations found in our ASD cohort. Chapter two of this thesis describes the SH-SY5Y cell model system using NaP-induced mitochondrial stress to recapitulate ASD mitochondrial dysfunction. MT-DNA copy number and ATP levels were significantly increased, confirming mitochondrial stress. Additionally, these increases in MT-DNA copy number and ATP levels were consistent with the hypothesis that mitochondrial biogenesis was upregulated; this links these data to the differential methylation of the biogenesis regulator, PGC-1α, in our cohort study (Bam *et al.*, 2021). In addition, TEM analysis used to visualise mitochondrial morphology

on our cell model system revealed that fission was favoured over fusion. This increase in fission and/or decrease in fusion was supported by significant decreases in gene expression of the fusion gene *STOML2*. Again, this change in the balance between fusion and fission is supported by differential methylation of fusion and fission genes described in chapter three and Bam *et al*. (2021). Further exploration of these findings led to the hypothesis that changes in mitochondrial dynamics were potentially associated with increased biogenesis and/or inhibition of mitophagy.

The use of TEM in the SH-SY5Y cell model highlighted the potential of this method in visualising cell ultrastructure, organelle morphology and cellular interactions. Instead of using gene and/or protein expression proxies to measure changes in morphology, morphological parameters such as area and perimeter could be measured in the cells. TEM remains one of the few methods capable of visualising the entirety and morphology of the mitochondria using a single method, as well as the interactions mitochondria have with other organelles, although these interactions could not be explored further in this thesis due to time constraints. Additionally, the collection of quantitative data from these images using Fiji/ImageJ further distinguishes this study as many previous studies have only qualitatively classified mitochondrial parameters and used them as supporting evidence for other gene and/or protein data.

Chapter two established a workflow to examine the relationship between mitochondrial function, dynamics and morphology *in vitro*. The cell model system described in chapter two can now be used in future experiments to continue to investigate mitochondrial dynamics or additional mitochondrial pathways implicated in ASD. This cell model system is poised to start unravelling the specific relationships that maintain mitochondrial homeostasis and mitostasis. These data have begun to identify relationships that regulate mitochondrial dynamics and morphology in the context of ASD. Given the role that mitochondrial dynamics is suggested to play in ASD and the unclear mechanisms regarding mitochondrial compensation, dysfunction and dynamics, the ability to study this in an *in vitro* system is useful and significantly contributes to the field.

The data from examining differential methylation in a South African cohort together with studying mitochondrial dysfunction in a recapitulated-ASD cell model system demonstrate that mitochondrial dynamics play a prominent role in ASD-associated mitochondrial

dysfunction. The changes found in the balance between fusion and fission in the SH-SY5Y model are consistent with changes in methylation patterns of these key genes in the ASD cohort. In addition, the possibility of biogenesis and mitophagy being involved in mitochondrial dynamics was also introduced due to the results of the SH-SY5Y model. This further supports the hypothesis of an imbalance between biogenesis and mitophagy in the context of mitochondrial dysfunction. Overall, the data in this thesis provide the foundation for future research to continue investigating the mechanisms behind the association between mitochondrial dynamics, biogenesis and mitophagy.

Supplementary Materials

Table S1: Primer sequences used for RT-qPCR

Primer	**Sequence (5’ to 3’)**
B2M Forward	5’-CCAGCAGAGAATGGAAAGTCAA-3’
B2M Reverse	5’-TCTCTCTCCATTCTTCAGTAAGTCAACT-’3
MT-ND1 Forward	5’-CCCTAAAACCCGCCACATCT-3’
MT-ND1 Reverse	5’-GAGCGATGGTGAGAGCTAAGGT-3'
STOML2 Forward	5’-GTGACTCTCGACAATGTAAC-3’
STOML2 Reverse	5’-TGATCTCATAACGGAGGCAG-3’

Table S2: Assays designed for targeted next-generation bisulfite sequencing to assess differential methylation

Gene	**Assay**	**Number of CpG sites**
DRP1	ASY2711	4
	ASY2713	7
FIS1	ASY2721	10
	ASY2722	5
	ASY2723	8
	ASY2724	7
MFN1	ASY1849	5
	ASY1850	18
	ASY1851	3
	ASY1852	5

MFN2	ASY2682	6
	ASY2683	12
	ASY2684	2
	ASY2685	3
	ASY2686	3
OPA1	ASY2677	1
	ASY2678	1
	ASY2679	3
	ASY2680	4
	ASY2681	16
STOML2	ADS5520	12
	ASY2579	8
	ASY2580	3
	ASY2581	3
	ASY2582	4
	ASY2583	20
	ASY2584	5
	ASY2585	3
	ASY2586	3
	ASY2587	3
	ASY2588	6

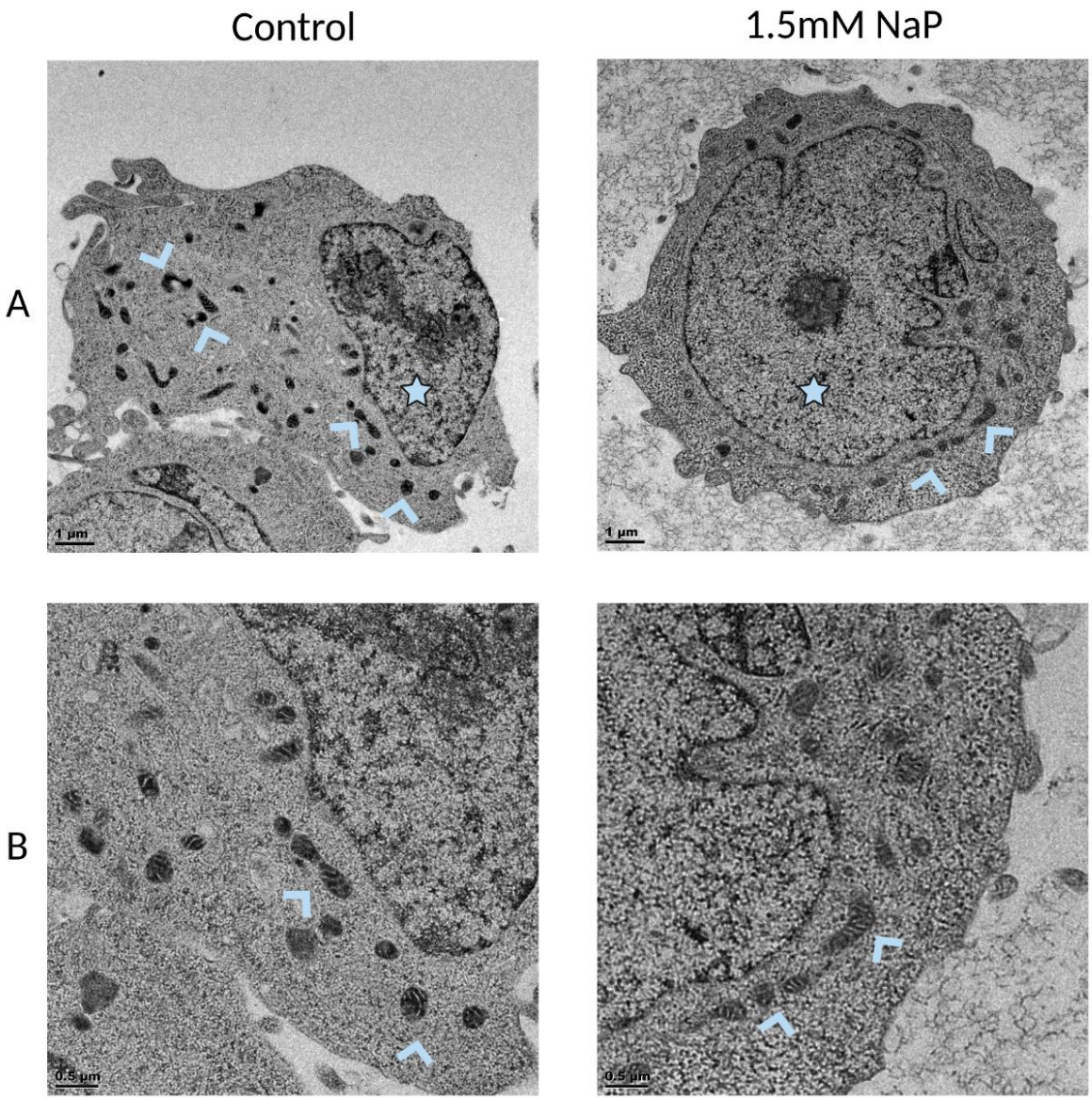

FIGURE S1: Unprocessed TEM images. Row **A.** Control and 1.5mM treatment cells showing the full cell image used in analysis. Row **B.** A zoomed in view of the cells. Blue arrows indicate mitochondria and blue stars indicate the nucleus. Figure made in BioRender.com

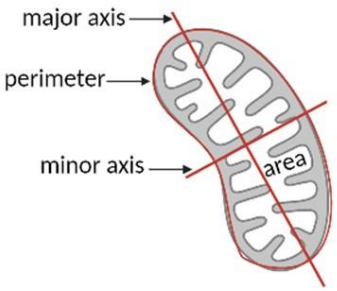

$$area = area\ of\ selection\ (square\ pixels)$$

$$perimeter = the\ length\ of\ the\ outside\ boudary\ of\ the\ selection\ (pixels)$$

$$aspect\ ratio = \frac{major\ axis}{minor\ axis}$$

$$form\ factor = \frac{perimeter^2}{4\pi(area)}$$

$$circularity = \frac{4\pi(area)}{perimeter^2}$$

$$area - weighted\ form\ factor = \frac{perimeter^2}{4\pi}$$

$$roundness = \frac{4(area)}{\pi(major\ axis)^2}$$

$$Feret's\ diameter = the\ longest\ distance\ between\ any\ two\ points\ along\ the\ selection\ boundary, also\ known\ as\ maximum\ caliper$$

FIGURE S2: Diagram and equations of mitochondrial parameters measured. Figure based on Merrill *et al*. (2017). Figure made in BioRender.com

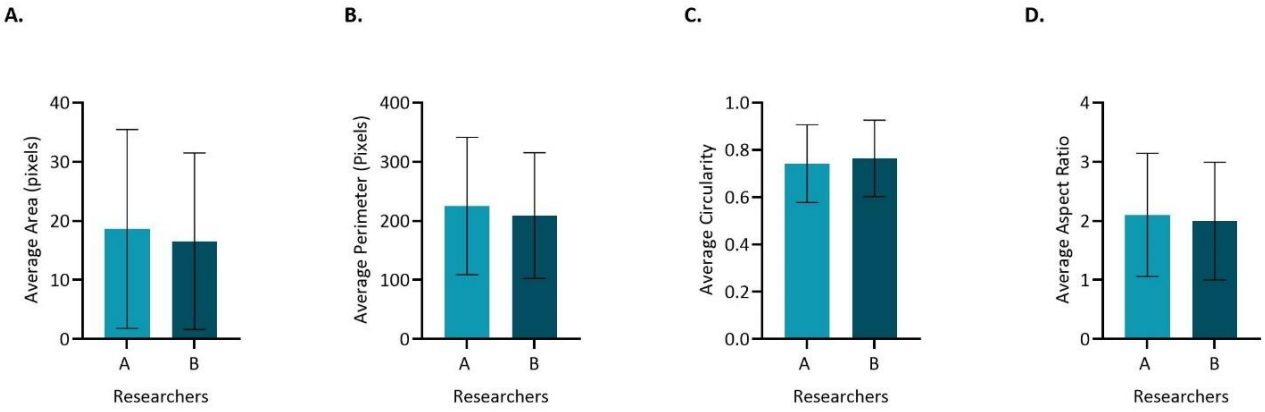

FIGURE S3: Pilot study comparing Free-Hand analysis method used by two researchers. Four parameters were measured: **A.** Average Area (pixels), **B.** Average Perimeter (pixels), **C.** Average Circularity and **D.** Average Aspect Ratio. The pilot study consisted of 10 randomised images across three biological repeats and controls, 1.5mM, 3mM and 5mM NaP treatments. Unpaired t-tests analysing the group of 10 images between the two researchers showed no significance ($p<0.05$). Bars represent mean parameters; error bars represent standard deviation. Data shown represents n=3 biological repeats.

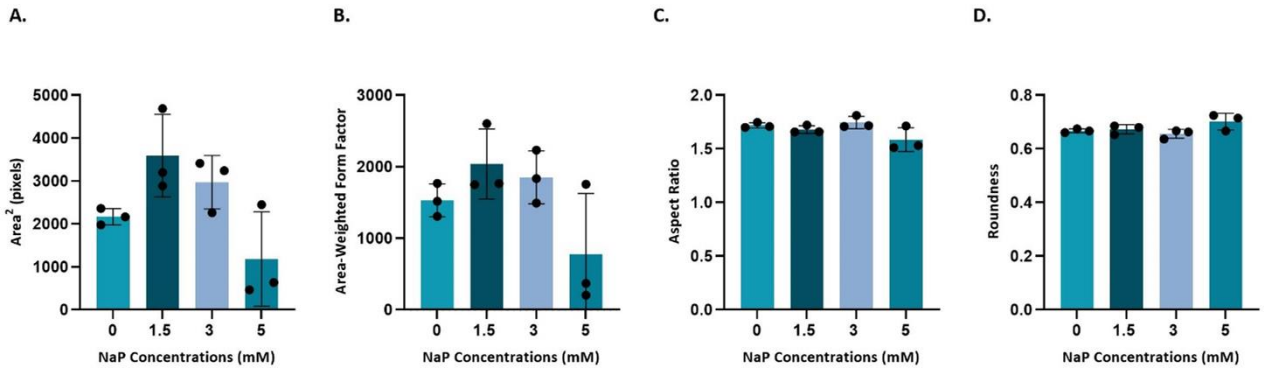

FIGURE S4: Mitochondrial morphology during mitochondrial stress. SH-SY5Y cells treated with NaP for 24 hours underwent preparation for TEM and results were analysed using Fiji/ImageJ. Four of the nine parameters showed no significant differences between control (0mM NaP) and treated (1.5mM, 3mM, 5mM NaP) cells. **A.** Area^2, **B.** Area-Weighted Form Factor, **C.** Aspect Ratio, **D.** Roundness. Significant differences were identified using one-way ANOVA (control compared to treatments) and Dunnett's test for multiple comparisons ($p<0.05$). Bars represent the mean parameters; error bars represent standard deviations. Data shown represents n=3 biological repeats; a total of 144 images; 2 000 mitochondria per treatment; 8 200 mitochondria in total; * indicates $p<0.05$, ** indicates $p<0.01$ and *** indicates $p<0.001$.

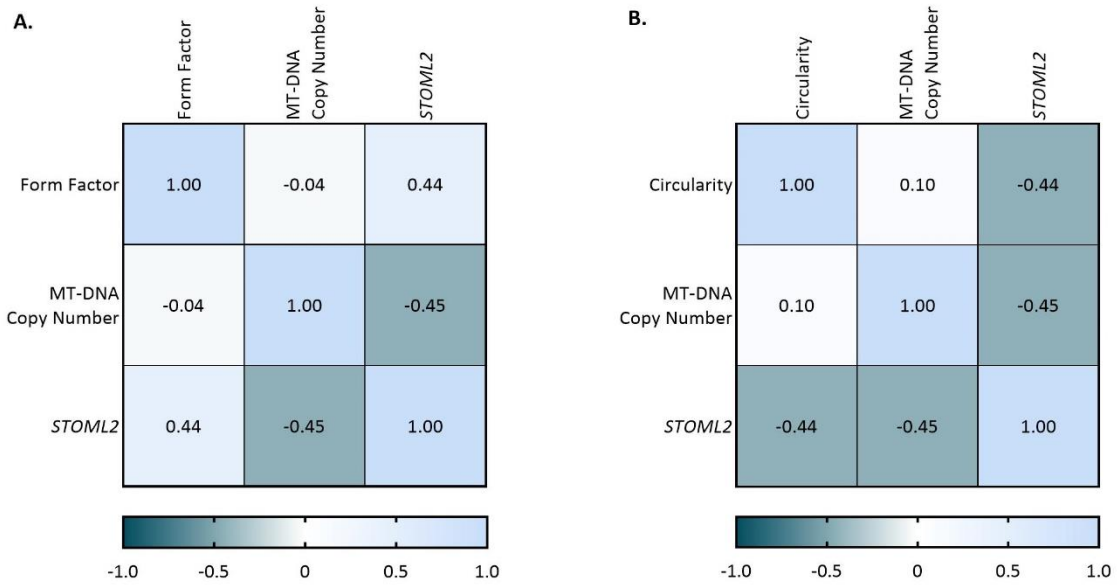

FIGURE S5: Relationship between MT-DNA copy number, STOML2 and morphological parameters. Heatmaps show the Pearson's rank correlations between MT-DNA copy number, STOML2 and the morphological parameters (form factor and circularity). Rho is represented according to the colour key provided, n=3 biological repeats for all groups. **A.** Form factor, **B.** Circularity.

ROIBatchGen Macro:

```
/*This macro asks for an input folder (directory), and file format (tif, jpg, etc).
It opens each of the specified files in the folder,and asks you to selct Regions of interest (ROIs) around the mitochondria (or other areas of interest).
The selected ROIs are saved as .zip files, to be used by the next macro
*/
input = getDirectory("Input directory"); //asks for folder where your image files are
print("Input folder for ROI generation = " +input);
File.makeDirectory(input+File.separator+"ROIs"+File.separator);
Dialog.create("File type");
Dialog.addString("File suffix: ", ".tif", 5);
Dialog.show();
suffix = Dialog.getString();
Dialog.create("Indicate Condition");
Dialog.addString("Experimental condition in this folder", "control or treatment?");
Dialog.show();
condition = Dialog.getString();
processFolder(input);
function processFolder(input) {
	list = getFileList(input);
	for (i = 0; i < list.length; i++) {
		if(File.isDirectory(input + list[i]))
			processFolder("" + input + list[i]);
		if(endsWith(list[i], suffix))
			//processFile(input, output, list[i]);
			processFile(input, list[i]);
	}
```

```
}
//function processFile(input, output, file) {
function processFile(input, file) {
	print("Processing: " + input + file);
	open(input+File.separator+file+"");
	title = getTitle();
	//removes the suffix from the name of the file
	if (endsWith(title, suffix)){
	index2=lastIndexOf(title, suffix);
	image= substring(title, 0, index2);
	}
	//roiManager("delete");
	waitForUser("Select ROIs", "Select ROIs around mitochondria. \n Press t to save each one to the ROI Manager before slecting the next one. \n \n Press OK when you're done.");
	n=roiManager("count");
	run("Select All");
	roiManager("Save",	""+input+File.separator+"ROIs"+File.separator+"ROIs-"+image+".zip");
	n=roiManager("count");
	print("ROIs selected and saved for "+title+" : "+n+".");
	roiManager("deselect");
	roiManager("delete");
	selectWindow(title);
	run("Close");
}
```

```
Dialog.create("Folder processing for ROIs finished!");
Dialog.addMessage("ROIs from all the images in the folder for <"+condition+"> have been generated and saved.");
Dialog.show();
```

Edge Detector Macro

```
input = getDirectory("Input directory");
print("Input folder = " +input);
File.makeDirectory(input+File.separator+"Canny"+File.separator);
Dialog.create("Indicate Condition");
Dialog.addString("Experimental condition in this folder", "control or treatment?");
Dialog.show();
condition = Dialog.getString();
Dialog.create("File type");
Dialog.addString("File suffix: ", ".tif", 5);
Dialog.show();
suffix = Dialog.getString();
processFolder(input);
function processFolder(input) {
	list = getFileList(input);
	for (i = 0; i < list.length; i++) {
		//if(File.isDirectory(input + list[i]))
			//processFolder("" + input + list[i]);
		if(endsWith(list[i], suffix))
			processFile(input, list[i]);
	}
}
function processFile(input, file) {
```

```
	open(input+File.separator+file+"");
	title = getTitle();
	print(title+ " is being processed.");

	//removes the suffix from the name of the file
	if (endsWith(title, suffix)){
	index2=lastIndexOf(title, suffix);
	image= substring(title, 0, index2);
	}
//Processing Image with Bandpass Filter
	run("Bandpass Filter...", "filter_large=60 filter_small=8 suppress=Vertical tolerance=5 autoscale saturate");
	//Applying the Canny Edge Detector using default settings
	run("Canny Edge Detector", "gaussian=2 low=2.5 high=7.5");
	rename("CannyImage");
	wait(1000);
	//Open up the corresponding ROIs file for the image.
	//Duplicate out each ROI from the mask as a new image. Analyse those particles.
	roiManager("open", input+"ROIs"+File.separator+"ROIs-"+image+".zip")
	run("Set Measurements...", "area perimeter fit shape feret's add redirect=None decimal=5");
	//Duplicate out each ROI from the mask as a new image. Analyse those particles. Generate count masks of those particles.
	n = roiManager("Count");
	for (i = 0; i < n; ++i) {
		m=i+1;
		selectWindow("CannyImage");
		roiManager("Select", i)
```

```
		//run("Duplicate...", "title=CannyImage-"+i"");

		run("Duplicate...", " ");

		selectWindow("CannyImage-"+m+"");

		//run("Analyze Particles...", "size=500-Infinity circularity=0.40-1.00
show=[Overlay Masks] display exclude");

		run("Analyze Particles...", "display exclude"); //measures particles
>600 pixels - excludes remaining background

		//measures particles >600 pixels - excludes remaining background

		saveAs("Results",  ""+input+File.separator+condition+"-Results.csv");
//saves the results table with all the measurements for each particle in each ROI
for each file in the folder.

	}

	wait(1000);

	//Closes the ROI windows from an image. Saves the new count masks as tiffs

	for (i = 0; i < n; ++i) {

		m=i+1;

		selectWindow("CannyImage-"+m+"");

		saveAs("tiff",   input+File.separator+"Canny"+File.separator+image+"-
Canny-"+m);

		//selectWindow(""+image+"-Canny-"+m+".tif");

		run("Close");

	}

	wait(1000);

	//clear and close the ROImanager and all open images

	roiManager("deselect");

	roiManager("delete");

	close("*");

}
```

```
//This section calculates parameters for mitochondrial morphology measurments, based on the measurements put out in the Results table

awff = ff = ar = sum_a = a2 = len = 0;

for (i = 0; i < nResults; i++) { // for every particle in table

	a = getResult("Area", i);

	p = getResult("Perim.", i);

	ar = getResult("Major", i) / getResult("Minor", i); /* aspect ratio = length / width */

	ar_sum+= ar;

	sum_a += a;

	sum_a_sq += a*a;

	ff = (p*p) / (4 * 3.14159265358979*a); // ff = p^2 / (4 * pi * a)

	//setResult("AspectRatio", i, ar);

	setResult("FormFactor", i, ff);

	ff_sum += ff;

	awff += (p * p) / (4 * 3.14159265358979 );

	}

//average and output

nParticles = nResults

sum_a /=nParticles

//a2 = sum_a_sq/(sum_a * sum_a);

awff /= sum_a;

ff_sum /= nParticles;

ar_sum /= nParticles;

print(condition+ " average measurements:" + "\t " + "nParticles" + "\t " + "Area" + "\t " + "Area2" + "\t " + "Area-WeightedFormFactor" + "\t " + "FormFactor" + "\t " + "AspectRatio");
```

```
print(condition+ " average measurements:" + "\t " + nParticles +"\t " + "\t " + sum_a +"\t " + "\t " + a2 +"\t " + "\t " + awff +"\t " + "\t " + ff_sum + "\t " + "\t " + ar_sum);

saveAs("Results", ""+input+File.separator+condition+"-Results with FF.csv"); //saves the results table with all the measurements for each particle in each ROI for each file in the folder.

//tidy up and confirm finished!

//run("Close");     //closes all image windows

close("Results");

close("ROI manager");

Dialog.create("Folder processing finished!");

      Dialog.addMessage("All the images in the folder for <"+condition+"> have been processed and analysed.");

      Dialog.show();
```

Mitochondrial Macro:

```
input = getDirectory("Input directory");

print("Input folder = " +input);

File.makeDirectory(input+File.separator+"Count Masks"+File.separator);

Dialog.create("Indicate Condition");

Dialog.addString("Experimental condition in this folder", "control or treatment?");

Dialog.show();

condition = Dialog.getString();

Dialog.create("File type");

Dialog.addString("File suffix: ", ".tif", 5);

Dialog.show();

suffix = Dialog.getString();

processFolder(input);

function processFolder(input) {

      list = getFileList(input);
```

```
	for (i = 0; i < list.length; i++) {
		//if(File.isDirectory(input + list[i]))
			//processFolder("" + input + list[i]);
		if(endsWith(list[i], suffix))
			processFile(input, list[i]);
	}
}
function processFile(input, file) {
	open(input+File.separator+file+"");
	title = getTitle();
	print(title+ " is being processed.");
	//removes the suffix from the name of the file
	if (endsWith(title, suffix)){
	index2=lastIndexOf(title, suffix);
	image= substring(title, 0, index2);
	}
	//Process the images to increase contrast and remove BG
	run("Invert");
	run("Subtract Background...", "rolling=60");
	run("Subtract...", "value=100");
	run("Bandpass Filter...", "filter_large=60 filter_small=8 suppress=Vertical
tolerance=5 autoscale saturate");
	//Threshold and make binary mask, fill in gaps in mask
	setAutoThreshold("MaxEntropy dark");
	setOption("BlackBackground", false);
	run("Convert to Mask");
	run("Dilate");
	run("Fill Holes");
```

```
	run("Dilate");

	run("Dilate");

	run("Dilate");

	run("Close-");

	run("Erode");

	run("Erode");

	run("Erode");

	run("Erode");

	run("Open");

	rename("Mask");

	//Open up the corresponding ROIs file for the image.

	//Duplicate out each ROI from the mask as a new image. Analyse those particles.

	roiManager("open", input+"ROIs"+File.separator+"ROIs-"+image+".zip")

	run("Set Measurements...", "area perimeter fit shape feret's add redirect=None decimal=5");

	//Duplicate out each ROI from the mask as a new image. Analyse those particles. Generate count masks of those particles.

	n = roiManager("Count");

	for (i = 0; i < n; ++i) {

		m=i+1;

		selectWindow("Mask");

		roiManager("Select", i)

		//run("Duplicate...", "title=Mask-"+i"");

		run("Duplicate...", " ");

		selectWindow("Mask-"+m+"");

		//run("Analyze Particles...", "size=500-Infinity circularity=0.40-1.00 show=[Overlay Masks] display exclude");

		run("Analyze Particles...", "size=0-Infinity show=[Count Masks] display exclude"); //measures particles >600 pixels - excludes remaining background
```

```
		saveAs("Results",  ""+input+File.separator+condition+"-Results.csv");
//saves the results table with all the measurements for each particle in each ROI
for each file in the folder.
	}
	wait(1000);
	//Closes the ROI windows from an image. Saves the new count masks as tiffs
	for (i = 0; i < n; ++i) {
		m=i+1;
		selectWindow("Mask-"+m+"");
		run("Close");
		selectWindow("Count Masks of Mask-"+m+"");
		run("3-3-2 RGB");
		saveAs("tiff",                          input+File.separator+"Count
Masks"+File.separator+image+"-CountMask-"+m);
	}
	wait(1000);
	//clear and close the ROImanager and all open images
	roiManager("deselect");
	roiManager("delete");
	close("*");
}
//This section calculates parameters for mitochondrial morphology measurments, based
on the measurements put out in the Results table
awff = ff = ar = sum_a = a2 = len = 0;
for (i = 0; i < nResults; i++) { // for every particle in table
	a = getResult("Area", i);
	p = getResult("Perim.", i);
	ar = getResult("Major", i) / getResult("Minor", i); /* aspect ratio = length
/ width */
```

```
        ar_sum+= ar;
        sum_a += a;
        sum_a_sq += a*a;
        ff = (p*p) / (4 * 3.14159265358979*a); // ff = p^2 / (4 * pi * a)
        //setResult("AspectRatio", i, ar);
        setResult("FormFactor", i, ff);
        ff_sum += ff;
        awff += (p * p) / (4 * 3.14159265358979 );
        }
//average and output
nParticles = nResults
sum_a /=nParticles
a2 = sum_a_sq/(sum_a * sum_a);
awff /= sum_a;
ff_sum /= nParticles;
ar_sum /= nParticles;
print(condition+ " average measurements:" + "\t " + "nParticles" + "\t " + "Area" + "\t " + "Area2" + "\t " + "Area-WeightedFormFactor" + "\t " + "FormFactor" + "\t " + "AspectRatio");
print(condition+ " average measurements:" + "\t " + nParticles +"\t " + "\t " + sum_a +"\t " + "\t " + a2 +"\t " + "\t " + awff +"\t " + "\t " + ff_sum + "\t " + "\t " + ar_sum);
saveAs("Results", ""+input+File.separator+condition+"-Results with FF.csv");
//saves the results table with all the measurements for each particle in each ROI for each file in the folder.
//tidy up and confirm finished!
//run("Close");    //closes all image windows
close("Results");
close("ROI manager");
```

```
Dialog.create("Folder processing finished!");
	Dialog.addMessage("All the images in the folder for <"+condition+"> have been processed and analysed.");
	Dialog.show();
```

References

Abubakar, A., Ssewanyana, D. and Newton, C.R. (2016) 'A systematic review of research on autism spectrum disorders in sub-Saharan Africa', *Behavioural Neurology*, 2016, Article ID: 3501910. Available at: https://doi.org/10.1155/2016/3501910.

Abubakar, A., Ssewanyana, D., de Vries, P.J. and Newton, C.R. (2016) 'Autism spectrum disorders in sub-Saharan Africa', *Lancet Psychiatry*, 3(9), pp. 800–802. Available at: https://doi.org/10.1016/S2215-0366(16)30138-9.

Ai, S., Shen, L., Guo, J., Feng, X. and Tang, B. (2012) 'DNA methylation as a biomarker for neuropsychiatric diseases', *International Journal of Neuroscience*, 122, pp. 165–176. Available at: https://doi.org/10.3109/00207454.2011.637654.

Al-Beltagi, M. (2021) 'Autism medical comorbidities', *World Journal of Clinical Pediatrics*, 10(3), pp. 15–28. Available at: https://doi.org/10.5409/wjcp.v10.i3.15.

Aljanabi, S.M. and Martinez, I. (1997) 'Universal and rapid salt-extraction of high quality genomic DNA for PCR-based techniques', *Nuclei Acids Research*, 25(22), pp. 4692–4693. Available at: https://doi.org/https://doi.org/10.1093/nar/25.22.4692.

American Psychiatric Association (2013) *Diagnostic and Statistical Manual of Mental Disorders*. 5th edn. American Psychiatric Association. Available at: https://doi.org/10.1176/appi.books.9780890425596.

Anand, R., Wai, T., Baker, M.J., Kladt, N., Schauss, A.C., Rugarli, E. and Langer, T. (2014) 'The i-AAA protease YME1L and OMA1 cleave OPA1 to balance mitochondrial fusion and fission', *Journal of Cell Biology*, 204(6), pp. 919–929. Available at: https://doi.org/10.1083/jcb.201308006.

Anitha, A., Nakamura, K., Thanseem, I., Matsuzaki, H., Miyachi, T., Tsujii, M., Iwata, Y., Suzuki, K., Sugiyama, T. and Mori, N. (2013) 'Downregulation of the expression of mitochondrial electron transport complex genes in autism brains', *Brain Pathology*, 23(3), pp. 294–302. Available at: https://doi.org/10.1111/bpa.12002.

Anitha, A., Nakamura, K., Thanseem, I., Yamada, K., Iwayama, Y., Toyota, T., Matsuzaki, H., Miyachi, T., Yamada, S., Tsujii, M., Tsuchiya, K.J., Matsumoto, K., Iwata, Y., Suzuki, K., Ichikawa,

H., Sugiyama, T., Yoshikawa, T. and Mori, N. (2012) 'Brain region-specific altered expression and association of mitochondria-related genes in autism', *Molecular Autism*, 3, p. 12. Available at: https://doi.org/10.1186/2040-2392-3-12.

Area-Gomez, E. and Schon, E.A. (2014) 'Mitochondrial genetics and disease', *Journal of Child Neurology*, 29(9), pp. 1208–1215. Available at: https://doi.org/10.1177/0883073814539561.

Baker, N., Patel, J. and Khacho, M. (2019) 'Linking mitochondrial dynamics, cristae remodeling and supercomplex formation: How mitochondrial structure can regulate bioenergetics', *Mitochondrion*, 49, pp. 259–268. Available at: https://doi.org/10.1016/j.mito.2019.06.003.

Balachandar, V., Rajagopalan, K., Jayaramayya, K., Jeevanandam, M. and Iyer, M. (2021) 'Mitochondrial dysfunction: A hidden trigger of autism?', *Genes and Diseases*, 8, pp. 629–639. Available at: https://doi.org/10.1016/j.gendis.2020.07.002.

Bam, S., Buchanan, E., Mahony, C. and O'Ryan, C. (2021) 'DNA methylation of PGC-1α is associated with elevated mtDNA copy number and altered urinary metabolites in autism spectrum disorder', *Frontiers in Cell and Developmental Biology*, 9, p. 696428. Available at: https://doi.org/10.3389/fcell.2021.696428.

Baranova, J., Dragunas, G., Botellho, M.C.S., Ayub, A.L.P., Bueno-Alves, R., Alencar, R.R., Papaiz, D.D., Sogayar, M.C., Ulrich, H. and Correa, R.G. (2021) 'Autism spectrum disorder: signaling pathways and prospective therapeutic targets', *Cellular and Molecular Neurobiology*, 41, pp. 619–649. Available at: https://doi.org/10.1007/s10571-020-00882-7.

Belenguer, P., Duarte, J.M.N., Schuck, P.F. and Ferreira, G.C. (2019) 'Mitochondria and the Brain: Bioenergetics and Beyond', *Neurotoxicity Research*, 36(2), pp. 219–238. Available at: https://doi.org/10.1007/s12640-019-00061-7.

de Brito, O.M. and Scorrano, L. (2008) 'Mitofusin 2 tethers endoplasmic reticulum to mitochondria', *Nature*, 456, pp. 605–610. Available at: https://doi.org/10.1038/nature07534.

Carrasco, M., Salazar, C., Tiznado, W. and Ruiz, L.M. (2019) 'Alterations of mitochondrial biology in the oral mucosa of Chilean children with autism spectrum disorder (ASD)', *Cells*, 8, p. 367. Available at: https://doi.org/10.3390/cells8040367.

Castellani, C.A., Longchamps, R.J., Sun, J., Guallar, E. and Arking, D.E. (2020) 'Thinking outside the nucleus: Mitochondrial DNA copy number in health and disease', *Mitochondrion*, 53, pp. 214–223. Available at: https://doi.org/10.1016/j.mito.2020.06.004.

Chang, D.T.W. and Reynolds, I.J. (2006) 'Mitochondrial trafficking and morphology in healthy and injured neurons', *Progress in Neurobiology*, 80, pp. 241–268. Available at: https://doi.org/10.1016/j.pneurobio.2006.09.003.

Chaudhary, S., Ganguly, S., Palanichamy, J.K., Singh, A., Bakhshi, R., Jain, A., Chopra, A. and Bakhshi, S. (2021) 'PGC1A driven enhanced mitochondrial DNA copy number predicts outcome in pediatric acute myeloid leukemia', *Mitochondrion*, 58, pp. 246–254. Available at: https://doi.org/10.1016/j.mito.2021.03.013.

Chen, H., Detmer, S.A., Ewald, A.J., Griffin, E.E., Fraser, S.E. and Chan, D.C. (2003) 'Mitofusins Mfn1 and Mfn2 coordinately regulate mitochondrial fusion and are essential for embryonic development', *The Journal of Cell Biology*, 160(2), pp. 189–200. Available at: https://doi.org/10.1083/jcb.200211046.

Chen, S., Li, Z., He, Y., Zhang, F., Li, H., Liao, Y., Wei, Z., Wan, G., Xiang, X., Hu, M., Xia, K., Chen, X. and Tang, J. (2015) 'Elevated mitochondrial DNA copy number in peripheral blood cells is associated with childhood autism', *BMC Psychiatry*, 15(1), pp. 1–7. Available at: https://doi.org/10.1186/s12888-015-0432-y.

Chen, S.-D., Yang, D.I., Lin, T.K., Shaw, F.Z., Liou, C.W. and Chuang, Y.C. (2011) 'Roles of oxidative stress, apoptosis, PGC-1α and mitochondrial biogenesis in cerebral ischemia', *International Journal of Molecular Sciences*, 12, pp. 7199–7215. Available at: https://doi.org/10.3390/ijms12107199.

Christie, D.A., Mitsopoulos, P., Blagih, J., Dunn, S.D., St-Pierre, J., Jones, R.G., Hatch, G.M. and Madrenas, J. (2012) 'Stomatin-like protein 2 deficiency in T cells is associated with altered mitochondrial respiration and defective CD4 + T cell responses', *The Journal of Immunology*, 189, pp. 4349–4360. Available at: https://doi.org/10.4049/jimmunol.1103829.

Chu, C.H., Tseng, W.W., Hsu, C.M. and Wei, A.C. (2022) 'Image Analysis of the Mitochondrial Network Morphology With Applications in Cancer Research', *Frontiers in Physics*, 10, p. 855755. Available at: https://doi.org/10.3389/fphy.2022.855775.

Chuang, Y.H., Paul, K.C., Bronstein, J.M., Bordelon, Y., Horvath, S. and Ritz, B. (2017) 'Parkinson's disease is associated with DNA methylation levels in human blood and saliva', *Genome Medicine*, 9, p. 76. Available at: https://doi.org/10.1186/s13073-017-0466-5.

Ciernia, A.V. and LaSalle, J. (2016) 'The landscape of DNA methylation amid a perfect storm of autism aetiologies', *Nature Reviews Neuroscience*, 17(7), pp. 411–423. Available at: https://doi.org/doi:10.1038/nrn.2016.41.

Citrigno, L., Muglia, M., Qualtieri, A., Spadafora, P., Cavalcanti, F., Pioggia, G. and Cerasa, A. (2020) 'The mitochondrial dysfunction hypothesis in autism spectrum disorders: current status and future perspectives', *International Journal of Molecular Sciences*, 21, p. 5785. Available at: https://doi.org/10.3390/ijms21165785.

Cogliati, S., Enriquez, J.A. and Scorrano, L. (2016) 'Mitochondrial Cristae: Where Beauty Meets Functionality', *Trends in Biochemical Sciences*, 41(3), pp. 261–273. Available at: https://doi.org/10.1016/j.tibs.2016.01.001.

Cogliati, S., Frezza, C., Soriano, M.E., Varanita, T., Quintana-Cabrera, R., Corrado, M., Cipolat, S., Costa, V., Casarin, A., Gomes, L.C., Perales-Clemente, E., Salviati, L., Fernandez-Silva, P., Enriquez, J.A. and Scorrano, L. (2013) 'Mitochondrial Cristae Shape Determines Respiratory Chain Supercomplexes Assembly and Respiratory Efficiency', *Cell*, 155, pp. 160–171. Available at: https://doi.org/10.1016/j.cell.2013.08.032.

Collins, H.E., Kane, M.S., Litovsky, S.H., Darley-Usmar, V.M., Young, M.E., Chatham, J.C. and Zhang, J. (2021) 'Mitochondrial morphology and mitophagy in heart diseases: qualitative and quantitative analyses using transmission electron microscopy', *Frontiers in Aging*, 2. Available at: https://doi.org/10.3389/fragi.2021.670267.

Corley, M.J., Vargas-Maya, N., Pang, A.P.S., Lum-Jones, A., Li, D., Khadka, V., Sultana, R., Blanchard, D.C. and Maunakea, A.K. (2019) 'Epigenetic delay in the neurodevelopmental trajectory of DNA methylation states in autism spectrum disorders', *Frontiers in Genetics*, 10, p. 907. Available at: https://doi.org/10.3389/fgene.2019.00907.

Dabrowska, A., Venero, J.L., Iwasawa, R., Hankir, M., Rahman, S., Boobis, A. and Hajji, N. (2015) 'PGC-1α controls mitochondrial biogenesis and dynamics in lead-induced neurotoxicity', *Aging (Albany NY)*, 7(9), pp. 629–643. Available at: https://doi.org/10.18632/aging.100790.

Desviat, L.R., Pérez, B., Pérez-Cerdá, C., Rodríguez-Pombo, P., Clavero, S. and Ugarte, M. (2004) 'Propionic acidemia: mutation update and functional and structural effects of the variant alleles', *Molecular Genetics and Metabolism*, 83, pp. 28–37. Available at: https://doi.org/10.1016/j.ymgme.2004.08.001.

Doherty, E. and Perl, A. (2017) 'Measurement of mitochondrial mass by flow cytometry during oxidative stress', *Reactive Oxygen Species*, 4(10), pp. 275–283. Available at: https://doi.org/10.20455/ros.2017.839.

Duvezin-Caubet, S., Jagasia, R., Wagener, J., Hofmann, S., Trifunovic, A., Hansson, A., Chomyn, A., Bauer, M.F., Attardi, G., Larsson, N.G., Neupert, W. and Reichert, A.S. (2006) 'Proteolytic processing of OPA1 links mitochondrial dysfunction to alterations in mitochondrial morphology', *Journal of Biological Chemistry*, 281(49), pp. 37972–37979. Available at: https://doi.org/10.1074/jbc.M606059200.

Dyrvig, M., Qvist, P., Lichota, J., Larsen, K., Nyegaard, M., Børglum, A.D. and Christensen, J.H. (2017) 'DNA methylation analysis of BRD1 promoter regions and the schizophrenia rs138880 risk allele', *PLoS ONE*, 12(1), p. e0170121. Available at: https://doi.org/10.1371/JOURNAL.PONE.0170121.

Ehrlich, M. (2019) 'DNA hypermethylation in disease: mechanisms and clinical relevance', *Epigenetics*, 14(12), pp. 1141–1163. Available at: https://doi.org/10.1080/15592294.2019.1638701.

El-Ansary, A.K., Bacha, A.B. and Kotb, M. (2012) 'Etiology of autistic features: the persisting neurotoxic effects of propionic acid', *Journal of Neuroinflammation*, 9, p. 174. Available at: https://doi.org/10.1186/1742-2094-9-74.

Elgass, K.D., Smith, E.A., LeGros, M.A., Larabell, C.A. and Ryan, M.T. (2015) 'Analysis of ER-mitochondria contacts using correlative fluorescence microscopy and soft X-ray tomography of mammalian cells', *Journal of Cell Science*, 128, pp. 2795–2804. Available at: https://doi.org/10.1242/jcs.169136.

Escobar-Henriques, M. and Langer, T. (2014) 'Dynamic survey of mitochondria by Ubiquitin', *EMBO Reports*, 15, pp. 231–243. Available at: https://doi.org/10.1002/embr.201338225.

Fan, X.-Y., Guo, L., Chen, L.-N., Yin, S., Wen, J., Li, S., Ma, J.-Y., Jing, T., Jiang, M.-X., Sun, X.-H., Chen, M., Wang, F., Wang, Z.-B., Zhang, C.-F., Wang, X.-H., Ge, Z.-J., Hu, C., Zeng, L., Shen, W., Sun, Q.-Y., Ou, X.-H. and Luo, S.-M. (2022) 'Reduction of mtDNA heteroplasmy in mitochondrial replacement therapy by inducing forced mitophagy', *Nature Biomedical Engineering*, 6, pp. 339–350. Available at: https://doi.org/10.1038/s41551-022-00881-7.

Feinberg, A.P., Koldobskiy, M.A. and Göndör, A. (2016) 'Epigenetic modulators, modifiers and mediators in cancer aetiology and progression', *Nature Reviews Genetics*, 17(5), pp. 284–299. Available at: https://doi.org/10.1038/nrg.2016.13.

Ferri, S.L., Abel, T. and Brodkin, E.S. (2018) 'Sex differences in autism spectrum disorder: a review', *Current Psychiatry Reports*, 20, p. 9. Available at: https://doi.org/10.1007/s11920-018-0874-2.

Filiano, J.J., Goldenthal, M.J., Harker Rhodes, C. and Marín-García, J. (2002) 'Mitochondrial dysfunction in patients with hypotonia, epilepsy, autism, and developmental delay: HEADD syndrome', *Journal of Child Neurology*, 17(6), pp. 435–439. Available at: https://doi.org/10.1177/088307380201700607.

Franz, L., Chambers, N., von Isenburg, M. and de Vries, P.J. (2017) 'Autism spectrum disorder in sub-Saharan Africa: a comprehensive scoping review', *Autism Res*, 10(5), pp. 723–749. Available at: https://doi.org/10.1002/aur.1766.

Frederick, R.L. and Shaw, J.M. (2007) 'Moving mitochondria: establishing distribution of an essential organelle', *Traffic*, 8, pp. 1668–1675. Available at: https://doi.org/10.1111/j.1600-0854.2007.00644.x.

Frezza, C., Cipolat, S., de Brito, O.M., Micaroni, M., Beznoussenko, G.V., Rudka, T., Bartoli, D., Polishuck, R.S., Danial, N.N., de Strooper, B. and Scorrano, L. (2006) 'OPA1 controls apoptotic cristae remodeling independently from mitochondrial fusion', *Cell*, 126, pp. 177–189. Available at: https://doi.org/10.1016/j.cell.2006.06.025.

Friedman, J.R., Lackner, L.L., West, M., DiBenedetto, J.R., Nunnari, J. and Voeltz, G.K. (2011) 'ER tubules mark sites of mitochondrial division', *Science*, 334(6054), pp. 358–362. Available at: https://doi.org/10.1126/science.1207385.

Frye, R.E. (2020) 'Mitochondrial dysfunction in autism spectrum disorder: unique abnormalities and targeted treatments', *Seminars in Pediatric Neurology*, 35, p. 100829. Available at: https://doi.org/10.1016/J.SPEN.2020.100829.

Frye, R.E., Cakir, J., Rose, S., Palmer, R.F., Austin, C., Curtin, P. and Arora, M. (2021) 'Mitochondria may mediate prenatal environmental influences in autism spectrum disorder', *Journal of Personalized Medicine*, 11, p. 218. Available at: https://doi.org/10.3390/jpm11030218.

Frye, R.E., Rose, S., Chacko, J., Wynne, R., Bennuri, S.C., Slattery, J.C., Tippett, M., Delhey, L., Melnyk, S., Kahler, S.G. and MacFabe, D.F. (2016) 'Modulation of mitochondrial function by the microbiome metabolite propionic acid in autism and control cell lines', *Translational Psychiatry*, 6, p. e927. Available at: https://doi.org/10.1038/tp.2016.189.

Frye, R.E. and Rossignol, D.A. (2011) 'Mitochondrial dysfunction can connect the diverse medical symptoms associated with autism spectrum disorders', *Pediatric Research*, 69(5 Pt 2), pp. 41–47. Available at: https://doi.org/10.1203/PDR.0b013e318212f16b.

Fu, W., Liu, Y. and Yin, H. (2019) 'Mitochondrial dynamics: biogenesis, fission, fusion, and mitophagy in the regulation of stem cell behaviors', *Stem Cells International*, 2019, Article ID: 9757201. Available at: https://doi.org/10.1155/2019/9757201.

Fu, X.-F., Yao, K., Du, X., Li, Y., Yang, X.-Y., Yu, M., Li, M.-Z. and Cui, Q.-H. (2016) 'PGC-1α regulates the cell cycle through ATP and ROS in CH1 cells *#', *Journal of Zhejiang University-SCIENCE B*, 17, pp. 136–146. Available at: https://doi.org/10.1631/jzus.B1500158.

Galloway, C.A., Lee, H. and Yoon, Y. (2012) 'Mitochondrial morphology – Emerging role in bioenergetics', *Free Radical Biology and Medicine*, 53(12). Available at: https://doi.org/10.1016/j.freeradbiomed.2012.09.035.Mitochondrial.

Gandal, M.J., Haney, J.R., Parikshak, N.N., Leppa, V., Ramaswami, G., Hartl, C., Schork, A.J., Appadurai, V., Buil, A., Werge, T.M., Liu, C., White, K.P., Horvath, S. and Geschwind, D.H. (2018) 'Shared molecular neuropathology across major psychiatric disorders parallels polygenic overlap', *Science*, 359, pp. 693–697. Available at: https://doi.org/10.1126/science.aad6469.

Gaziev, A.I., Abdullaev, S. and Podlutsky, A. (2014) 'Mitochondrial function and mitochondrial DNA maintenance with advancing age', *Biogerontology*, 15, pp. 417–438. Available at: https://doi.org/10.1007/s10522-014-9515-2.

Giddings, T.H. (2003) 'Freeze-substitution protocols for improved visualization of membranes in high-pressure frozen samples', *Journal of Microscopy*, 212(Pt 1), pp. 53–61. Available at: https://doi.org/https://doi.org/10.1046/j.1365-2818.2003.01228.x.

Good, K.V., Vincent, J.B. and Ausió, J. (2021) 'MeCP2: the genetic driver of Rett syndrome epigenetics', *Frontiers in Genetics*, 12, p. 620859. Available at: https://doi.org/10.3389/fgene.2021.620859.

Grady, J.P., Murphy, J.L., Blakely, E.L., Haller, R.G., Taylor, R.W., Turnbull, D.M. and Tuppen, H.A.L. (2014) 'Accurate measurement of mitochondrial DNA deletion level and copy number differences in human skeletal muscle', *PLoS ONE*, 9(12), p. e114462. Available at: https://doi.org/10.1371/journal.pone.0114462.

Griffiths, K.K. and Levy, R.J. (2017) 'Evidence of mitochondrial dysfunction in autism: biochemical links, genetic-based associations, and non-energy-related mechanisms', *Oxidative Medicine and Cellular Longevity*, 2017, Article ID 4314025. Available at: https://doi.org/10.1155/2017/4314025.

Gu, F., Chauhan, V., Kaur, K., Brown, W.T., LaFauci, G., Wegiel, J. and Chauhan, A. (2013) 'Alterations in mitochondrial DNA copy number and the activities of electron transport chain complexes and pyruvate dehydrogenase in the frontal cortex from subjects with autism', *Translational psychiatry*, 3, p. e299. Available at: https://doi.org/10.1038/tp.2013.68.

Haas, R.H. (2010) 'Autism and Mitochondrial Disease', *Developmental Disabilities Research Reviews*, 16, pp. 144–153. Available at: https://doi.org/10.1002/ddrr.112.

Hájek, P., Chomyn, A. and Attardi, G. (2007) 'Identification of a novel mitochondrial complex containing mitofusin 2 and stomatin-like protein 2', *Journal of Biological Chemistry*, 282(8), pp. 5670–5681. Available at: https://doi.org/10.1074/jbc.M608168200.

Hawes, P., Netherton, C.L., Mueller, M., Wileman, T. and Monaghan, P. (2007) 'Rapid freeze-substitution preserves membranes in high-pressure frozen tissue culture cells', *Journal of*

Microscopy, 226(Pt 2), pp. 182–189. Available at: https://doi.org/10.1111/j.1365-2818.2007.01767.x.

Heinz, S., Freyberger, A., Lawrenz, B., Schladt, L., Schmuck, G. and Ellinger-Ziegelbauer, H. (2017) 'Mechanistic investigations of the mitochondrial complex I inhibitor rotenone in the context of pharmacological and safety evaluation', *Scientific Reports*, 7, p. 45465. Available at: https://doi.org/10.1038/srep45465.

Hoitzing, H., Johnston, I.G. and Jones, N.S. (2015) 'What is the function of mitochondrial networks? A theoretical assessment of hypotheses and proposal for future research', *Bioessays*, 37(6), pp. 687–700. Available at: https://doi.org/10.1002/bies.201400188.

Hon, G.C., Hawkins, R.D., Caballero, O.L., Lo, C., Lister, R., Pelizzola, M., Valsesia, A., Ye, Z., Kuan, S., Edsall, L.E., Camargo, A.A., Stevenson, B.J., Ecker, J.R., Bafna, V., Strausberg, R.L., Simpson, A.J. and Ren, B. (2012) 'Global DNA hypomethylation coupled to repressive chromatin domain formation and gene silencing in breast cancer', *Genome Research*, 22, pp. 246–258. Available at: https://doi.org/10.1101/gr.125872.111.

Hu, C., Shu, L., Huang, X., Yu, J., Li, liuju, Gong, L., Yang, M., Wu, Z., Gao, Z., Zhao, Y., Chen, L. and Song, Z. (2020) 'OPA1 and MICOS Regulate mitochondrial crista dynamics and formation', *Cell Death and Disease*, 11, p. 940. Available at: https://doi.org/10.1038/s41419-020-03152-y.

Hu, G., Zhang, J., Xu, F., Deng, H., Zhang, W., Kang, S. and Liang, W. (2018) 'Stomatin-like protein 2 inhibits cisplatin-induced apoptosis through MEK/ERK signaling and the mitochondrial apoptosis pathway in cervical cancer cells', *Cancer Science*, 109(5), pp. 1357–1368. Available at: https://doi.org/10.1111/cas.13563.

Ishihara, N., Fujita, Y., Oka, T. and Mihara, K. (2006) 'Regulation of mitochondrial morphology through proteolytic cleavage of OPA1', *EMBO Journal*, 25, pp. 2966–2977. Available at: https://doi.org/10.1038/sj.emboj.7601184.

Jaenisch, R. and Bird, A. (2003) 'Epigenetic regulation of gene expression: how the genome integrates intrinsic and environmental signals', *Nature Genetics*, 33, pp. 245–254. Available at: https://doi.org/10.1038/ng1089.

Jin, Z. and Liu, Y. (2018) 'DNA methylation in human diseases', *Genes and Diseases*, 5, pp. 1–8. Available at: https://doi.org/10.1016/j.gendis.2018.01.002.

Juven-Gershon, T. and Kadonaga, J.T. (2010) 'Regulation of gene expression via the core promoter and the basal transcriptional machinery', *Developmental Biology*, 339, pp. 225–229. Available at: https://doi.org/10.1016/j.ydbio.2009.08.009.

Karbowski, M. and Youle, R.J. (2003) 'Dynamics of mitochondrial morphology in healthy cells and during apoptosis', *Cell Death and Differentiation*, 10, pp. 870–880. Available at: https://doi.org/10.1038/sj.cdd.4401260.

Khacho, M. and Slack, R.S. (2018) 'Mitochondrial dynamics in the regulation of neurogenesis: from development to the adult brain', *Developmental Dynamics*, 247, pp. 47–53. Available at: https://doi.org/10.1002/dvdy.

Khera, R., Mehan, S., Bhalla, S., Kumar, S., Alshammari, A., Alharbi, M. and Sadhu, S.S. (2022) 'Guggulsterone mediated JAK/STAT and PPAR-gamma modulation prevents neurobehavioral and neurochemical abnormalities in propionic acid-induced experimental model of autism', *Molecules*, 27, p. 889. Available at: https://doi.org/10.3390/molecules27030889.

Kim, S.A., Jang, E.H., Mun, J.Y. and Choi, H. (2019) 'Propionic acid induces mitochondrial dysfunction and affects gene expression for mitochondria biogenesis and neuronal differentiation in SH-SY5Y cell line', *NeuroToxicology*, 75, pp. 116–122. Available at: https://doi.org/10.1016/j.neuro.2019.09.009.

Klein, C.J., Botuyan, M., Wu, Y., Ward, C.J., Nicholson, G.A., Hammans, S., Hojo, K., Yamanishi, H., Karpf, A.R., Wallace, D.C., Simon, M., Lander, C., Boardman, L.A., Cunningham, J.M., Smith, G.E., Litchy, W.J., Boes, B., Atkinson, E.J., Middha, S., Dyck, P James, Parisi, J.E., Mer, G., Smith, D.I. and Dyck, Peter J (2011) 'Mutations in DNMT1 cause hereditary sensory neuropathy with dementia and hearing loss', *Nature Genetics*, 43(6), pp. 595–600. Available at: https://doi.org/10.1038/ng.830.Mutations.

Kuratomi, G., Iwamoto, K., Bundo, M., Kusumi, I., Kato, N., Iwata, N., Ozaki, N. and Kato, T. (2008) 'Aberrant DNA methylation associated with bipolar disorder identified from discordant monozygotic twins', *Molecular Psychiatry*, 13, pp. 429–441. Available at: https://doi.org/https://doi.org/10.1038/sj.mp.4002001.

Ladd-Acosta, C., Hansen, K.D., Briem, E., Fallin, M.D., Kaufmann, W.E. and Fienberg, A.P. (2014) 'Common DNA methylation alterations in multiple brain regions in autism', *Molecular Psychiatry*, 19(8), pp. 862–871. Available at: https://doi.org/10.1038/mp.2013.114.

Lam, J., Katti, P., Biete, M., Mungai, M., Ashshareef, S., Neikirk, K., Lopez, E.G., Vue, Z., Christensen, T.A., Beasley, H.K., Rodman, T.A., Murray, S.A., Salisbury, J.L., Glancy, B., Shao, J., Pereira, R.O., Abel, E.D. and Hinton Jr., A. (2021) 'A universal approach to analyzing transmission electron microscopy with ImageJ', *Cells*, 10(9), p. 2177. Available at: https://doi.org/10.3390/cells10092177.

Levenson, V.V. (2010) 'DNA methylation as a universal biomarker', *Expert Review of Molecular Diagnostics*, 10(4), pp. 481–488. Available at: https://doi.org/10.1586/erm.10.17.

Liesa, M. and Shirihai, O.S. (2013) 'Mitochondrial dynamics in the regulation of nutrient utilization and energy expenditure', *Cell Metabolism*, 17(4), pp. 491–506. Available at: https://doi.org/10.1016/j.cmet.2013.03.002.

Lim, K.L., Ng, X.H., Grace, L.G.Y. and Yao, T.P. (2012) 'Mitochondrial dynamics and Parkinson's disease: focus on Parkin', *Antioxidants and Redox Signaling*, 16(9), pp. 935–949. Available at: https://doi.org/10.1089/ars.2011.4105.

Livak, K.J. and Schmittgen, T.D. (2001) 'Analysis of relative gene expression data using real-time quantitative PCR and the 2-ΔΔCT method', *Methods*, 25, pp. 402–408. Available at: https://doi.org/10.1006/meth.2001.1262.

Losón, O.C., Song, Z., Chen, H. and Chan, D.C. (2013) 'Fis1, Mff, MiD49, and MiD51 mediate Drp1 recruitment in mitochondrial fission', *Molecular Biology of the Cell*, 24, pp. 659–667. Available at: https://doi.org/10.1091/mbc.E12-10-0721.

Lowe, R., Gemma, C., Beyan, H., Hawa, M.I., Bazeos, A., David Leslie, R., Montpetit, A., Rakyan, V.K. and Ramagopalan, S.V (2013) 'Buccals are likely to be a more informative surrogate tissue than blood for epigenome-wide association studies', *Epigenetics*, 8(4), pp. 445–454. Available at: https://doi.org/10.4161/epi.24362.

Mandal, A., Wong, H.T.C., Pinter, K., Mosqueda, N., Beirl, A., Lomash, R.M., Won, S., Kindt, K.S. and Drerup, C.M. (2021) 'Retrograde mitochondrial transport is essential for organelle

distribution and health in zebrafish neurons', *Journal of Neuroscience*, 41(7), pp. 1371–1392. Available at: https://doi.org/10.1523/JNEUROSCI.1316-20.2020.

Martin, A.R., Teferra, S., Möller, M., Hoal, E.G. and Daly, M.J. (2018) 'The critical needs and challenges for genetic architecture studies in Africa', *Current Opinion in Genetics and Development*, 53, pp. 113–120. Available at: https://doi.org/10.1016/j.gde.2018.08.005.

Mattson, M.P., Gleichmann, M. and Cheng, A. (2008) 'Mitochondria in Neuroplasticity and Neurological Disorders', *Neuron*, 60(5), pp. 748–766. Available at: https://doi.org/10.1016/j.neuron.2008.10.010.

Maunakea, A.K., Nagarajan, R.P., Bilenky, M., Ballinger, T.J., Dsouza, C., Fouse, S.D., Johnson, B.E., Hong, C., Nielsen, C., Zhao, Y., Turecki, G., Delaney, A., Varhol, R., Thiessen, N., Shchors, K., Heine, V.M., Rowitch, D.H., Xing, X., Fiore, C., Schillebeeckx, M., Jones, S.J.M., Haussler, D., Marra, M.A., Hirst, M., Wang, T. and Costello, J.F. (2010) 'Conserved role of intragenic DNA methylation in regulating alternative promoters', *Nature*, 466, pp. 253–257. Available at: https://doi.org/10.1038/nature09165.

Merrill, R.A., Flippo, K.H. and Strack, S. (2017) 'Measuring mitochondrial shape with imageJ', in S. Strack and Y. Usachev (eds) *Techniques to Investigate Mitochondrial Function in Neurons.* Neuromethods. New York, NY: Humana Press, pp. 31–48. Available at: https://doi.org/10.1007/978-1-4939-6890-9_2.

Mill, J., Tang, T., Kaminsky, Z., Khare, T., Yazdanpanah, S., Bouchard, L., Jia, P., Assadzadeh, A., Flanagan, J., Schumacher, A., Wang, S. and Petronis, A. (2008) 'Epigenomic profiling reveals DNA-methylation changes associated with major psychosis.', *American Journal of Human Genetics*, 82, pp. 696–711. Available at: https://doi.org/10.1016/j.ajhg.2008.01.008.

Misgeld, T. and Schwarz, T.L. (2017) 'Mitostasis in neurons: Maintaining mitochondria in an extended cellular architecture', *Neuron*, 96(3), pp. 651–666. Available at: https://doi.org/10.1016/j.neuron.2017.09.055.

Mitsopoulos, P., Chang, Y.-H., Wai, T., König, T., Dunn, S.D., Langer, T. and Madrenas, J. (2015) 'Stomatin-like protein 2 is required for in vivo mitochondrial respiratory chain supercomplex formation and optimal cell function', *Molecular and Cellular Biology*, 35(10), pp. 1838–1847. Available at: https://doi.org/10.1128/mcb.00047-15.

Moore, L.D., Le, T. and Fan, G. (2013) 'DNA methylation and its basic function', *Neuropsychopharmacology*, 38, pp. 23–38. Available at: https://doi.org/10.1038/npp.2012.112.

Nardone, S., Sharan Sams, D., Reuveni, E., Getselter, D., Oron, O., Karpuj, M. and Elliott, E. (2014) 'DNA methylation analysis of the autistic brain reveals multiple dysregulated biological pathways', *Translational Psychiatry*, 4, p. e433. Available at: https://doi.org/10.1038/tp.2014.70.

Nardone, S., Sharan Sams, D., Zito, A., Reuveni, E. and Elliott, E. (2017) 'Dysregulation of cortical neuron DNA methylation profile in autism spectrum disorder', *Cerebral Cortex*, 27, pp. 5739–5754. Available at: https://doi.org/10.1093/cercor/bhx250.

Oliveira, G., Diogo, L., Grazina, M., Garcia, P., Ataíde, A., Marques, C., Miguel, T., Borges, L., Vicente, A.M. and Oliveira, C.R. (2005) 'Mitochondrial dysfunction in autism spectrum disorders: A population-based study', *Developmental Medicine and Child Neurology*, 47, pp. 185–189. Available at: https://doi.org/10.1017/S0012162205000332.

Otera, H., Miyata, N., Kuge, O. and Mihara, K. (2016) 'Drp1-dependent mitochondrial fission via MiD49/51 is essential for apoptotic cristae remodeling', *Journal of Cell Biology*, 212(5), pp. 531–544. Available at: https://doi.org/10.1083/jcb.201508099.

Otera, H., Wang, C., Cleland, M.M., Setoguchi, K., Yokota, S., Youle, R.J. and Mihara, K. (2010) 'Mff is an essential factor for mitochondrial recruitment of Drp1 during mitochondrial fission in mammalian cells', *Journal of Cell Biology*, 191(6), pp. 1141–1158. Available at: https://doi.org/10.1083/jcb.201007152.

Palikaras, K. and Tavernarakis, N. (2014) 'Mitochondrial homeostasis: The interplay between mitophagy and mitochondrial biogenesis', *Experimental Gerontology*, 56, pp. 182–188. Available at: https://doi.org/10.1016/j.exger.2014.01.021.

Palmer, C.S., Osellame, L.D., Stojanovski, D. and Ryan, M.T. (2011) 'The regulation of mitochondrial morphology: Intricate mechanisms and dynamic machinery', *Cellular Signalling*, 23, pp. 1534–1545. Available at: https://doi.org/10.1016/j.cellsig.2011.05.021.

Pecorelli, A., Ferrara, F., Messano, N., Cordone, V., Schiavone, M.L., Cervellati, F., Woodby, B., Cervellati, C., Hayek, J. and Valacchi, G. (2020) 'Alterations of mitochondrial bioenergetics,

dynamics, and morphology support the theory of oxidative damage involvement in autism spectrum disorder', *The FASEB Journal*, 34(5), pp. 6521–6538. Available at: https://doi.org/10.1096/fj.201902677r.

Peng, K., Yang, L., Wang, J., Ye, F., Dan, G., Zhao, Y., Cai, Y., Cui, Z., Ao, L., Liu, J., Zou, Z., Sai, Y. and Cao, J. (2017) 'The interaction of mitochondrial biogenesis and fission/fusion mediated by PGC-1α regulates rotenone-induced dopaminergic neurotoxicity', *Molecular Neurobiology*, 54, pp. 3783–3797. Available at: https://doi.org/10.1007/s12035-016-9944-9.

Popov, L.D. (2020) 'Mitochondrial biogenesis: An update', *Journal of Cellular and Molecular Medicine*, 24, pp. 4892–4899. Available at: https://doi.org/10.1111/jcmm.15194.

Qu, H., Jiang, W., Wang, Y. and Chen, P. (2019) 'Stoml2 as a novel prognostic biomarker modulates cell proliferation, motility and chemo-sensitivity via IL6-Stat3 pathway in head and neck squamous cell carcinoma', *American Journal of Translational Research*, 11(2), pp. 683–695.

Rangaraju, V., Lewis, T.L., Hirabayashi, Y., Bergami, M., Motori, E., Cartoni, R., Kwon, S.K. and Courchet, J. (2019) 'Pleiotropic mitochondria: the influence of mitochondria on neuronal development and disease', *Journal of Neuroscience*, 39(42), pp. 8200–8208. Available at: https://doi.org/10.1523/JNEUROSCI.1157-19.2019.

Reynolds, E.S. (1963) 'The use of lead citrate at high pH as an electron-opaque stain in electron microscopy', *Journal of Cell Biology*, 17(1), pp. 208–212. Available at: https://doi.org/https://doi.org/10.1083/jcb.17.1.208.

Rodriguez-Gomez, D.A., Garcia-Guaqueta, D.P., Charry-Sánchez, J.D., Sarquis-Buitrago, E., Blanco, M., Velez-van-Meerbeke, A. and Talero-Gutiérrez, C. (2021) 'A systematic review of common genetic variation and biological pathways in autism spectrum disorder', *BMC Neuroscience*, 22, p. 60. Available at: https://doi.org/10.1186/s12868-021-00662-z.

Rossignol, D.A. and Frye, R.E. (2012) 'Mitochondrial dysfunction in autism spectrum disorders: A systematic review and meta-analysis', *Molecular Psychiatry*, 17, pp. 290–314. Available at: https://doi.org/10.1038/mp.2010.136.

Rugarli, E.I. and Langer, T. (2012) 'Mitochondrial quality control: A matter of life and death for neurons', *EMBO Journal*, 31, pp. 1336–1349. Available at: https://doi.org/10.1038/emboj.2012.38.

Rylaarsdam, L. and Guemez-Gamboa, A. (2019) 'Genetic causes and modifiers of autism spectrum disorder', *Frontiers in Cellular Neuroscience*, 13, p. 385. Available at: https://doi.org/10.3389/fncel.2019.00385.

Ryoo, I. and Kwak, M.-K. (2018) 'Regulatory crosstalk between the oxidative stress-related transcription factor Nfe2l2/Nrf2 and mitochondria', *Toxicology and Applied Pharmacology*, 359, pp. 24–33. Available at: https://doi.org/10.1016/j.taap.2018.09.014.

Santel, A. and Fuller, M.T. (2001) 'Control of mitochondrial morphology by a human mitofusin', *Journal of Cell Science*, 114(Pt 5), pp. 867–874.

Schenkel, L.C., Schwartz, C., Skinner, C., Rodenhiser, D.I., Ainsworth, P.J., Pare, G. and Sadikovic, B. (2016) 'Clinical validation of fragile X syndrome screening by DNA methylation array', *The Journal of Molecular Diagnostics*, 18(6), pp. 834–841. Available at: https://doi.org/10.1016/j.jmoldx.2016.06.005.

Schindelin, J., Arganda-Carreras, I., Frise, E., Kaynig, V., Longair, M., Pietzsch, T., Preibisch, S., Rueden, C., Saalfeld, S., Schmid, B., Tinevez, J.-Y., White, D.J., Hartenstein, V., Eliceiri, K., Tomancak, P. and Cardona, A. (2012) 'Fiji: an open-source platform for biological-image analysis', *Nature Methods*, 9, pp. 676–682. Available at: https://doi.org/10.1038/nmeth.2019.

Semick, S.A., Bharadwaj, R.A., Collado-Torres, L., Tao, R., Shin, J.H., Deep-Soboslay, A., Weiss, J.R., Weinberger, D.R., Hyde, T.M., Kleinman, J.E., Jaffe, A.E. and Mattay, V.S. (2019) 'Integrated DNA methylation and gene expression profiling across multiple brain regions implicate novel genes in Alzheimer's disease', *Acta Neuropathologica*, 137, pp. 557–569. Available at: https://doi.org/10.1007/s00401-019-01966-5.

Siddiqui, M.F., Elwell, C. and Johnson, M.H. (2016) 'Mitochondrial Dysfunction in Autism Spectrum Disorders', *Autism Open Access*, 6(5). Available at: https://doi.org/10.4172/2165-7890.1000190.Mitochondrial.

Smirnova, E., Griparic, L., Shurland, D.-L. and van der Bliek, A.M. (2001) 'Dynamin-related protein Drp1 is required for mitochondrial division in mammalian cells', *Molecular Biology of*

the Cell, 12, pp. 2245–2256. Available at: https://doi.org/https://doi.org/10.1091/mbc.12.8.2245.

Smith, A.K., Kilaru, V., Klengel, T., Mercer, K.B., Bradley, B., Conneely, K.N., Ressler, K.J. and Binder, E.B. (2015) 'DNA extracted from saliva for methylation studies of psychiatric traits: evidence tissue specificity and relatedness to brain', *Neuropsychiatric Genetics, Part B of the American Journal of Medical Genetics*, 0(1), pp. 36–44. Available at: https://doi.org/:10.1002/ajmg.b.32278.

Stathopoulos, S., Gaujoux, R., Lindeque, Z., Mahony, C., van der Colff, R., van der Westhuizen, F. and O'Ryan, C. (2020) 'DNA methylation associated with mitochondrial dysfunction in a South African autism spectrum disorder cohort', *Autism Research*, 13(7), pp. 1079–1093. Available at: https://doi.org/10.1002/aur.2310.

Stojanovski, D., Koutsopoulos, O.S., Okamoto, K. and Ryan, M.T. (2004) 'Levels of human Fis1 at the mitochondrial outer membrane regulate mitochondrial morphology', *Journal of Cell Science*, 117(7), pp. 1201–1210. Available at: https://doi.org/10.1242/jcs.01058.

Stremming, J., Chang, E.I., Knaub, L.A., Armstrong, M.L., Baker, P.R., Wesolowski, S.R., Reisdorph, N., Reusch, J.E.B. and Brown, L.D. (2012) 'Lower citrate synthase activity, mitochondrial complex expression, and fewer oxidative myofibers characterize skeletal muscle from growth-restricted fetal sheep', *American Journal of Physiology-Regulatory, Integrative and Comparative Physiology*, 14, pp. 3349–3360. Available at: https://doi.org/10.1152/ajpregu.00222.2021.

Tang, G., Rios, P.G., Kuo, S.-H., Akman, H.O., Rosoklija, G., Tanji, K., Dwork, A., Schon, E.A., DiMauro, S., Goldman, J. and Sulzer, D. (2013) 'Mitochondrial abnormalities in temporal lobe of autistic brain', *Neurobiology of Disease*, 54, pp. 349–361. Available at: https://doi.org/10.1016/j.nbd.2013.01.006.

Thompson, K., Majd, H., Dallabona, C., Reinson, K., King, M.S., Alston, C.L., He, L., Lodi, T., Jones, S.A., Fattal-Valevski, A., Fraenkel, N.D., Saada, A., Haham, A., Isohanni, P., Vara, R., Barbosa, I.A., Simpson, M.A., Deshpande, C., Puusepp, S., Bonnen, P.E., Rodenburg, R.J., Suomalainen, A., Õunap, K., Elpeleg, O., Ferrero, I., McFarland, R., Kunji, E.R.S. and Taylor, R.W. (2016) 'Recurrent de novo dominant mutations in SLC25A4 cause severe early-onset mitochondrial disease and loss of mitochondrial DNA copy number', *American Journal of*

Human Genetics, 99(4), pp. 860–876. Available at: https://doi.org/10.1016/j.ajhg.2016.08.014.

Tondera, D., Grandemange, S., Jourdain, A., Karbowski, M., Mattenberger, Y., Herzig, S., da Cruz, S., Clerc, P., Raschke, I., Merkwirth, C., Ehses, S., Krause, F., Chan, D.C., Alexander, C., Bauer, C., Youle, R., Langer, T. and Martinou, J.C. (2009) 'SLP-2 is required for stress-induced mitochondrial hyperfusion', *EMBO Journal*, 28, pp. 1589–1600. Available at: https://doi.org/10.1038/emboj.2009.89.

Tremblay, M.W. and Jiang, Y.H. (2019) 'DNA methylation and susceptibility to autism spectrum disorder', *Annual Review of Medicine*, 70, pp. 151–166. Available at: https://doi.org/10.1146/annurev-med-120417-091431.

Uittenbogaard, M. and Chiaramello, A. (2014) 'Mitochondrial biogenesis: a therapeutic target for neurodevelopmental disorders and neurodegenerative diseases', *Current pharmaceutical design*, 20(35), pp. 5574–5593. Available at: https://doi.org/10.2174/1381612820666140305224906.

Vaarmann, A., Mandel, M., Zeb, A., Wareski, P., Liiv, J., Kuum, M., Antsov, E., Liiv, M., Cagalinec, M., Choubey, V. and Kaasik, A. (2016) 'Mitochondrial biogenesis is required for axonal growth', *Development*, 143, pp. 1981–1992. Available at: https://doi.org/10.1242/dev.128926.

Viscomi, C., Bottani, E., Civiletto, G., Cerutti, R., Moggio, M., Fagiolari, G., Schon, E.A., Lamperti, C. and Zeviani, M. (2011) 'In vivo correction of COX deficiency by activation of the AMPK/PGC-1α axis', *Cell Metabolism*, 14, pp. 80–90. Available at: https://doi.org/10.1016/j.cmet.2011.04.011.

Wai, T. and Langer, T. (2016) 'Mitochondrial Dynamics and Metabolic Regulation', *Trends in Endocrinology and Metabolism*, 27(2), pp. 105–117. Available at: https://doi.org/10.1016/j.tem.2015.12.001.

Wang, Y.M., Qiu, M.Y., Liu, Q., Tang, H. and Gu, H.F. (2021) 'Critical role of dysfunctional mitochondria and defective mitophagy in autism spectrum disorders', *Brain Research Bulletin*, 168, pp. 138–145. Available at: https://doi.org/10.1016/j.brainresbull.2020.12.022.

Weissman, J.R., Kelley, R.I., Bauman, M.L., Cohen, B.H., Murray, K.F., Mitchell, R.L., Kern, R.L. and Natowicz, M.R. (2008) 'Mitochondrial disease in autism spectrum disorder patients: A cohort analysis', *PLoS ONE*, 3(11), pp. 1–6. Available at: https://doi.org/10.1371/journal.pone.0003815.

Weng, Y.L., An, R., Shin, J., Song, H. and Ming, G. li (2013) 'DNA Modifications and Neurological Disorders', *Neurotherapeutics*, 10, pp. 556–567. Available at: https://doi.org/10.1007/s13311-013-0223-4.

Winey, M., Meehl, J.B., O'Toole, E.T. and Giddings Jr, T.H. (2014) 'Conventional transmission electron microscopy', *Molecular Biology of the Cell*, 25, pp. 319–323. Available at: https://doi.org/10.1091/mbc.E12-12-0863.

Wiśniowiecka-Kowalnik, B. and Nowakowska, B.A. (2019) 'Genetics and epigenetics of autism spectrum disorder – current evidence in the field', *Journal of Applied Genetics*, 60, pp. 37–47. Available at: https://doi.org/10.1007/s13353-018-00480-w.

Wong, C.C.Y., Meaburn, E.L., Ronald, A., Price, T.S., Jeffries, A.R., Schalkwyk, L.C., Plomin, R. and Mill, J. (2014) 'Methylomic analysis of monozygotic twins discordant for autism spectrum disorder and related behavioural traits', *Molecular Psychiatry*, 19, pp. 495–503. Available at: https://doi.org/10.1038/mp.2013.41.

Yang, D., Ying, J., Wang, X., Zhao, T., Yoon, S., Fang, Y., Zheng, Q., Liu, X., Yu, W. and Hua, F. (2021) 'Mitochondrial dynamics: a key role in neurodegeneration and a potential target for neurodegenerative disease', *Frontiers in Neuroscience*, 15, p. 654785. Available at: https://doi.org/10.3389/fnins.2021.654785.

Yoon, S.H., Choi, J., Lee, W.J. and Do, J.T. (2020) 'Genetic and epigenetic etiology underlying autism spectrum disorder', *Journal of Clinical Medicine*, 9(4), p. 966. Available at: https://doi.org/10.3390/jcm9040966.

Youle, R.J. and Bliek, A.M. van der (2012) 'Mitochondrial Fission, Fusion, and Stress', *Science*, 337(6098), pp. 1062–1065. Available at: https://doi.org/10.1126/science.1219855.

Yu, R., Lendahl, U., Nistér, M. and Zhao, J. (2020) 'Regulation of mammalian mitochondrial dynamics: opportunities and challenges', *Frontiers in Endocrinology*, 11, p. 374. Available at: https://doi.org/10.3389/fendo.2020.00374.

Zeidan, J., Fombonne, E., Scorah, J., Ibrahim, A., Durkin, M.S., Saxena, S., Yusuf, A., Shih, A. and Elsabbagh, M. (2022) 'Global prevalence of autism: A systematic review update', *Autism Research*, 15, pp. 778–790. Available at: https://doi.org/10.1002/aur.2696.

Zeng, Y., Pan, Q., Wang, X., Li, D., Lin, Y., Man, F., Xiao, F. and Guo, L. (2019) 'Impaired mitochondrial fusion and oxidative phosphorylation triggered by high glucose is mediated by Tom22 in endothelial cells', *Oxidative Medicine and Cellular Longevity*, 2019, Article ID 4508762. Available at: https://doi.org/10.1155/2019/4508762.

Zheng, Y., Huang, C., Lu, L., Yu, K., Zhao, J., Chen, M., Liu, L., Sun, Q., Lin, Z., Zheng, J., Chen, J. and Zhang, J. (2021) 'STOML2 potentiates metastasis of hepatocellular carcinoma by promoting PINK1-mediated mitophagy and regulates sensitivity to lenvatinib', *Journal of Hematology and Oncology*, 14, p. 16. Available at: https://doi.org/10.1186/s13045-020-01029-3.

Zhu, J., Wang, K.Z.Q. and Chu, C.T. (2013) 'After the banquet', *Autophagy*, 9(11), pp. 1663–1676. Available at: https://doi.org/10.4161/auto.24135.

Zick, M., Rabl, R. and Reichert, A.S. (2009) 'Cristae formation-linking ultrastructure and function of mitochondria', *Biochimica et Biophysica Acta Molecular Cell Research*, 1793(1), pp. 5–19. Available at: https://doi.org/10.1016/j.bbamcr.2008.06.013.